EXPLORING THE MOLECULAR MECHANISMS OF INSECT ODORANT RECEPTORS

By

Gregory M. Pask

Dissertation

Submitted to the Faculty of the

Graduate School of Vanderbilt University

in partial fulfillment of the requirements

for the degree of

DOCTOR OF PHILOSOPHY

in

Biological Sciences

May, 2013

Nashville, TN

Approved:

Dr. Terry Page

Dr. Douglas McMahon

Dr. Aurelio Galli

Dr. David Piston

Dr. Laurence Zwiebel

To my Mom and Dad, for teaching me

to continually strive for excellence

and

To my loving wife, Heather, for encouraging me

to pursue my ever-changing curiosity

ACKNOWLEDGEMENTS

I would first like to thank my advisor, Larry Zwiebel, who graciously welcomed me into the laboratory despite a fruitless rotation project. Since joining the lab in May 2009, Larry has continued to push me to become an independent researcher and has encouraged me to pursue the research questions that interested me the most. Through this practice, Larry has imparted the following belief that I now share; interest and curiosity are the best motivators. I also wish to thank Jason Pitts, who has been an amazing source of mosquito knowledge, past lab endeavors, and sports talk. Jason has always been willing to talk about planned, successful, or failed experiments, and has had a major role in my graduate training even while obtaining his own PhD.

I would also like to thank the members of the Zwiebel lab for their helpful discussions/critiques throughout my training, as well as their contributions to a fun and cooperative lab environment. In particular, I would like to thank Patrick Jones, who helped me get started as an independent researcher in the lab. I also wish to thank David Rinker, who is always ready for a spontaneous and scientific “bull session,” whether it takes place over a rack to tubes, a pint of stout, or a Pepperfire leg quarter. I wish to also thank Zhen Li, for continually providing assistance in molecular cloning when I was either busy or simply had some recent bad luck. Even though we only had a couple years of overlap, I thank Jesse Slone for our ongoing discussions (in no particular order) concerning cloning strategies, ants, college basketball, and Breaking Bad.

My committee has been extremely supportive and responsive during my graduate career. Terry Page has been an excellent committee chair, and he has not only taught me about Cellular Neurobiology in his class, but how to effectively relate complicated systems to eager undergraduates. I thank Aurelio Galli for the opportunity to learn patch clamp electrophysiology during my rotation in his lab and the continued assistance from Aurelio and a postdoc in his lab, Kevin Erreger, as I tackled more complex recording paradigms. I would also like to thank Dave Piston, for serving as my fluorescence microscopy resource and his eagerness to help me get a handle on single-molecule TIRF imaging.

The Biological Sciences Administrative Support Staff has been outstanding, especially in dealing with the submission and logistics of my predoctoral fellowship. In particular, Carol Wiley and Alicia Goostree were able to immediately answer my questions or could find an answer within a couple hours. Leslie Maxwell has been the ultimate resource, dealing with all of my issues regarding student registration, remaining travel funds, and several other matters. I would also like to recognize the Gisela Mosig Travel Fund, which has allowed me to travel to across the globe to share my research at conferences and attend a PhD course in Sweden. I have been fortunate to have these funds made available to me and I hope future graduate students take advantage of this wonderful opportunity.

Finally, I would like to give a special thank you to my parents, for supporting me every step of the way. As my role models, they have led by example to demonstrate that intelligence and hard work are a great recipe for a

successful career, but more importantly, a rewarding life. I wish to thank my brother, Jim, for allowing me to follow him to Vanderbilt for graduate school and helping me get acclimated to Southern living, and also for having my back in a impromptu intramural basketball or softball fracas. Finally I would like to thank my at-home support team of Lincoln and Heather. Even on days when experiments didn't work out, Lincoln always had a couple tail wags and licks of encouragement to help keep me sane. I am extremely fortunate that Heather, my best friend and wife, finds my work exciting and fully understands when I want to stay late to pursue an interesting experiment. I feel like the luckiest researcher in the world to have a wife who enjoys the subject of my curiosity and is eager to hear about every experiment and insect "fun fact" when I come home.

TABLE OF CONTENTS

Page

LIST OF TABLES

LIST OF FIGURES

CHAPTER I

THE IMPORTANCE OF INSECT OLFACTION: FROM OLFACTORY-DRIVEN BEHAVIOR TO CHEMOSENSORY RECEPTORS

Olfaction in Insect Behavior

In an environment filled with a complex spectrum of chemical stimuli, animals use the sensory modality of olfaction to discern a wide range of volatile cues of ecological importance. Many odorant molecules function as semiochemicals, or chemicals that convey specific messages among organisms. Intraspecific semiochemicals, collectively termed pheromones, can signal for a wide variety of behaviors in conspecifics, such as aggregation, alarm, and mating[1]. Other semiochemicals allow for communication between different species, and these can benefit the emitter (allomones), the receiver (kairomones), or both (synomones)[1].

Insects, in particular, rely on the olfactory system to drive several key behaviors. In the 1870s, Jean-Henri Fabre observed that a female great peacock moth was able to attract over forty males in one evening[2]. Fabre later postulated that the female was emitting some odor that was highly attractive to the opposite sex[2]. Almost a century later, the first insect sex pheromone, bombykol, was identified by Adolph Butenandt in 1959 who found that a pure extract of bombykol from *Bombyx mori* females was sufficient to induce mating responses in *B. mori* males[3]. In addition to pheromone-based communication within an insect species, volatile semiochemicals from other sources can trigger robust behaviors. For example, when a female *Anopheles gambiae* mosquito is

searching for a suitable host to obtain a bloodmeal, it is attracted to several volatile cues emitted from humans, such as carbon dioxide and other volatile components found in human sweat[4]. Another example is from the hawkmoth *Manduca sexta*, which uses floral volatiles to orient towards a host plant, *Datura wrightii*, where these odorant cues elicit both nectar-feeding or oviposition behaviors[5].

As the field began to recognize the significance of odor-guided behaviors in insects, it was not surprising that targeting the olfactory system became a successful approach to control the destructive behaviors of both agricultural pests and disease vectors. By using the sex pheromone as a lure, several coleopteran and lepidopteran agricultural pests have been controlled by mass-trapping techniques[6]. Pheromones have also proven to be an effective and efficient way to detect and monitor the population of a particular pest species due to the great specificity in pheromone-based communication. Another widely-used pest control technique in lepidopterans is mating disruption, where dispensers are placed throughout an agricultural plot and slowly release synthetic sex pheromone[6]. Consequently, the male moth has difficulty locating a calling female due to several sources of pheromone, resulting in a reduction of successful mating events[6]. Kairomones can also be used as bait in insect trapping, as demonstrated by trapping of *An. gambiae*[7,8]. A synthetic blend of volatiles identified from humans can be an effect lure in trapping *An. gambiae*, and one assay shows a blend that is ~4 times more attractive than an actual

human[7]. As a means to modify insect behaviors, the olfactory system still remains a potent and viable target for control strategies.

Olfactory Signaling: Sensilla to the Brain

Insects are able to detect volatiles through several chemosensory appendages. The primary olfactory appendages are the antennae, but other head structures, such as the maxillary palps and proboscis, have been shown to detect volatiles[9-11]. Covering the olfactory appendages are tiny cuticular projections called sensilla, which display a wide range of morphological diversity[12,13]. Olfactory sensilla are multiporous, and odorant molecules traverse these cuticular pores enter into the sensillum lymph (Figure 1.1A). Although several odorants are quite hydrophobic and will not readily solubilize in the aqueous lymph, the lymph contains an abundance of proteins termed odorant-binding proteins (OBPs) that are thought to facilitate odorant solubilization (Figure 1.1B)[14,15]. With the odorant molecule able to diffuse through the sensillum lymph, it can interact with the dendrites of olfactory receptors neurons (ORNS) that project into the sensillum (Figure 1.1A). Cell-surface chemoreceptors on the dendritic membrane of ORNs are able to detect a specific range of odorants (Figure 1.1B). Upon odorant binding, the chemoreceptors depolarize the ORN with an influx of cations, and the signal is relayed to the antennal lobe and into higher centers of the brain[16].

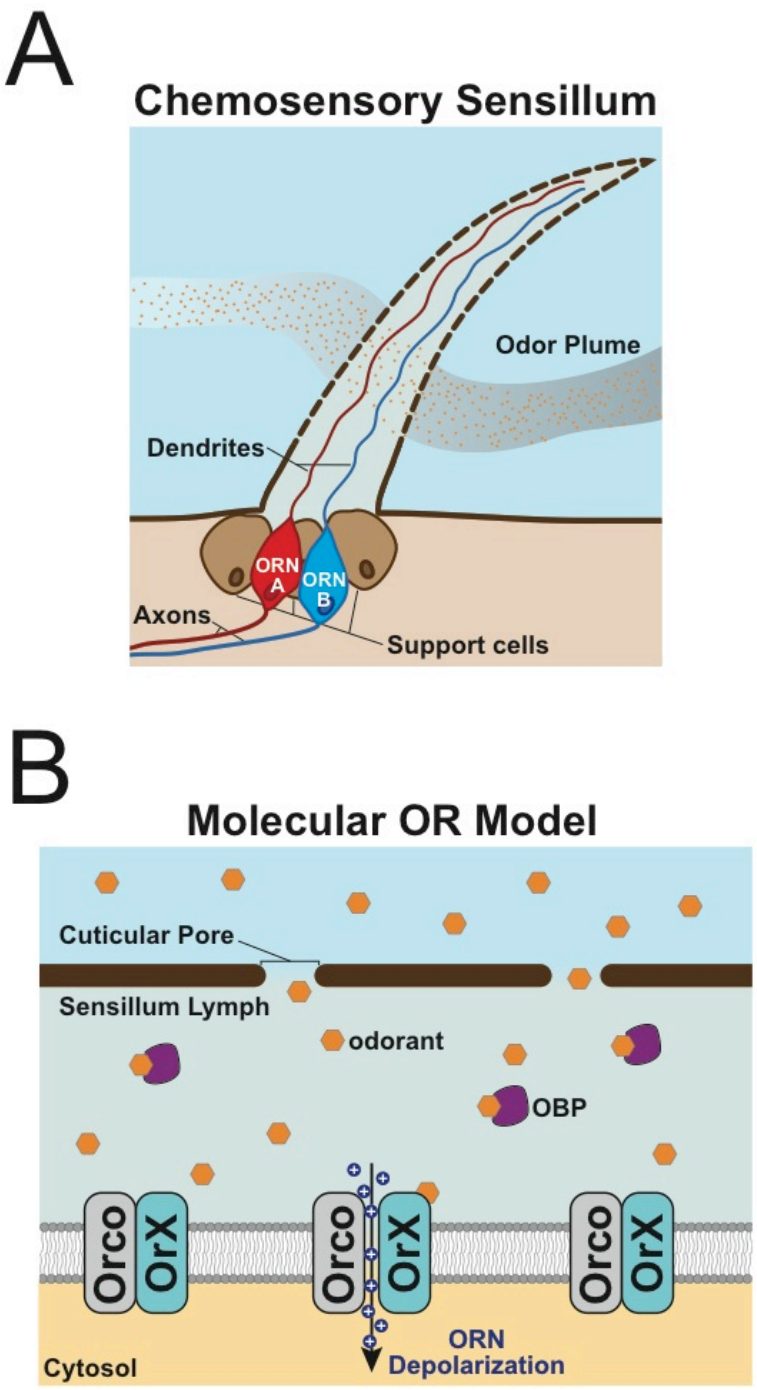

Figure 1.1 Schematic of the peripheral olfactory system in insects.

Olfactory Chemoreceptors

A variety of chemoreceptors can be expressed in the dendrites of ORNs. The 2 largest families of olfactory receptors consist of the chemosensory ionotropic receptors (IRs) and the odorant receptors (ORs). The IRs are related to the ionotropic glutamate receptors, but have evolved a divergent ligand-binding domain that lacks the residues for glutamate binding[17]. Initial functional work has demonstrated that several IR sensilla from *Drosophila melanogaster* are narrowly tuned to acids and amines[18]. IRs also appear to be conserved beyond insects into other arthropods, namely crustaceans and arachnids[18]. The OR family, on the other hand, seems to have appeared at some point during the insect lineage, as only IRs, not ORs, were not detected in the silverfish *Lepismachilis y-signata*, a basal wingless insect (Miβbach et al, presented at ISOT 2012). The OR family is believed to have evolved from insect gustatory receptors (GRs), a chemoreceptor family involved in detecting tastants such as sugars and glycerol[19-21]. In some cases GRs have also been shown to function in the olfactory system, where combinations of GRs are responsible for CO_2 sensitivity[22]. Although there is still much to learn about each of these chemoreceptor families, research within the last 14 years has resulted in a significant increase in the understanding of OR function.

The first insect ORs were identified in 1999 in *D. melanogaster* by three separate groups, 8 years after Buck and Axel discovered mammalian ORs in the rat[23-26]. The identification of ORs in *Drosophila* proved to be more challenging due to the lack of homology to the rat ORs and other GPCRs, and it was later

demonstrated that insect ORs possess an inverted heptahelical topology[27,28]. In insects, functional OR complexes exist as heteromultimers consisting of two types of subunits, the Orco coreceptor and an odorant-specific tuning OR in an unknown stoichiometry[29].

Orco, first described in *Drosophila*, is extremely conserved across several insect taxa, and it is quickly identified as new insect genomes are sequenced[30-32]. In *Drosophila*, Orco, formerly known as OR83b, has been implicated in dendritic localization of the OR complex, as tuning ORs are absent from chemosensory dendrites when expressed without Orco[33]. The functional conservation of Orco across insects has been demonstrated by rescuing olfactory responses of *Orco* null mutant flies through expression of Orco orthologs as well as in heterologous expression systems[34-36].

In contrast to Orco, tuning ORs are quite divergent across insects. For example, between 2 mosquito species, ~95% of *Aedes aegypti* ORs shared less than 20% identity to those in *An. gambiae*[37]. Among ants, it has been shown that the tuning ORs experience rapid rates of gene birth and death, and this has resulted in several species-specific expansions[38]. The number of tuning ORs from an insect can be quite variable. For example, *D. melanogaster* (60 ORs) and *Bombyx mori* (48 ORs) have a relatively smaller number of tuning ORs compared to *Nasonia vitripennis* (301 ORs) and *Tribolium castaneum* (341 ORs)[23-25,39-41]. For some insects, odorant agonists have been identified for subsets of tuning ORs. Through the use of heterologous expression systems, such as the *Drosophila* empty neuron and the *Xenopus laevis* oocyte, tuning

ORs have been successfully deorphanized by screening against both large odorant panels and ecologically-relevant semiochemicals[35,36,38,42-45].

Several studies have shown that the expression of insect ORs was necessary and sufficient for odorant-dependent responses in *Xenopus* oocytes and cultured mammalian cells, even in the absence of OBPs or other expressed proteins[36,37,43-45]. As more research groups began studying insect OR function, an interesting dilemma in the field. How are insect ORs, which were thought to function as GPCRs like their vertebrate counterparts, able to interact with intracellular G-proteins when they posses an inverted topology and lack the conserved amino acid motifs common to all GPCRs[27,28]? In addition, several previous reports had implicated specific G-proteins and arrestins in peripheral olfactory signaling[46-48]. In 2008, two reports were published together that demonstrated that insect OR complexes function as odorant-gated non-selective cation channels[49,50]. However, these findings led to a disagreement about the specific mechanism and whether a metabotropic component had a role in gating the channel. One model proposed that the heteromeric OR complex is gated by an odorant agonist and results in an ionotropic current through a pore surround by both Orco and tuning OR subunits[49]. The other model claimed that the binding of an odorant to the tuning OR triggers both a short ionotropic current and a prolonged metabotropic current, in which Orco formed a channel that was directly gated by cyclic nucleotides[50]. This debate is ongoing even as other groups are unable to detect a metabotropic current, but a consensus model

suggests that the G-protein pathway produces a post-translational modification on the OR complex that results in a functional change[51].

The finding that insect ORs function as heteromeric cation channels has yielded many new research directions and questions. For example, how do Orco and tuning OR subunits assemble to form a channel pore? Do different tuning ORs impart distinct channel properties other than odorant binding? As demonstrated in the following chapters, we can made relatively quick advances in understanding insect OR function through the techniques and strategies from the previous literature on ion channel characterization. Additionally, a pharmacological approach that was initially proposed to identify compounds that modify insect behavior (attractants/repellents) can prove most useful in the basic research of OR function.

References

1. Herrmann, A. *The chemistry and biology of volatiles*. (Wiley Online Library, 2010).

2. Fabre, J. H. *Social life in the insect world*. (TF Unwin, 1911).

3. Butenandt, A., Beckmann, R., Stamm, D. & Hecker, E. Uber den Sexual-Lockstoff des Seidenspinners Bombyx mori. Reindarstellung und Konstitution. *Z. Naturforsch* **14**, 283–284 (1959).

4. Takken, W. & Knols, B. G. Odor-mediated behavior of Afrotropical malaria mosquitoes. *Annu Rev Entomol* **44**, 131–157 (1999).

5. Riffell, J. A., Lei, H., Christensen, T. A. & Hildebrand, J. G. Characterization and Coding of Behaviorally Significant Odor Mixtures. *Curr Biol* **19**, 335–340 (2009).

6. Witzgall, P., Kirsch, P. & Cork, A. Sex pheromones and their impact on pest management. *J Chem Ecol* **36**, 80–100 (2010).

7. Okumu, F. O. *et al.* Development and field evaluation of a synthetic mosquito lure that is more attractive than humans. *PLoS ONE* **5**, e8951 (2010).

8. Mukabana, W. R. *et al.* A Novel Synthetic Odorant Blend for Trapping of Malaria and Other African Mosquito Species. *J Chem Ecol* (2012).doi:10.1007/s10886-012-0088-8

9. de Bruyne, M., Clyne, P. J. & Carlson, J. R. Odor coding in a model olfactory organ: the Drosophila maxillary palp. *Journal of Neuroscience* **19**, 4520–4532 (1999).

10. Lu, T. *et al.* Odor coding in the maxillary palp of the malaria vector mosquito Anopheles gambiae. *Curr Biol* **17**, 1533–1544 (2007).

11. Kwon, H.-W., Lu, T., Rützler, M. & Zwiebel, L. J. Olfactory responses in a gustatory organ of the malaria vector mosquito Anopheles gambiae. *Proc Natl Acad Sci USA* **103**, 13526–13531 (2006).

12. Hull, C. D. & Cribb, B. W. Ultrastructure of the antennal sensilla of Queensland fruit fly, Bactrocera tryoni(Froggatt)(Diptera: Tephritidae). *Int J Insect Morphol* **26**, 27–34 (1997).

13. Pitts, R. J. & Zwiebel, L. J. Antennal sensilla of two female anopheline sibling species with differing host ranges. *Malar J* **5**, 26 (2006).

14. Hekmat-Scafe, D., Steinbrecht, R. & Carlson Olfactory coding in a compound nose - Coexpression of odorant-binding proteins in Drosophila. *Ann Ny Acad Sci* **855**, 311–315 (1998).

15. Galindo, K. & Smith, D. P. A large family of divergent Drosophila odorant-binding proteins expressed in gustatory and olfactory sensilla. *Genetics* **159**, 1059–1072 (2001).

16. Hansson, B. S. & Stensmyr, M. C. Evolution of insect olfaction. *Neuron* **72**, 698–711 (2011).

17. Benton, R., Vannice, K. S., Gomez-Diaz, C. & Vosshall, L. B. Variant ionotropic glutamate receptors as chemosensory receptors in Drosophila. *Cell* **136**, 149–162 (2009).

18. Silbering, A. F. *et al.* Complementary Function and Integrated Wiring of the Evolutionarily Distinct Drosophila Olfactory Subsystems. *Journal of Neuroscience* **31**, 13357–13375 (2011).

19. Robertson, H. M., Warr, C. G. & Carlson, J. R. Molecular evolution of the insect chemoreceptor gene superfamily in Drosophila melanogaster. *Proc Natl Acad Sci USA* **100 Suppl 2**, 14537–14542 (2003).

20. Dahanukar, A., Foster, K., der Goes van Naters, van, W. M. & Carlson, J. R. A Gr receptor is required for response to the sugar trehalose in taste neurons of Drosophila. *Nat Neurosci* **4**, 1182–1186 (2001).

21. Wisotsky, Z., Medina, A., Freeman, E. & Dahanukar, A. Evolutionary differences in food preference rely on Gr64e, a receptor for glycerol. *Nat Neurosci* **14**, 1534–1541 (2011).

22. Jones, W. D., Cayirlioglu, P., Kadow, I. G. & Vosshall, L. B. Two chemosensory receptors together mediate carbon dioxide detection in Drosophila. *Nature* **445**, 86–90 (2007).

23. Clyne, P. J. *et al.* A novel family of divergent seven-transmembrane proteins: candidate odorant receptors in Drosophila. *Neuron* **22**, 327–338 (1999).

24. Gao, Q. & Chess, A. Identification of candidate Drosophila olfactory receptors from genomic DNA sequence. *Genomics* **60**, 31–39 (1999).

25. Vosshall, L. B., Amrein, H., Morozov, P. S., Rzhetsky, A. & Axel, R. A spatial map of olfactory receptor expression in the Drosophila antenna. *Cell* **96**, 725–736 (1999).

26. Buck, L. & Axel, R. A novel multigene family may encode odorant receptors: a molecular basis for odor recognition. *Cell* **65**, 175–187 (1991).

27. Benton, R., Sachse, S., Michnick, S. W. & Vosshall, L. B. Atypical membrane topology and heteromeric function of Drosophila odorant receptors in vivo. *PLoS Biol* **4**, e20 (2006).

28. Lundin, C. *et al.* Membrane topology of the Drosophila OR83b odorant receptor. *FEBS Lett* **581**, 5601–5604 (2007).

29. Kaupp, U. B. Olfactory signalling in vertebrates and insects: differences and commonalities. *Nat Rev Neurosci* **11**, 188 (2010).

30. Pitts, R. J., Fox, A. N. & Zwiebel, L. J. A highly conserved candidate chemoreceptor expressed in both olfactory and gustatory tissues in the malaria vector Anopheles gambiae. *Proc Natl Acad Sci USA* **101**, 5058–5063 (2004).

31. Krieger, J., Klink, O., Mohl, C., Raming, K. & Breer, H. A candidate olfactory receptor subtype highly conserved across different insect orders. *J Comp Physiol A* **189**, 519–526 (2003).
32. Hull, J. J., Hoffmann, E. J., Perera, O. P. & Snodgrass, G. L. Identification of the western tarnished plant bug (*Lygus hesperus*) olfactory co-receptor Orco: Expression profile and confirmation of atypical membrane topology. *Arch Insect Biochem Physiol* **81**, 179–198 (2012).

33. Larsson, M. C. *et al.* Or83b encodes a broadly expressed odorant receptor essential for Drosophila olfaction. *Neuron* **43**, 703–714 (2004).

34. Jones, W. D., Nguyen, T.-A. T., Kloss, B., Lee, K. J. & Vosshall, L. B. Functional conservation of an insect odorant receptor gene across 250 million years of evolution. *Curr Biol* **15**, R119–21 (2005).

35. Carey, A. F., Wang, G., Su, C.-Y., Zwiebel, L. J. & Carlson, J. R. Odorant reception in the malaria mosquito Anopheles gambiae. *Nature* **464**, 66–71 (2010).

36. Nakagawa, T., Sakurai, T., Nishioka, T. & Touhara, K. Insect sex-pheromone signals mediated by specific combinations of olfactory receptors. *Science* **307**, 1638–1642 (2005).

37. Bohbot, J. D. *et al.* Conservation of indole responsive odorant receptors in mosquitoes reveals an ancient olfactory trait. *Chem Senses* **36**, 149–160 (2011).

38. Zhou, X. *et al.* Phylogenetic and transcriptomic analysis of chemosensory receptors in a pair of divergent ant species reveals sex-specific signatures of odor coding. *PLoS Genet* **8**, e1002930 (2012).

39. Wanner, K. W. *et al.* Female-biased expression of odourant receptor genes in the adult antennae of the silkworm, Bombyx mori. *Insect Mol Biol* **16**, 107–119 (2007).

40. Robertson, H. M., Gadau, J. & Wanner, K. W. The insect chemoreceptor superfamily of the parasitoid jewel wasp Nasonia vitripennis. *Insect Mol Biol* **19**, 121–136 (2010).

41. Engsontia, P. *et al.* The red flour beetle's large nose: An expanded odorant receptor gene family in Tribolium castaneum. *Insect Biochem Mol Biol* **38**, 387–397 (2008).

42. Hallem, E. A., Ho, M. G. & Carlson, J. R. The molecular basis of odor coding in the Drosophila antenna. *Cell* **117**, 965–979 (2004).

43. Wanner, K. W. *et al.* A honey bee odorant receptor for the queen substance 9-oxo-2-decenoic acid. *Proc Natl Acad Sci USA* **104**, 14383–14388 (2007).
44. Wang, G., Carey, A. F., Carlson, J. R. & Zwiebel, L. J. Molecular basis of odor coding in the malaria vector mosquito Anopheles gambiae. *Proceedings of the National Academy of Sciences* **107**, 4418–4423 (2010).

45. Mitchell, R. F. *et al.* Sequencing and characterizing odorant receptors of the cerambycid beetle Megacyllene caryae. *Insect Biochem Mol Biol* (2012).doi:10.1016/j.ibmb.2012.03.007

46. Michael Rutzler, T. L. & Zwiebel, L. J. G[alpha] encoding gene family of the malaria vector mosquito Anopheles gambiae: Expression analysis and immunolocalization of AG[alpha]q and AG[alpha]o in female antennae. *J Comp Neurol* (2006).

47. Walker, W. B., Smith, E. M., Jan, T. & Zwiebel, L. J. A functional role for Anopheles gambiae Arrestin1 in olfactory signal transduction. *J Insect Physiol* **54**, 680–690 (2008).

48. Sakurai, T. *et al.* Identification and functional characterization of a sex pheromone receptor in the silkmoth Bombyx mori. *Proc Natl Acad Sci USA* **101**, 16653–16658 (2004).

49. Sato, K. *et al.* Insect olfactory receptors are heteromeric ligand-gated ion channels. *Nature* **452**, 1002–1006 (2008).

50. Wicher, D. *et al.* Drosophila odorant receptors are both ligand-gated and cyclic-nucleotide-activated cation channels. *Nature* **452**, 1007–1011 (2008).

51. Nakagawa, T. & Vosshall Controversy and consensus: noncanonical signaling mechanisms in the insect olfactory system. *Curr Opin Neurobiol* **19**, 284–292 (2009).

CHAPTER II

FUNCTIONAL AGONISM OF INSECT ODORANT RECEPTORS

Patrick L. Jones*, Gregory M. Pask*, David C. Rinker, and Laurence J. Zwiebel

**denotes equal contributions to this work*

Preface

The work in this chapter has been published in *PNAS* (2011 vol. 108 (21) pp. 8821-8825) and I was a co-first author of this work. My experimental contributions ranged from experimental design, molecular cloning of several OR constructs, generation of the AgOrco cell line, and all patch clamp electrophysiology experiments. In addition, I significantly contributed to figure design and manuscript writing. This work was supported by a grant from the Foundation for the National Institutes of Health to L.J.Z through the Grand Challenges in Global Health Initiative.

Introduction

A single insect OR complex has the ability to bind a variety of structurally different odorants and then relay the signal to the olfactory receptor neurons (ORNs) at the periphery[1,2]. It is even possible that several odorant binding sites may exist on a single receptor in order to detect such chemical diversity. In this light, it is conceivable that a small molecule may be able to interact at an odorant-binding region and modulate insect OR function. Using the high-throughput techniques common used in the drug discovery field, a large library of

small molecules can be screened against an insect OR complex in a cell-based Ca^{++}-mobilization assay to identify new agonists, potentiators, or antagonists[3,4]. In our high-throughput screen, we expressed ORs from the principal afro-tropical malaria vector, *Anopheles* gambiae, as any active modulators may prove useful in reducing the efficiency of host-seeking and potentially disease transmission.

Results

We carried out high-throughput, calcium-imaging screens for novel modulators of the AgOrco + AgOr10 complex expressed in human embryonic kidney (HEK293) cell lines. AgOr10 was chosen in particular on the basis of its molecular and functional conservation across multiple mosquito species[5,6].

Unlike the many novel agonists identified in our small molecule screens against AgOrco + AgOr10 expressing cells, only one of the 118,720 compounds tested (denoted here as VUAA1; Figure 2.1A) elicited activity consistent with allosteric agonism. Classification as an allosteric agonist was based on VUAA1's intrinsic efficacy and capacity to potentiate the complex's response to a natural ligand. The chemical identity of VUAA1 was verified using high-resolution mass spectrometry (HRMS) as well as ^{1}H and ^{13}C NMR [see methods]. VUAA1 was re-validated against AgOrco + AgOr10 cells and elicited concentration-dependent responses that were not seen in control cells (Figure 2.1B). In addition, VUAA1 activated several other AgOrco + AgOrX cell lines in the context of other, ongoing HTS screens. We pursued VUAA1 on the basis of its novelty,

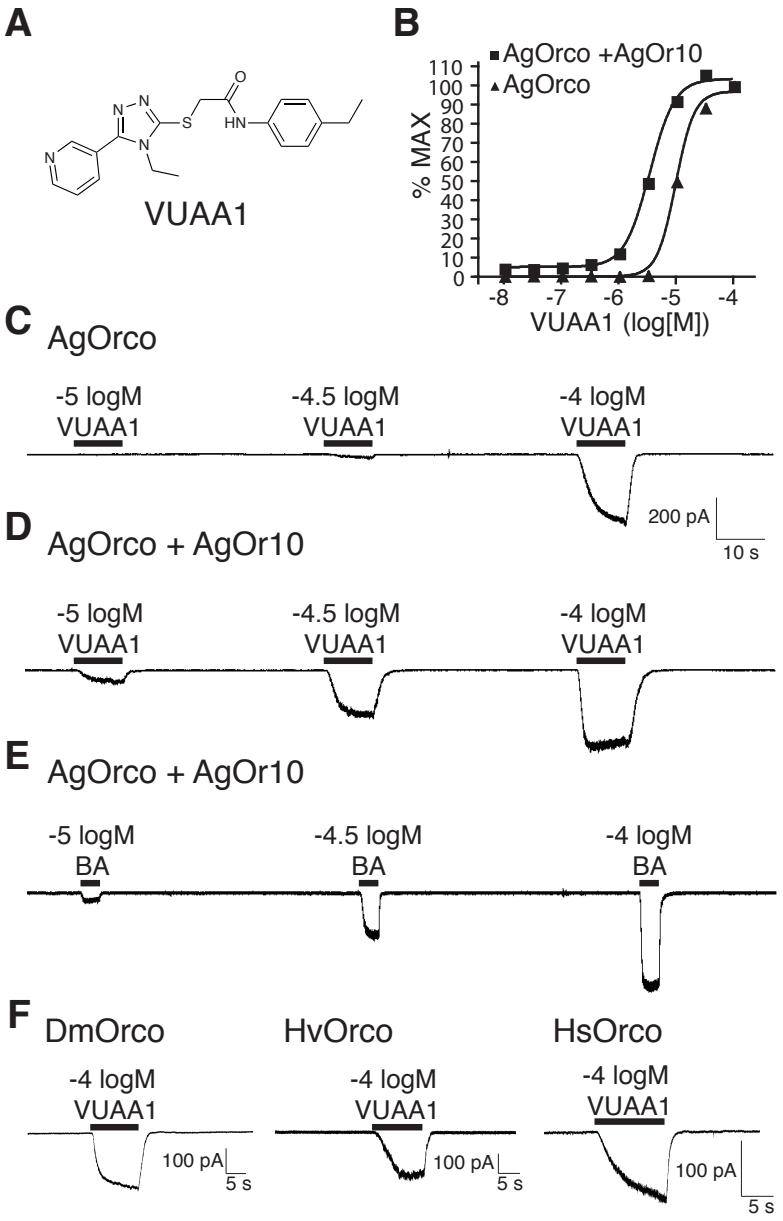

FIGURE 2.1 VUAA1 evokes macroscopic currents in HEK293 cells expressing AgOrco and its orthologs. (**A**) Structure of VUAA1**.** (**B**) Concentration–response curves (CRCs) generated from Fluo-4 acetoxymethyl ester-based Ca^{2+} imaging with AgOrco and AgOrco + AgOr10 cell lines in response to VUAA1. (**C-D**), Whole-cell patch clamp recordings of concentration-dependent responses to VUAA1 in cells stably expressing AgOrco alone (**C**) and AgOrco + AgOr10 (**D**). (**E**) Benzaldehyde (BA), an AgOr10 agonist, elicits concentration-dependent responses in AgOrco + AgOr10 cells. (**F**) Whole-cell current responses to VUAA1 in HEK293 cells expressing DmOrco, HvOrco, and HsOrco. Holding potentials of −60 mV were used in (**C-F**)**.**

as a probe for AgOR pharmacology, and in light of its potential role as a modulator of olfactory driven behaviors in *An. gambiae*.

As AgOrco was the common element among the functional responses of numerous AgOrco + AgOrx cell lines, we postulated that VUAA1 was a potential AgOrco agonist. To test this hypothesis, whole-cell patch clamp responses were examined in AgOrco + AgOr10-expressing cells and HEK293 cells stably expressing AgOrco alone. In these experiments, VUAA1 elicited concentration-dependent inward currents in both AgOrco- and AgOrco + AgOr10-expressing cells (Figure 2.1C-D) demonstrating both that VUAA1 is an AgOrco agonist and that currents were AgOrco-dependent. The VUAA1-induced currents in AgOrco + AgOr10 cells resembled those resulting from application of benzaldehyde, an AgOr10 agonist (Figure 2.1E). AgOrco + AgOr10 cells were more sensitive to VUAA1 than AgOrco cells, producing inward currents at −5.0 logM, a concentration at which AgOrco had no response. All currents induced by VUAA1 were AgOrco dependent; no responses were observed in control cells (Figure S2.1).

To further investigate the specificity of VUAA1 agonism, and to determine if it was capable of activating related orthologs, we tested Orco orthologs across Dipteran, Lepidopteran, and Hymenopteran taxa. When we transiently transfected HEK cells with the Orco orthologs of *Drosophila melanogaster* (DmOrco), *Heliothis virescens* (HvOrco), and *Harpegnathos saltator* (HsOrco), VUAA1 elicited robust inward currents similar to AgOrco-expressing cells (Figure 2.1F). These results demonstrate that VUAA1 is a broad-spectrum Orco family

agonist capable of activating OR coreceptors within and across multiple insect orders. This is consistent with the high sequence identity that is characteristic of Orco family members (76% to DmOrco, 67% to HvOrco, and 62% to HsOrco) as well as their previously demonstrated functional overlap[7,8].

It has been previously demonstrated that insect OR complexes function ionotropically, so we set out to characterize the conductive properties of the anopheline complex in response to VUAA1[9,10]. Using whole-cell patch clamp experiments, we determined the current–voltage relationships of AgOrco on its own and in complex with AgOr10. Currents induced by VUAA1 in AgOrco-expressing cells as well as those induced by VUAA1 or benzaldehyde in AgOrco + AgOr10 cells were all nearly symmetrical (Figure S2.2A-C). The reversal potential of AgOrco alone in the presence of VUAA1 was −4.74 ± 3.17 mV, while AgOrco + AgOr10 reversal potentials were +0.18 ± 0.02 mV with VUAA1 and −0.81 ± 2.12 mV with benzaldehyde (mean ± SEM, Figure S2.2D). These current–voltage relationships do not indicate any voltage-dependent gating, and the near-zero reversal potentials are consistent with previous reports that described non-selective cation conductance[9,10]. We next examined whether VUAA1-induced responses could be attenuated by ruthenium red (RR), a general cation channel blocker previously found to inhibit insect OR currents[9]. Application of RR reduced the VUAA1-elicited currents of AgOrco cells by 79.4 ± 4.0%, while RR reduced VUAA1 and benzaldehyde responses of AgOrco + AgOr10 cells by 68.3 ± 2.8% and 87.8 ± 1.8%, respectively (Figure 2.2). Taken

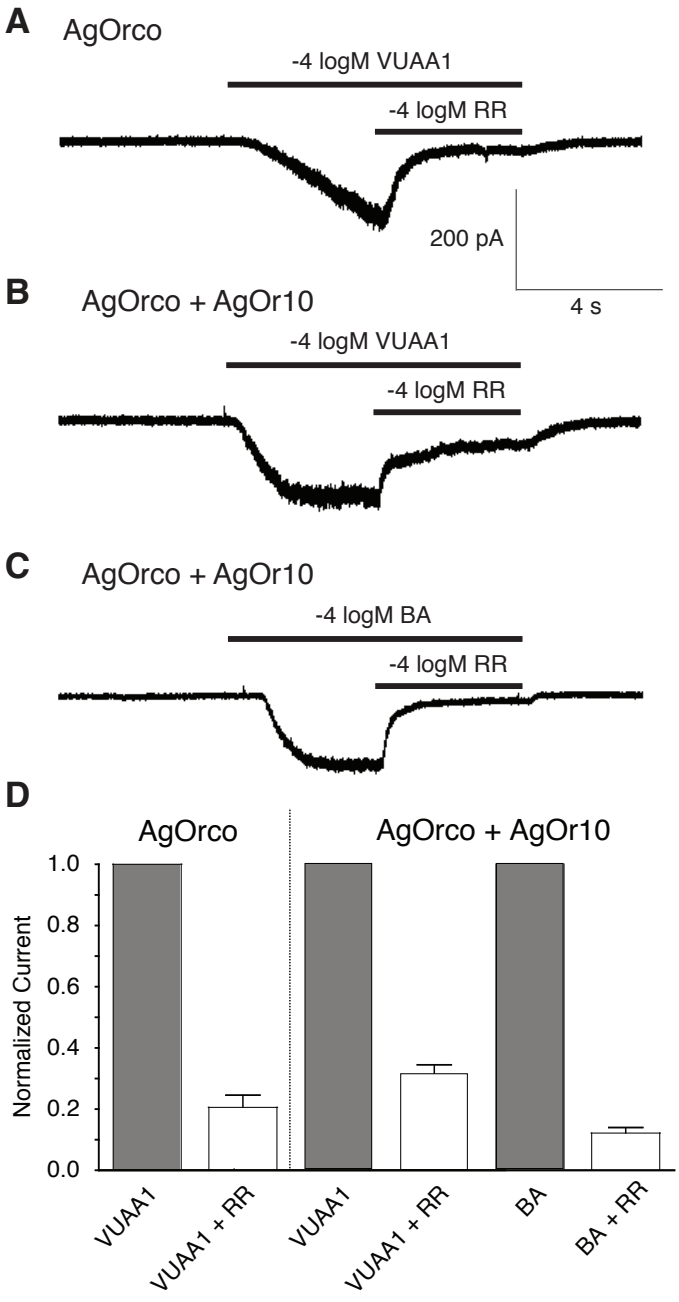

FIGURE 2.2 Ruthenium red blocks inward currents of AgOrco alone and in complex (**A-C**) Representative traces of ruthenium-red-blocked inward currents in AgOrco (**A**) and AgOrco + AgOr10 (**B-C**) cells. Holding potential was −60 mV for (**A-C**). (**D**) Analysis of Ruthenium Red blockage of VUAA1 and BA-induced currents from **A** (n=5), **B** (n=5), **C** (n=4).

together, these data indicate that AgOrco exhibits channel-like properties consistent with a non-selective cation channel.

In the next set of studies, outside-out membrane patches were excised from AgOrco-expressing cells to examine single-channel currents evoked by VUAA1 (Figure 2.3A). Here, spontaneous channel opening was observed before VUAA1 stimulation, but with very low probability (P_o= 0.02) (Figure 2.3B). During a 5-s application of VUAA1, channel opening probability increased to P_o= 0.38 (Figure 2.3C). Subsequent to agonist washout, channel opening probability decreased to 0.00 (Figure 2.3D). The average unitary current of AgOrco was 1.3 ± 0.3 pA (mean ± st. dev) (Figure 2.3C inset), which is comparable to previous single-channel studies of insect ORs[9]. Taken together, these data support the hypothesis that VUAA1 agonizes AgOrco in the absence of other intracellular components and provide additional support for the ionotropic nature of this channel as well as the role of VUAA1 as a direct agonist of AgOrco and other Orco family members.

We then investigated whether activation of AgOrco involves second-messenger-based signaling, which has been reported to contribute to insect olfactory signaling[10]. In these studies, which are consistent with a previously published report, two cyclic nucleotide analogs (8-Br-cAMP and 8-Br-cGMP) were unable to evoke whole-cell currents in AgOrco or AgOrco + AgOr10 cells (Figure 2.4A-B)[9]. Importantly, *Rattus norvegicus* cyclic-nucleotide gated channel A2 (rCNGA2) demonstrated robust responses to 8-Br cGMP (Figure 2.4C)[11].

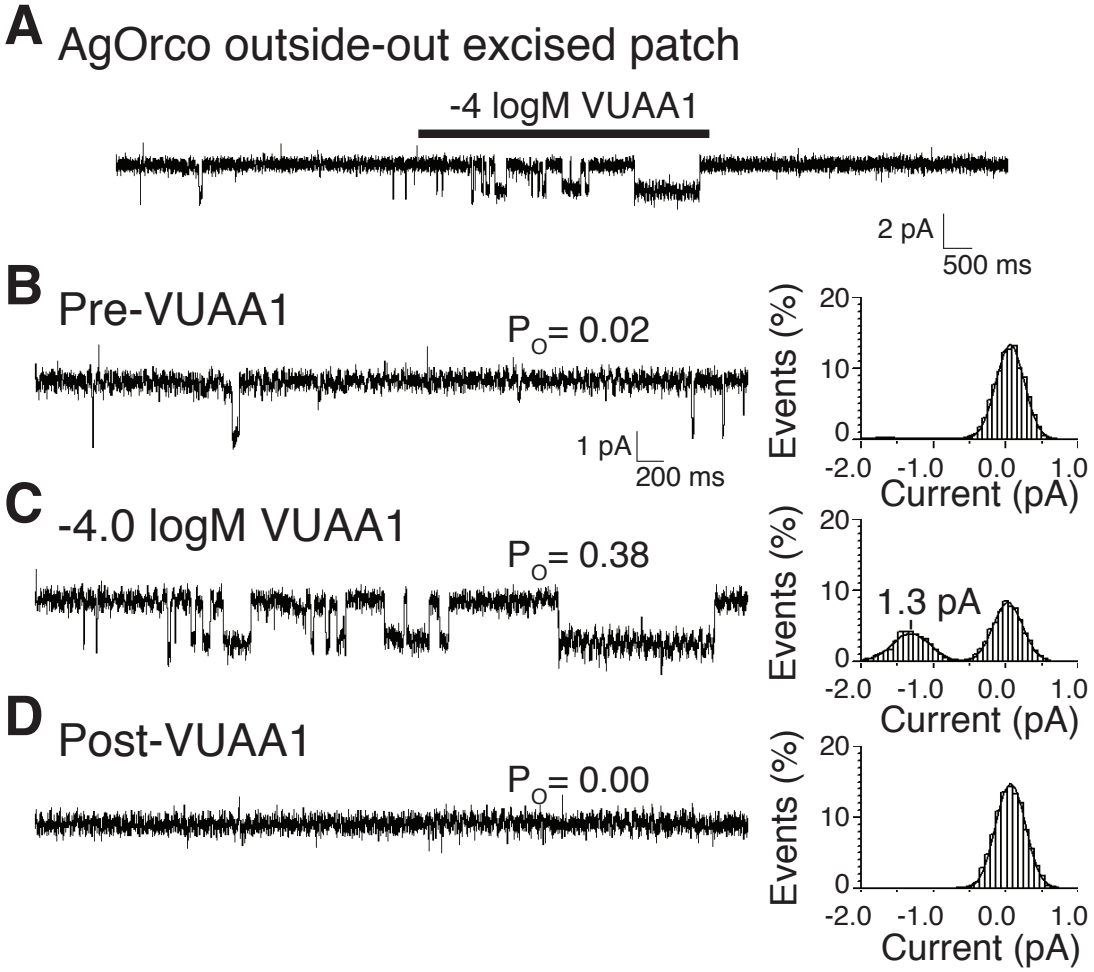

FIGURE 2.3 AgOrco is a functional channel and responds to VUAA1 in outside-out membrane patches. (**A**) Single-channel recording from an outside-out excised patch pulled from a cell-expressing AgOrco. (**B-D**) Expansions of trace **A** before (**B**), during (**C**), and after (**D**) a 5-s application of −4.0 logM VUAA1. All-point current histograms of trace expansions are in the right panel of **B-D**. Excised membrane patch was held at −60 mV.

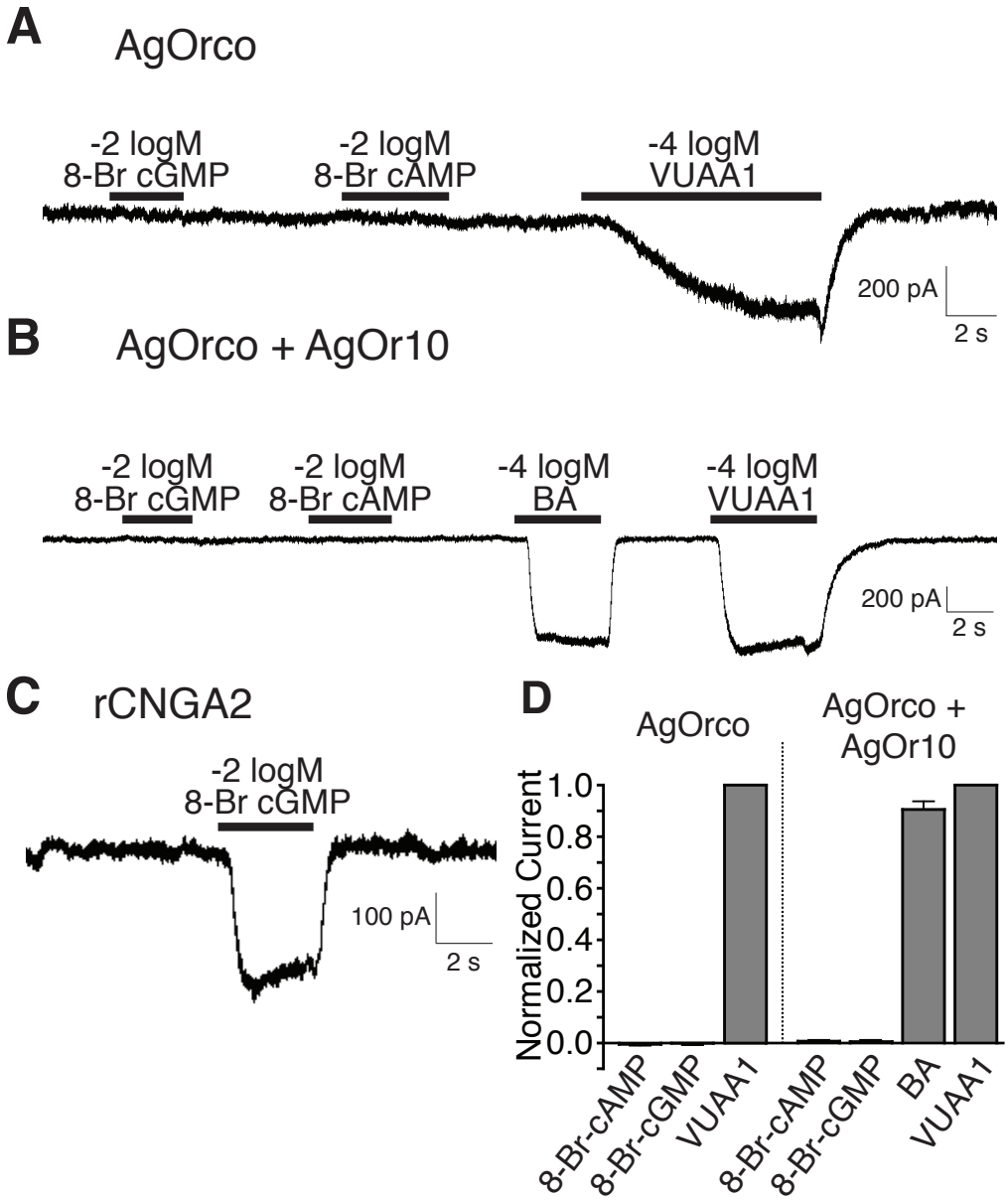

FIGURE 2.4 Cyclic nucleotides did not elicit currents in AgOrco or AgOrco + AgOr10 cells. (**A**) Representative trace from whole-cell recordings from cells expressing AgOrco-expressing cells with application of 8-Br-cAMP, 8-Br-cGMP, and VUAA1. (**B**) Representative trace from cells expressing AgOrco + AgOr10 with application of 8-Br-cAMP, 8-Br-cGMP, BA, and VUAA1. (**C**) Representative trace from cells expressing rCNGA2 with application of 8-Br-cGMP. Holding potentials for all recordings were −60mV. (**D**) Histogram of normalized currents from cyclic nucleotide and control responses (n=4). All currents normalized to VUAA1 responses.

These data support a hypothesis in which an ionotropic mechanism is the principal, if not sole, signaling mechanism of functional AgOR complexes.

In addition to demonstrating that AgOrco alone and AgOrco + AgOr10 complexes act as functional, ligand-gated ion channels, these studies have shown that VUAA1 elicits AgOR currents similar to those evoked by odorants. As an additional indicator of the specificity of VUAA1 for non-conventional Orco's, we tested VUAA1 on another non-selective cation channel, the rat transient receptor potential vanilloid receptor 1 (rTRPV1)[12,13]. In these controls, VUAA1 failed to evoke any response, while capsaicin elicited robust responses in TRPV1-expressing cells, thereby demonstrating that VUAA1 does not act as a general cation channel agonist (Figure S2.2F).

We next performed single unit, extracellular electrophysiological recordings on the maxillary palp of adult female *An. gambiae* to determine whether VUAA1 could activate AgOrco-expressing olfactory receptor neurons (ORNs) *in vivo.* We have previously demonstrated that the maxillary palp, an elongate olfactory appendage emanating from the head, contains only a single sensilla type, the capitate peg (Cp), and that all capitate pegs contain 3 chemosensory neurons[14]. The highly stereotypic Cp sensilla, contain two AgOrco/conventional OR-expressing ORNs (CpB and CpC), as well as a CO_2 sensitive neuron (CpA), which does not express AgOrco. Single sensillum recordings (SSRs) involve puncturing the sensillum wall with a glass electrode, which enables the passive sampling of all sensillum neurons simultaneously. The activities of individual neurons are discriminated from each other based on

compound response profiles and action potential amplitudes. In these preparations, CpA spike activity is clearly distinguished from those of CpB/C by its large action potential amplitude. CpB/C spikes were much smaller and in some preparations indistinguishable from each other. Consequently, the spike activities of CpB/C neurons were binned for data analysis. Accordingly, we reasoned that if VUAA1 acts as a specific AgOrco agonist, we would expect it to selectively increase the spike frequency of the CpB/C neurons, but have no effect on CpA responses.

Because of its relatively high molecular weight, and despite multiple attempts, volatile delivery of VUAA1 was not feasible. As a result, VUAA1 was directly introduced to each sensillum via the glass-recording electrode, rather than through the more conventional method of volatile delivery. When VUAA1 was added to the electrode solution it increased the spike frequency of CpB/C neurons in a dose-dependent manner, while vehicle alone had no effect (Figure 2.5A-B,D). Differential CpB/C spike activity was observed immediately after puncturing each sensillum, suggesting millisecond compound diffusion rates into the sensillum (Figure 2.5A-B,D). At the completion of each assay, a CO_2 pulse was delivered to the sensillum to test whether VUAA1 affected the CpA neuron; in contrast to the responsiveness of the AgOrco-expressing CpB/C neurons, CpA activity was unchanged in the presence of vehicle and/or VUAA1 (Figure 2.5C). The ability of VUAA1 to activate AgOrco-expressing ORNs *in vivo* further demonstrates that AgOrco is an accessible biological target in *An. gambiae*.,

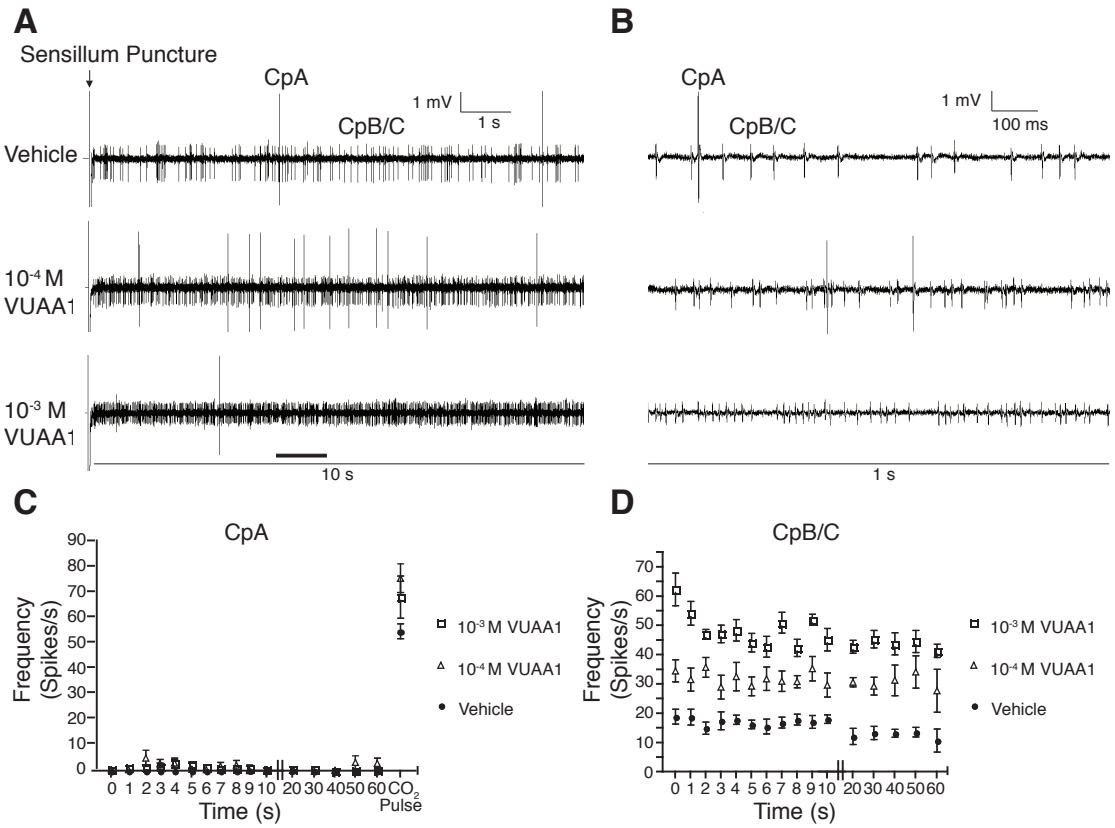

FIGURE 2.5 VUAA1 activates AgOrco-expressing neurons in *Anopheles gambiae* females. (**A**) Representative traces of SSR recordings from capitate peg sensilla upon electrode puncture. VUAA1 or vehicle alone (DMSO) was delivered through the glass- recording electrode. CpA is discernible from the smaller CpB/C action potentials. (**B**) Expansions of traces in *A*. (**C**) Activity of CpA neuron in response to VUAA1. Spike frequency was calculated every second for the first 10 s after sensillum puncture and every 10 s thereafter. After 60 s, the preparation was pulsed for 2 s with atmospheric air to confirm a functional CpA neuron (n=6). (**D**) Activity of CpB/CpC neurons in response to VUAA1, as in **C**.

Discussion

Here we report the identification and characterization of VUAA1, the first Orco family agonist that is capable of gating orthologs across multiple insect taxa. In contrast to previous models, these data support a hypothesis whereby AgOrco and related Orco orthologs act as ion channels, which can function independently of their heteromeric partners and are indifferent to cyclic nucleotide modulation[9,10,15]. Other than the unique activity of VUAA1 there are currently no known natural ligands for Orco family members. Therefore, we suggest that AgOrco and other Orco family members should be recognized as independently-gated ion channels or channel subunits rather than odorant receptors.

As Orco functionality is required for OR-mediated chemoreception across all insects, an Orco agonist would theoretically be capable of activating all OR-expressing ORNs. Accordingly, Orco agonism would be expected to severely impact the discrimination of odors across all insect taxa, affecting a broad range of chemosensory driven behaviors. In *An. gambiae* females universal ORN activation would likely disrupt a variety of olfactory-driven behaviors, most notably human host-seeking, which serves as the foundation for their ability to transmit malaria[16]. The discovery of a universal Orco agonist is also an important step towards the development of a new generation of broad-spectrum agents for integrated management of nuisance insects and agricultural pests.

The *in vivo* VUAA1-mediated activation of AgOrco-expressing cells serves as a proof-of-principle that targeting AgOrco and other Orco orthologs is a viable approach for the development of behaviorally disruptive olfactory compounds

(BDOCs) to control a wide range of insect pests and vectors. While it is premature to speculate as to the ultimate utility of VUAA1 as an anti-malarial BDOC or as a general modulator of insect chemosensory-driven behaviors, VUAA1 nevertheless represents an important tool for the direct study of AgOrco and other Orco orthologs in insect chemosensory signal transduction.

Materials and Methods

Cell Culture and Ca^{2+} imaging

Transient transfections of pCI (Promega)-containing OR constructs were performed with FuGENE 6 (Roche) into FLP-IN T-REX 293 (Invitrogen) cell lines. TRPV1 cells were a gift from Dr. D. Julius[12]. Construction of the AgOrco + AgOr10 cell line has been previously described[5]. Fluo-4AM-dye-loaded cells were assayed for ligand response in an FDSS6000 (Hammamatsu) as previously described[5].

Chemicals

Benzaldehyde (CAS 100-52-7) and Capsaicin (CAS 404-86-4) were purchased from Sigma-Aldrich. 8-Br-cAMP and 8-Br-cGMP were obtained from Enzo Life Sciences. VUAA1 (N-(4-Ethylphenyl)-2-((4-Et-5-(3-Pyridinyl)-4H-1,2,4-Triazol-3-yl)Thio)acetamide) was purchased from Sigma-Aldrich's Rare Chemical Library (CAS # 525582-84-7). To ensure that observed activity was elicited from VUAA1, and not from a contaminant present in the mixture, we performed preparative High Performance Liquid Chromatography (HPLC). Briefly, 20mg VUAA1 was dissolved in a 50/50 mixture of methanol and DMSO, and HPLC was

performed on a Phenomenex Luna 30x50-mm C18 prep column with 0.1% Trifluoracetic acid (TFA) in H_20 coupled to an acetonitrile gradient. Appropriate fractions were pooled and passed over a TFA scavenger column (Polymer labs, StratoSpheres SPE PL-HCO3 MP-resin). The solvent was removed by rotary evaporation with a Biotage V10 Roto-vap, yielding white powder. VUAA1 was subsequently re-dissolved in DMSO and assayed as described.

Characterization of chemical materials

^{1}H-NMR (400 MHz, DMSO-$_{d6}$) d 8.73 (d, *J* = 1.8 Hz, 1H), 8.65 (dd, *J* = 1.5, 4.8 Hz, 1H), 7.97 (dt, *J*= 1.9, 8.0 Hz, 1H), 7.49 (dd, *J* = 2.5, 8.3 Hz, 1H), 7.37 (d, *J* = 8.4 Hz, 2H), 7.04 (d, *J* = 8.4 HZ, 2H), 4.10 (s, 1H), 3.95 (q, *J* = 7.2 Hz, 2H), 2.43 (q, *J* = 7.6 Hz, 2H), 1.13 (t, *J* = 8.0 Hz, 3H), 1.04 (t, *J* = 8.0 Hz, 3H).^{13}C-NMR(400 MHz, DMSO-$_{d6}$) d 165.71, 152.92, 151.32, 150.95, 149.07, 139.35, 136.87, 136.33, 128.38, 124.34, 123.90, 119.58, 37.91, 27.97, 16.05, 15.42. HRMS (m/z) $[M]^+$ calculated for $C_{19}H_{22}N_5OS$, 368.1544 found 368.1545.

Patch-clamp recording in HEK cells

Currents from OR-expressing HEK293 cells were amplified using an Axopatch 200b Amplifier (Axon Instruments) and digitized through a Digidata 1322A (Axon Instruments). Electrophysiological data was recorded and analyzed using pCLAMP 10 (Axon Instruments). Electrodes were fabricated from quartz tubing (Sutter Instruments) and pulled to 4–6 MΩ for whole-cell recording. Electrodes were filled with internal solution [120mM KCl, 30mM D-glucose, 10mM HEPES, 2mM $MgCl_2$, 1.1mM EGTA, and 0.1 $CaCl_2$ (pH 7.35, 280mOsm)]. External (bath) solution contained 130mM NaCl, 34mM D-glucose, 10mM

HEPES, 1.5mM $CaCl_2$, 1.3mM KH_2PO_4, and 0.5 $MgSO_4$ (pH 7.35, 300mOsm). Compounds were diluted in external solution and locally perfused to the recording cell using Perfusion Pencil (Automate Scientific) and controlled by a ValveLink 8.2 controller (Automate Scientific). Whole-cell recordings were sampled at 10kHz and filtered at 5kHz. Outside-out patches were obtained using 10- to 15-MΩ electrodes pulled from standard glass capillaries (World Precision Instruments) and fire-polished with an MF-830 micro forge (Narishige). Single-channel recordings were sampled at 20kHz. Recordings were reduced to 1kHz and low-pass filtered at 500Hz for display and analysis using QuB (SUNY at Buffalo).

Cloning of HsOrco

The full-length coding sequence of *HsOrco* was PCR amplified from *Harpegnathos saltator* antennal cDNA using the primers 5'-ATGATGAAGATGAAGCAGCAGGGCCT-3' and 5'-TTTCATGGTGCTGGTACAACTGAAGTGA-3'. The subsequent PCR fragment was then cloned into pENTR/D-TOPO (Invitrogen) and then subcloned into the pCI mammalian expression vector.

Single sensillum recordings:

Single sensillum recordings were performed on 4- to 7-day-old, non-blood-fed *Anopheles gambiae* females maintained on 10% sucrose and a 12h/12h light/dark cycle. Legs, wings and antennae were removed from cold-anesthetized females that were then restrained on double-stick tape with thread. A glass reference electrode filled with sensillar lymph Ringers (SLR) was placed in the

eye, and the recording electrode filled with DMSO or VUAA1 diluted in SLR was used to puncture sensilla at their base[17]. Preparations were kept under a steady stream of humidified, synthetic air (21% O_2/ 79% N_2) to limit the basal activity of CpA. Sensilla that did not respond to CO_2 or 1-octen-3-ol were excluded from analysis. Responses were recorded and digitized using a Syntech IDAC-4 and analyzed with AutoSpike software (Syntech). A new glass recording pipette was used for every recording. Data was sampled at 12kHz.

References

1. Hallem, E. A. & Carlson, J. R. Coding of odors by a receptor repertoire. *Cell* **125**, 143–160 (2006).

2. Carey, A. F., Wang, G., Su, C.-Y., Zwiebel, L. J. & Carlson, J. R. Odorant reception in the malaria mosquito Anopheles gambiae. *Nature* **464**, 66–71 (2010).

3. Lindsley, C. W., Weaver, D., Jones, C., Marnett, L. & Conn, P. J. Preclinical drug discovery research and training at Vanderbilt. *ACS Chem. Biol.* **2**, 17–20 (2007).

4. Rinker, D. C. *et al.* Novel high-throughput screens of Anopheles gambiae odorant receptors reveal candidate behaviour-modifying chemicals for mosquitoes. *Physiol Entomol* **37**, 33–41 (2012).

5. Bohbot, J. D. *et al.* Conservation of indole responsive odorant receptors in mosquitoes reveals an ancient olfactory trait. *Chem Senses* **36**, 149–160 (2011).

6. Pelletier, J., Hughes, D. T., Luetje, C. W. & Leal, W. S. An odorant receptor from the southern house mosquito Culex pipiens quinquefasciatus sensitive to oviposition attractants. *PLoS ONE* **5**, e10090 (2010).

7. Jones, W. D., Nguyen, T.-A. T., Kloss, B., Lee, K. J. & Vosshall, L. B. Functional conservation of an insect odorant receptor gene across 250 million years of evolution. *Curr Biol* **15**, R119–21 (2005).

8. Nakagawa, T., Sakurai, T., Nishioka, T. & Touhara, K. Insect sex-pheromone signals mediated by specific combinations of olfactory receptors. *Science* **307**, 1638–1642 (2005).

9. Sato, K. *et al.* Insect olfactory receptors are heteromeric ligand-gated ion channels. *Nature* **452**, 1002–1006 (2008).

10. Wicher, D. *et al.* Drosophila odorant receptors are both ligand-gated and cyclic-nucleotide-activated cation channels. *Nature* **452**, 1007–1011 (2008).

11. Dhallan, R. S., Yau, K. W., Schrader, K. A. & Reed, R. R. Primary structure and functional expression of a cyclic nucleotide-activated channel from olfactory neurons. *Nature* **347**, 184–187 (1990).

12. Bohlen, C. J. *et al.* A Bivalent Tarantula Toxin Activates the Capsaicin Receptor, TRPV1, by Targeting the Outer Pore Domain. *Cell* **141**, 834–845 (2010).

13. Caterina, M. J. *et al.* The capsaicin receptor: a heat-activated ion channel in the pain pathway. *Nature* **389**, 816–824 (1997).

14. Lu, T. *et al.* Odor coding in the maxillary palp of the malaria vector mosquito Anopheles gambiae. *Curr Biol* **17**, 1533–1544 (2007).

15. Smart, R. *et al.* Drosophila odorant receptors are novel seven transmembrane domain proteins that can signal independently of heterotrimeric G proteins. *Insect Biochem Mol Biol* **38**, 770–780 (2008).

16. Zwiebel, L. & Takken Olfactory regulation of mosquito-host interactions. *Insect Biochem Mol Biol* **34**, 645–652 (2004).

17. Xu, P., Atkinson, R., Jones, D. N. M. & Smith, D. P. Drosophila OBP LUSH is required for activity of pheromone-sensitive neurons. *Neuron* **45**, 193–200 (2005).

Supporting Information

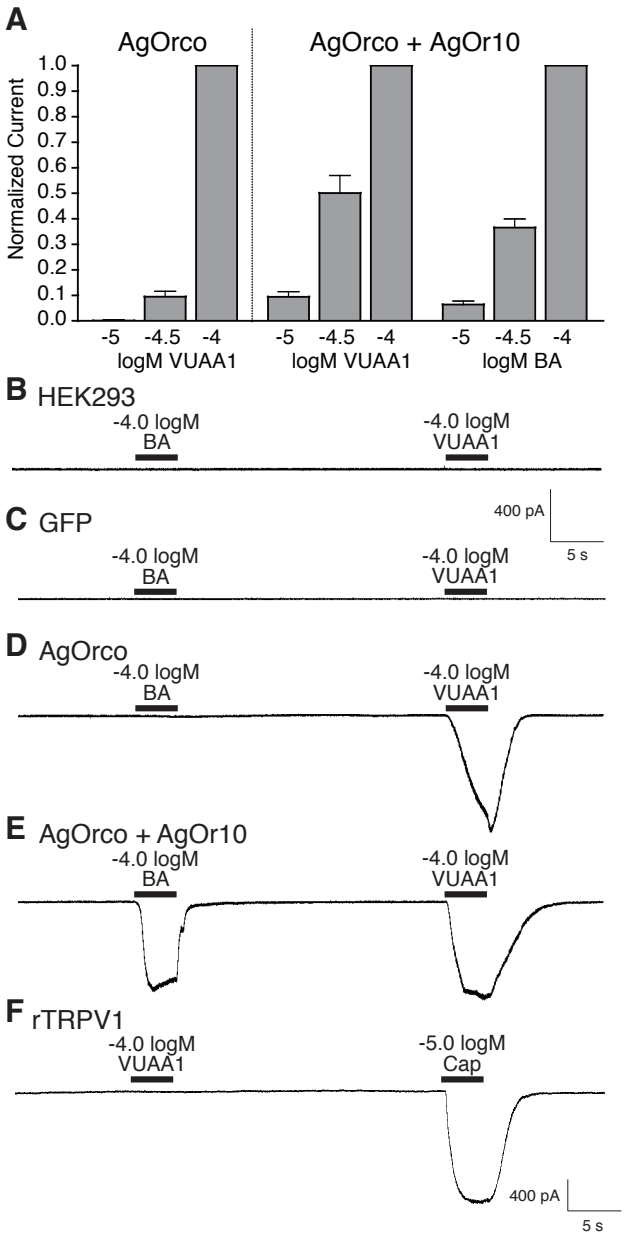

Figure S2.1 VUAA1 and BA responses are AgOr specific. (**A**) Histogram of normalized currents from concentration-dependent responses in Figure 1*C-E* (n=5). (**B**) Un-transfected HEK293 cells did not respond to either VUAA1 or BA (n=5). (**C**) GFP was co-transfected with Orco orthologs to identify cells expressing the OR. GFP-alone cells had no currents from VUAA1 or BA (n=4). (**D-E**) For comparison, both AgOrco and AgOrco+AgOr10 cells depolarized during VUAA1 application, while only AgOrco+AgOr10 cells responded to BA. Holding potentials for all recordings were −60mV. (**F**) VUAA1 did not elicit currents in cells stably expressing another cation channel, rat transient receptor potential vanilloid 1 (rTRPV1), but did respond to the agonist capsaicin (n=4).

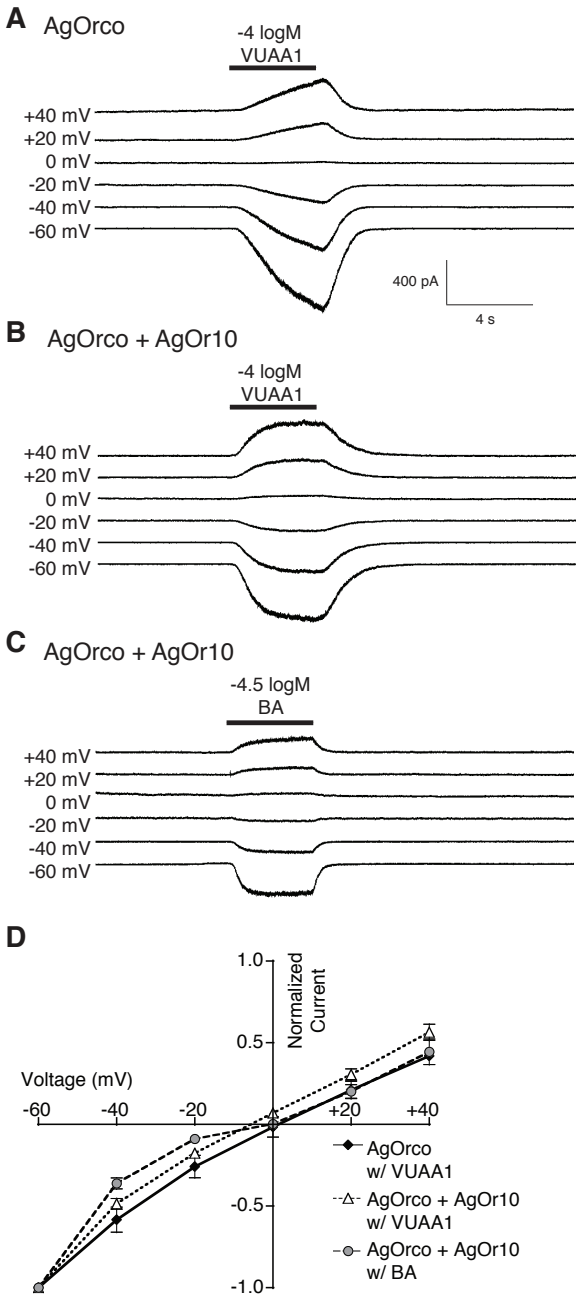

Figure S2.2 Channel-like currents elicited by application of VUAA1 to cells expressing AgOrco alone or in complex. (**A-C),** Representative traces of voltage-dependent currents in AgOrco (**A**) and AgOrco+AgOr10 (**B-C**) cells. Holding potentials ranged from −60 mV to +40 mV in 20-mV increments. (**D**) Current–voltage relationships of **A** (n=3), **B** (n=7), and **C** (n=4) from normalized peak currents.

CHAPTER III

HETEROMERIC ANOPHELINE ODORANT RECEPTORS EXHIBIT DISTINCT CHANNEL PROPERTIES

Gregory M. Pask, Patrick L. Jones, Michael Rützler, David C. Rinker, and Laurence J. Zwiebel

Preface

The following work has been published in *PLoS ONE* (2011 vol. 6(12) p. e28774). I designed and performed all of the experiments with contributions of reagents and analysis tools from PLJ, MR, and DCR. I wrote the manuscript with comments/edits from other co-authors. This work was supported by grants from the Foundation for the National Institutes of Health (NIH) through the Grand Challenges in Global Health Initiative and the NIH (AI056402) to LJZ.

Introduction

It has been previously been demonstrated that Orco can form functional homomeric channels when solely expressed in HEK cells[1,2]. Additionally, a putative pore region in Orco has been identified due to its similarity to a K^+ channel selectivity filter[2]. However, when Orco is in complex with a conventional OR, the makeup of the ion channel pore remains unclear. Regarding Orco's contribution to the channel pore, only slight differences in cation permeability and channel blockade have been observed when varying Orco subunits have been paired with a conventional OR, most likely due to the high conservation across insect taxa[3,4]. Conversely, the expression of different odorant-binding ORs in the

Drosophila empty neuron system imparts unique spontaneous ORN spike frequencies, suggesting that heteromeric OR complexes possess distinct conductive properties[5]. Within this context it is possible that Orco alone could form the ion channel pore, with the conventional OR providing distinct odorant recognition and channel gating domains. Conversely, both the Orco and conventional OR could form a single heteromultimeric complex that forms the channel pore and functions in odorant recognition/gating, comparable to the different subunits that comprise the pore of other, more characterized ligand-gated ion channels[6-8]. Additionally, certain subunits of cyclic-nucleotide gated (CNG) and transient receptor potential (TRP) channels can form functional homomeric channels, often with properties distinct from the heteromeric conformation[6,7].

Olfactory signaling plays a critical role in mediating the vectorial capacity in the principal afrotropical malaria vector mosquito *Anopheles gambiae*[9]. By examining the potential for OR-specific properties of AgOr channel pores, these studies aim to develop a better understanding of the diverse molecular architecture of heteromeric OR complexes. Along with the ongoing efforts to characterize odorant sensitivity and tuning profiles in *An. gambiae* and other insects, these studies provide an enhanced understanding of the contribution of conventional ORs to channel function[5,10,11]. In light of our results, we propose a molecular model of insect OR function, where the odorant-binding OR also influences the conductive properties, and consequently the downstream odor coding capacity of odorant-evoked ORN signaling.

Results

To determine the potential role of conventional OR subunits in forming the channel pore, we examined cation permeability and susceptibility to channel block across four conventional ORs from *An. gambiae,* each paired with AgOrco. The primary sequences and odorant sensitivities across these odorant-binding AgOrs are divergent, leading one to expect differences in conductive properties if the conventional AgOr contributes to the channel pore. In order to compare currents across different AgOr pairs that respond to different odorants, the recently identified Orco agonist, VUAA1, served as the control for potential agonist-related differences[1]. It is possible that AgOrco homomers may also exist in our cell lines expressing both AgOrco and another AgOr, which could potential affect interpretation of the VUAA1-based experiments. To address these concerns, each stable cell line uses the same insertion site and the identical dual promoter system. Importantly, AgOr complex properties were also assayed using odorants identified as strong agonists to assure that currents are not primarily due to homomeric AgOrco channels, which are non-responsive to the odorants used in this study (Figure S3.1).

The representative set of conventional AgOrs assayed in this study spans AgOrs 8, 10, 28, and 65, which are diverse in primary sequence (<20% identity), odorant-specificity, and expression[10-12]. In adult mosquitoes, AgOrs 8 and 28 are the only ORs expressed in the maxillary palp, while AgOrs 10 and 28 are both in the reduced set of ORs expressed during the larval stage[13,14]. Furthermore, AgOr10 is one of the few ORs highly conserved across Anophelinae and

Culicinae mosquitoes[15,16]. From an odor-coding perspective, AgOr65 is narrowly tuned to eugenol, while AgOrs 10 and 28 respond to a wider variety of odorants[10,11,13].

The relative permeability of monovalent cations across different AgOr combinations functionally expressed in HEK cells was determined through whole-cell patch clamp electrophysiology. In these studies, agonist-induced currents were subjected to a voltage ramp to determine the reversal potential, where net current through the channel is zero, in the presence of a single monovalent cation. As seen in Figure 3.1A, the more permeable cations have rightward shifts in reversal potential. When the Orco agonist VUAA1 was applied, significant differences in the relative permeability of K^+ and Rb^+ were observed between different AgOrs paired with AgOrco, suggesting that VUAA1 is acting on heteromeric AgOR complexes, not simply AgOrco homomers (Figure 3.1B). For each AgOr combination, the same permeability sequence of $Rb^+ \geq K^+ > Cs^+ > Na^+ > Li^+$ (Eisenman sequence III) was observed, which corresponds to a weak field strength binding site in the channel pore, where the permeability of the ion is largely determined by the hydration energy[17-19]. AgOrco + AgOr28-expressing cells were significantly more permeable to K^+ and Rb^+ with respective relative permeabilities to Na^+ of 2.05 ± 0.10 and 2.40 ± 0.17.

When the same combinations of AgOrco + AgOr-expressing cells, excluding AgOrco alone, were assayed with strong odorant agonists specific to the conventional AgOr subunits, AgOrco + AgOr28 again displayed significantly

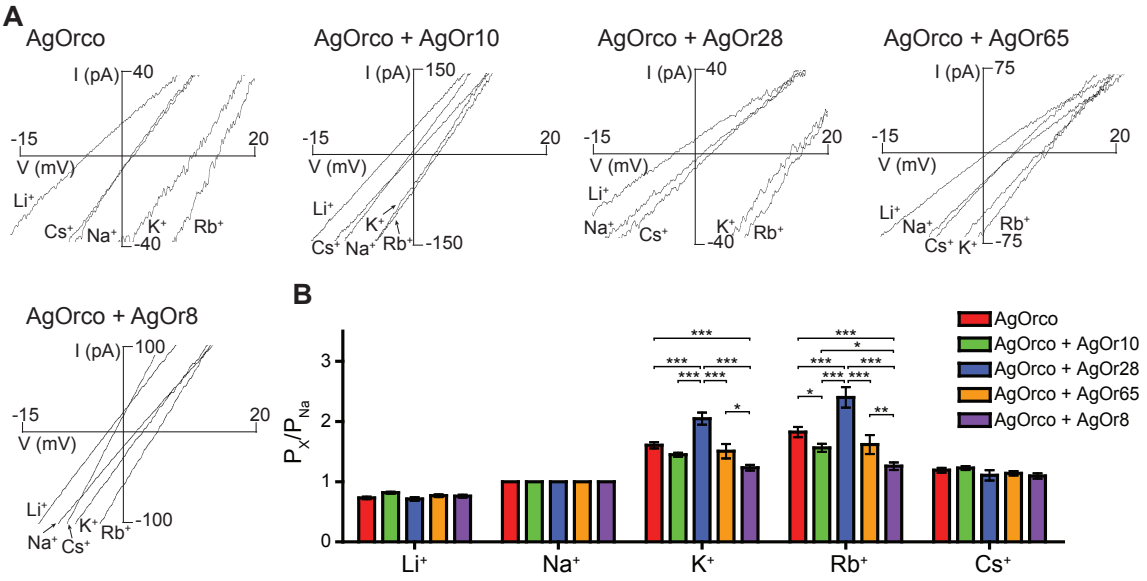

Figure 3.1 Monovalent cation permeation varies across AgOrs with VUAA1 agonism. (**A**) Representative VUAA1-induced currents across different AgOrs in extracellular solution containing 150 mM of the indicated monovalent cation and 100 μM VUAA1. (**B**) Histogram of the relative permeation of the monovalent cations to Na^+ for each AgOr (n=5 for each). Significance of the AgOr and the cation were determined by a two-factor ANOVA ($p<0.0001$ for both), and a Bonferroni correction was performed for individual comparisons (*** = $p<0.001$, ** = $p<0.01$, * = $p<0.05$).

higher permeabilities of K^+ and Rb^+, 2.87 ± 0.38 and 2.80 ± 0.32 (Figure 3.2). In some cases, agonist-specific differences in relative permeability were observed when comparing the odorant-induced currents to those from VUAA1 (Figure S3.2). These data suggest that channel gating mediated by either AgOrco or the conventional AgOr results in a different architecture of the channel pore, thus allowing particular ions to be more or less permeant.

Insect ORs are also permeable to divalent cations, previously demonstrated by Ca^{++} mobilization assays used to assess OR function[1-3,16]. Extracellular solutions containing a single divalent cation were used to determine the relative permeability of Ca^{++} and Mg^{++} among the different AgOr cell lines as in Figures 1 and 2. In the context of VUAA1 agonism, both divalent cations were less permeable than Na^+ across each AgOr combination (Figure 3.3). However, AgOrco + AgOr10 was significantly more permeable to both Ca^{++} and Mg^{++} than the other AgOrs with permeability ratios of 0.72 ± 0.03 and 0.60 ± 0.03, respectively. When activated by the odorant, Ca^{++} and Mg^{++} permeability was dependent on the conventional AgOr (Figure 3.4). In cells expressing AgOrco + AgOr65 and AgOrco + AgOr8, significant increases in permeability for both divalent cations were observed when compared to VUAA1 agonism, again demonstrating differences in permeability related to the agonist (Figure S3.3). Significant macroscopic currents were observed for all cations tested, confirming the role of insect ORs as non-selective cation channels, with a preference for monovalent over divalent cations.

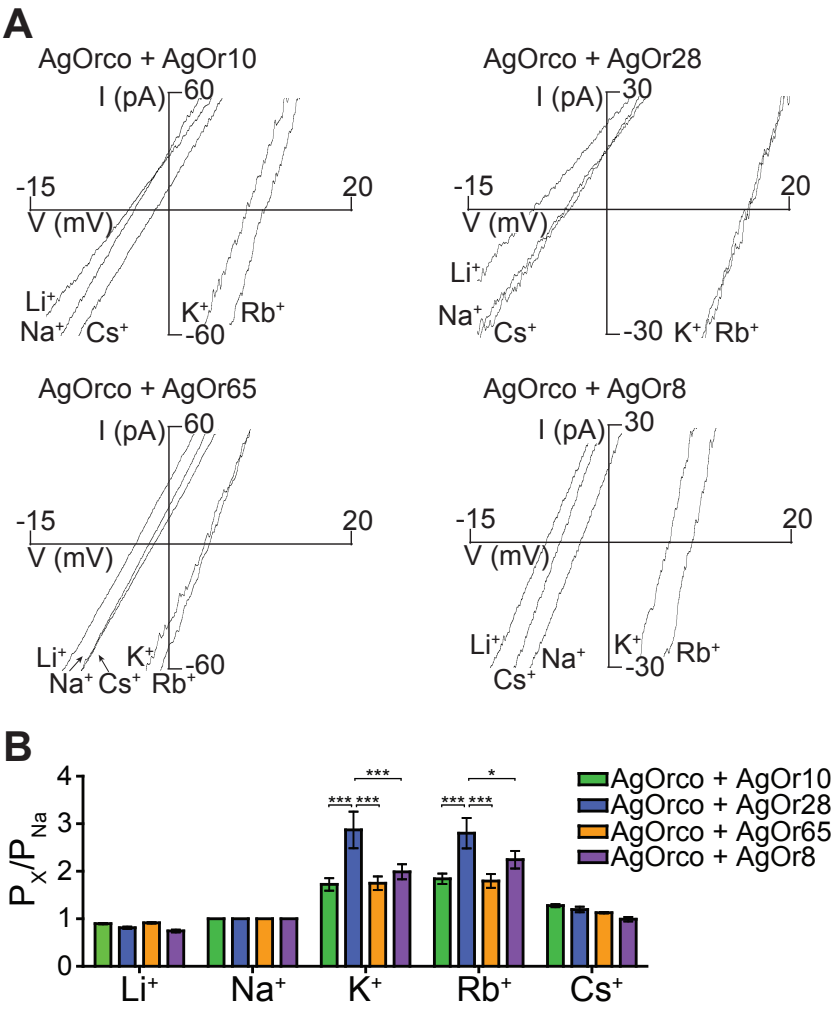

Figure 3.2 Odorant-induced monovalent permeation of heteromeric AgOrs. (**A**) Representative currents from AgOrs when activated by an odorant in extracellular solution containing 150 mM of the specified monovalent cation. AgOr:odorant pairs are as follows AgOr10:benzaldehyde (100 μM), AgOr28:2,4,5-trimethylthiazole (100 μM), AgOr65:eugenol (100 nM), and AgOr8:1-octen-3-ol (100 μM). (**B**) Histogram of the relative permeation of the monovalent cations to Na^+ for each AgOr (n=5 for each). Significance of the AgOr and the cation were determined by a two-factor ANOVA ($p<0.0001$ for both), and a Bonferroni correction was performed for individual comparisons (*** = $p<0.001$, * = $p<0.05$).

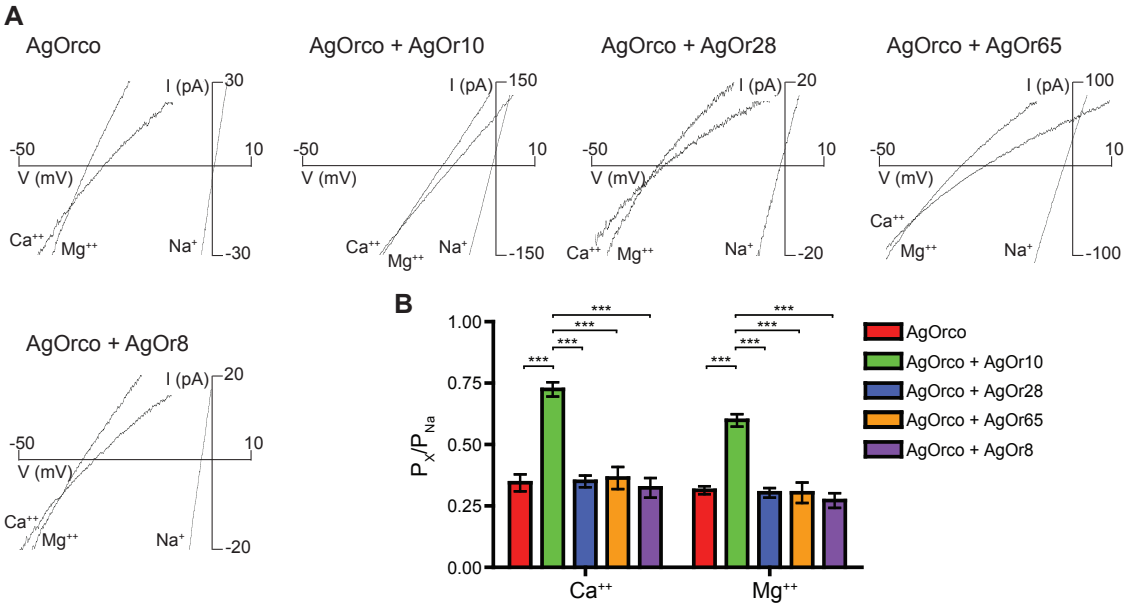

Figure 3.3 Divalent cation permeability between AgOrs activated by VUAA1. (**A**) Representative divalent cation currents from external solution containing 30mM of either Ca^{++} or Mg^{++} and 100 μM VUAA1. Currents from 150 mM Na^{+} are included for comparison. (**B**) Histogram of the relative permeation of the divalent cations to Na^{+} for each AgOr (n=5 for each). Significance of the AgOr and the cation were determined by a two-factor ANOVA ($p<0.0001$ for both), and a Bonferroni correction was performed for individual comparisons (*** = $p<0.001$).

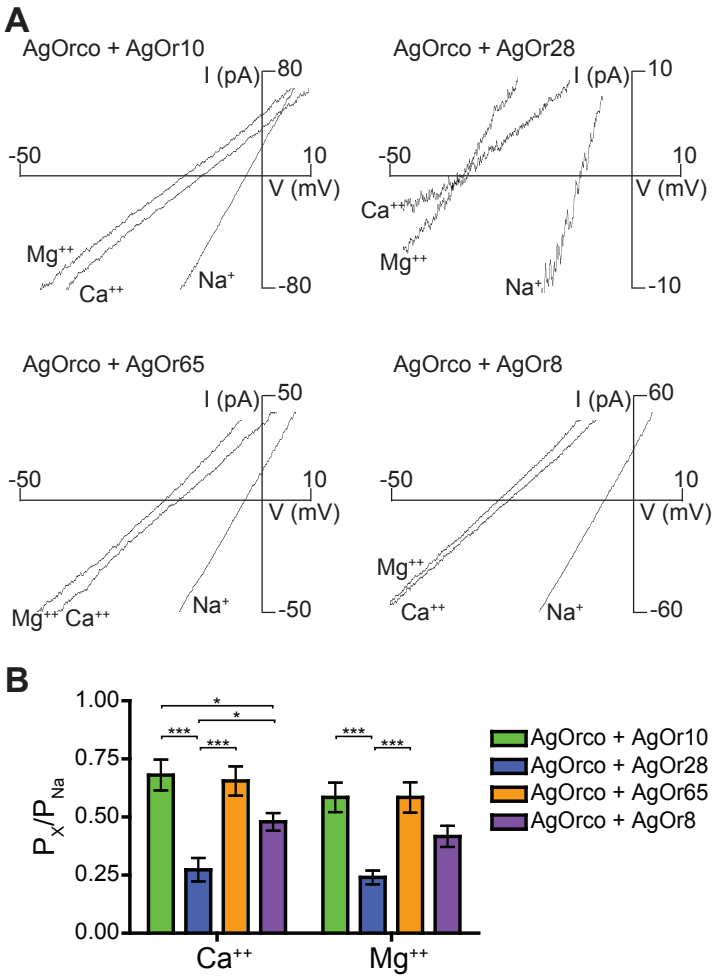

Figure 3.4 Divalent permeability differs between heteromeric AgOrs with odorant agonism. (**A**) Divalent currents from AgOrs in 30 mM Ca^{++} or Mg^{++} and the corresponding odorant. Currents from 150 mM Na^{+} are included for comparison. AgOr:odorant pairs are the same as in Figure 2. (**B**) Histogram of the relative permeation of the divalent cations to Na^{+} for each AgOr (n=5 for each). Significance of the AgOr and the cation were determined by a two-factor ANOVA ($p<0.0001$ for both), and a Bonferroni correction was performed for individual comparisons (*** = $p<0.001$, * = $p<0.05$).

Ruthenium red (RR) has been used as a blocker of insect ORs and other cation channels and is believed to bind to the extracellular entrance to the channel pore[1,3,4,20,21]. In addition to the differences in cation permeability, differences in the ability of RR to block VUAA1 or odorant-induced currents across different AgOr pairs would further support the hypothesis that the conventional odorant-binding ORs contribute to the OR ion channel pore.

In these studies, when VUAA1-currents were blocked by 100 μM RR, AgOrco + AgOr10 and AgOrco + AgOr28 were significantly less susceptible to RR blockade than AgOrco alone (Figure 3.5A-B). Furthermore, AgOrco + AgOr10 demonstrates significantly faster activation kinetics when compared to the other AgOrs, most likely due to the previously observed differences in sensitivity when compared to cells expressing AgOrco alone (Table S3.2)[1]. Varying the concentration of VUAA1 did not alter the sensitivity to RR, demonstrating that RR is noncompetitive with VUAA1 agonism (Figure 3.5C). In addition, each AgOr complex displayed concentration-dependent responses to VUAA1 in a Ca^{++}-based imaging assay. Significantly different sensitivities to the Orco agonist were observed, further suggesting that different AgOrs for variant complexes.

RR susceptibility was also examined when AgOr-expressing cells were stimulated by strong odorant agonists. A previous study on insect ORs found that odorants were also noncompetitive with RR blockade[4]. Here, AgOrco + AgOr10 currents were reduced by 78.5 ± 1.4%, a significantly higher reduction than the other three AgOr complexes (Figure 3.6A-B). With the exception of

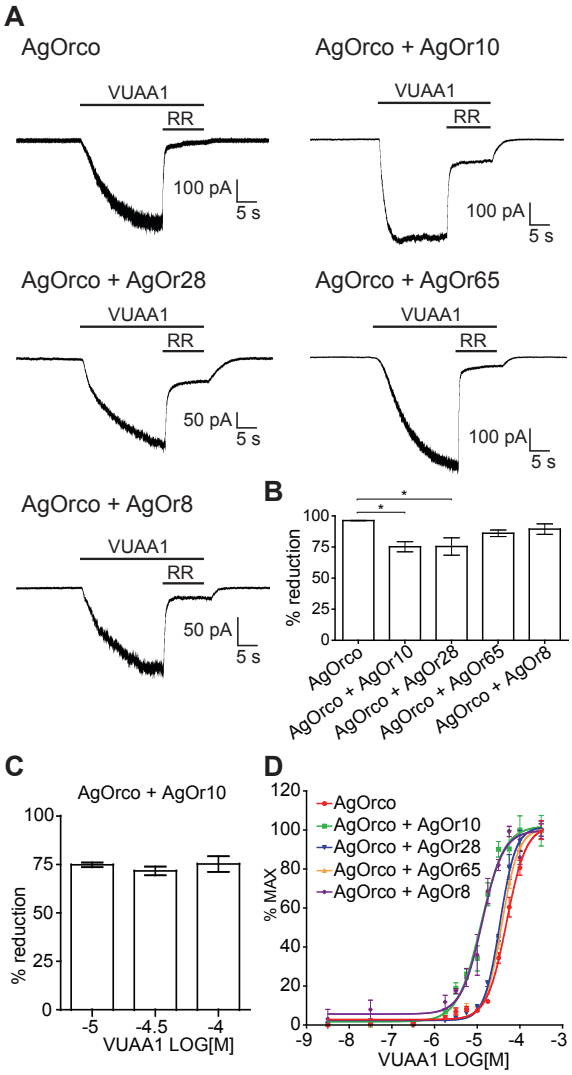

Figure 3.5 RR sensitivity varies across VUAA1-stimulated AgOrs. (**A**) Representative traces of macroscopic currents from 100 μM VUAA1, with subsequent current block by application of 100 μM RR. Holding potential for each recording is -60 mV. (**B**) The percent current reduction upon RR application across each AgOr combination (n=5 for each). Statistical significance was determined by a one-factor ANOVA ($p<0.01$), and a Bonferroni correction was performed for individual comparisons (* = $p<0.05$). (**C**) RR (100 μM) sensitivity across varying concentrations of VUAA1 agonist in AgOrco + AgOr10 cells (n=5). (**D**) Concentration-response curves generated from Ca^{++} imaging with AgOr cell lines in response to VUAA1 (n=4). EC_{50} values for each AgOr complex: AgOrco, –4.31 ± 0.03 logM; AgOrco + AgOr10, –4.91 ± 0.05 logM; AgOrco + AgOr28, –4.47 ± 0.02 logM; AgOrco + AgOr65, –4.42 ± 0.02 logM; AgOrco + AgOr8, –4.88 ± 0.05 logM. Statistical significance was determined by a one-factor ANOVA ($p<0.0001$), and individual comparisons (Bonferroni) resulted in two statistically different ($p<0.001$) groups *a* (AgOrco + AgOr10 and AgOrco + AgOr8) and *b* (AgOrco, AgOrco + AgOr28 and AgOrco + AgOr65).

AgOrco + AgOr10, each AgOrco + AgOr combination demonstrated significantly less reduction of odorant-induced currents when compared to VUAA1 agonism (Figure 3.6C). These results suggest that the odorant-specific AgOr influences the channel's susceptibility to RR and agree with previous results with *Drosophila* ORs, providing further support for its contribution to pore diversity among the OR ion channels in *An. gambiae*[4].

Discussion

This study of the channel properties across a diverse set of AgOr complexes provides compelling evidence that the conventional OR, known to impart odorant specificity, also significantly contributes to the function of the channel pore. We observed that all of the AgOr complexes used in this study displayed an Eisenman III cation permeability sequence, and significant differences in the relative permeability of some individual ions were observed between conventional AgOrs coexpressed with AgOrco in the context of both VUAA1 and odorant-evoked responses. While the differences in permeability between the AgOrco + AgOr complexes in the VUAA1 studies could potentially be affected by a mixed population of AgOrco homomers, the overall variance between AgOrco-only cells and the AgOrco + AgOr cells indicates that the conventional AgOr can influence the cation permeability in the heteromeric channel.

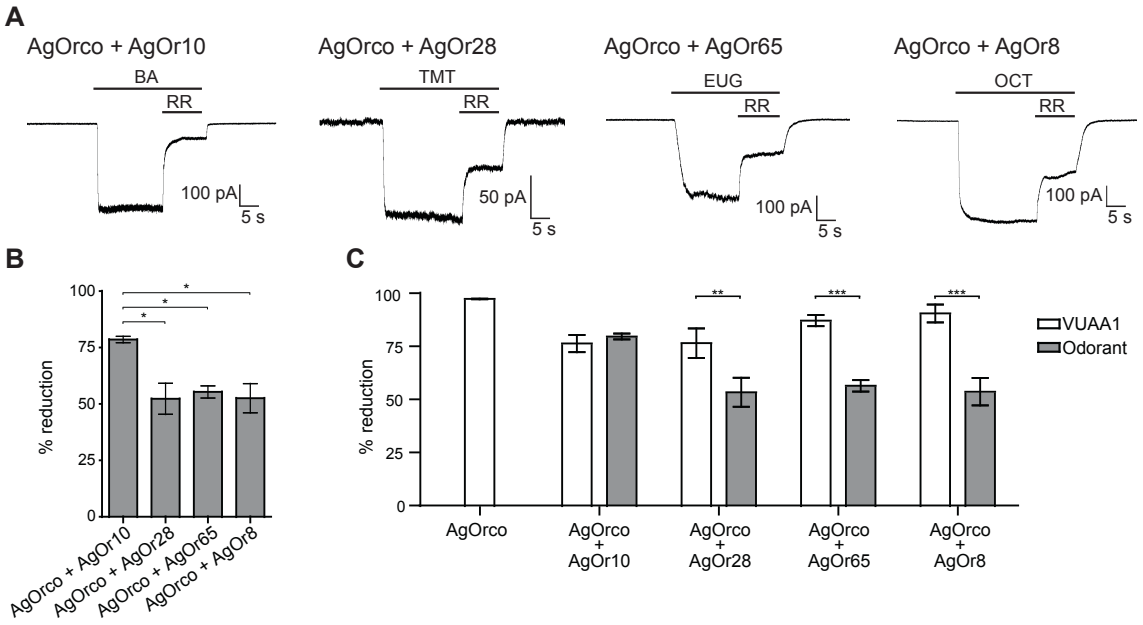

Figure 3.6 Susceptibility to RR depends on the AgOr and the agonist. (**A**) Representative traces of odorant-induced currents with subsequent current block by application of 100 μM RR. Odorant concentrations and abbreviations: 100 μM benzaldehyde (BA), 100 μM 2,4,5-trimethylthiazole (TMT), 100 nM eugenol (EUG), 100 μM 1-octen-3-ol (OCT). Holding potential for each recording is -60 mV. (**B**) The percent current reduction upon RR application across each AgOr combination (n=5 for each). Statistical significance was determined by a one-factor ANOVA ($p<0.01$), and a Bonferroni correction was performed for individual comparisons (* = $p<0.05$). (**C**) Histogram comparing RR sensitivity by AgOr and agonist. Statistical significance was determined by a two-factor ANOVA ($p<0.01$), and a Bonferroni correction was performed for individual comparisons (*** = $p<0.001$, ** = $p<0.01$).

Similarly, differences in RR sensitivity across the different AgOr complexes are consistent with the hypothesis that different heteromeric ORs have structurally distinct channel pores, in agreement with a previous study observing differences in RR susceptibility in a subset of *Drosophila* OR complexes[4]. Furthermore, while Rb^+ was the most permeant cation among the AgOr complexes in this study, we note that a Rb^+ gradient is not commonly established in biological systems. Interestingly, reports have found high concentrations of K^+ (~200 mM) in the sensillum lymph of moths[22,23]. Together with the observed relative permeability of K^+ in AgOr complexes, it is possible that influx of K^+ may significantly contribute to depolarizing ORNs *in vivo*, in addition to Na^+ and Ca^{++}, which typically have favorable gradients for cation influx.

While this study has characterized OR complexes from *An. gambiae*, these data support a molecular model that should broadly apply to OR-mediated olfactory signaling across insects. Though these data cannot conclusively rule out the possibility of the conventional OR indirectly altering the channel pore architecture, our data supports the newly proposed model in which both the Orco coreceptor and the conventional OR directly contribute to the channel pore, similar to different channel subunits surrounding the pores of cyclic nucleotide gated channels and those of the nicotinic acetylcholine receptor superfamily[6,8]. In this model, the conventional OR subunit that is responsible for odorant recognition has direct access to the channel pore where it can theoretically facilitate direct channel gating[3,4]. Comparable to other ion channels, one subunit,

Orco, can form functional homomeric channels in the absence of conventional OR[1,6,7]. The exact stoichiometry of Orco to the odorant-binding OR still remains as an important aspect in understanding the molecular mechanism of insect olfactory signaling.

The proposed model would have important implications for insect odor coding in that differences in odorant-evoked responses originate at the periphery, beginning with unique channel properties of each OR complex. The odorant-binding OR detects the specific odorant molecule, but it also can contribute to the qualitative and quantitative ability to flux cations through the OR channel pore. Along with the variables of OR expression, temporal dynamics of odorant mixtures, ORN morphology, and odorant concentration, the differences in the conductive properties of individual ORs may play a significant role in odorant-evoked depolarization of the ORN, which may ultimately result in propagation of the signal through an action potential[12,24]. These findings define the additional role for conventional ORs in establishing the ion channel characteristics of insect ORs that goes significantly beyond odorant specificity.

Materials and Methods

Chemicals

VUAA1 was purchased from ChemBridge corporation (ID# 7116565). Benzaldehyde (CAS 100-52-7), 2,4,5-trimethylthiazole (CAS 13623-11-5), eugenol (CAS 97-53-0), 1-octen-3-ol (CAS 3391-86-4), and ruthenium red (CAS

11103-72-3) were all purchased from Sigma-Aldrich. All compounds were first dissolved in DMSO and subsequently diluted in external solution.

Cell Culture, Ca^{++} Imaging, and Patch Clamp Electrophysiology

Generation of AgOrco + AgOrX cell lines and Ca^{++} imaging assays was performed as previously described[1,16]. AgOr expression was induced by incubation with 0.3 µg/mL tetracycline for 18-42 hours before functional assays.

Whole-cell patch clamp recording from AgOr-expressing HEK cells were performed as previously described[1]. For cation permeability assays, the external solution for monovalent cations contained 150 mM *X*Cl, 1 mM $MgCl_2$, 10 mM glucose, 10 mM HEPES, pH=7.4 (*X*= Li, Na, K, Rb, or Cs)[1]. The divalent cation external solution contained 30 mM XCl_2, 120mM NMDG-Cl, 1 mM $MgCl_2$, 10 mM glucose, 10 mM HEPES, pH 7.4 (*X*= Ca or Mg). The internal (pipette) solution for cation permeability assays contained 150 mM NaCl, 1 mM $MgCl_2$, 4 mM Na_2ATP, 0.037 mM $CaCl_2$, 5 mM EGTA, 10 mM HEPES, pH 7.2. The standard external solution for ruthenium red susceptibility assays contained 130 mM NaCl, 34 mM glucose, 10 mM HEPES, 1.5 mM $CaCl_2$, 1.3 mM KH_2PO_4, and 0.5 mM $MgSO_4$, pH 7.35 and the standard internal solution contained 120 mM KCl, 30 mM glucose, 10 mM HEPES, 2 mM $MgCl_2$, 1.1 mM EGTA, and 0.1 mM $CaCl_2$, pH 7.35.

To determine cation permeability, the agonist-induced current (-60 mV) was allowed to reach a steady state, and then a 2-second voltage ramp from -60 mV to +60 mV was applied to measure the reversal potential for each cation.

Recordings were performed at room temperature (20-22°C) and reversal potentials were corrected for liquid junction potentials using pCLAMP 10 (Axon Instruments) under the Ag-AgCl wire reference electrode parameter (note that all current-voltage relationship traces in Figures (3.1-3.4) are not corrected for liquid junction potential). The ruthenium red protocol consisted of agonist application to steady-state current followed by the application of 100 μM ruthenium red with agonist. Percent current reduction was calculated from steady-state currents before and during ruthenium red application.

Relative Permeability Calculations

The relative permeability of each monovalent cation to sodium was calculated according to the following equation:

$$P_X / P_{Na} = \exp(\Delta V_{rev} \bullet F / RT)$$

where ΔV_{rev} is the difference in reversal potential between the specific cation and sodium[25]. Permeability of divalent cations was calculated using the following equation:

$$P_X / P_{Na} = (1 + \exp(\Delta V_{rev} \bullet F / RT)) \bullet ([Na]_i \exp(V_{rev} \bullet F / RT)) / 4[X]_e$$

where V_{rev} is the absolute reversal potential of the divalent cation, $[Na]_i$ represents the intracellular sodium concentration, and $[X]_e$ is the extracellular concentration of the specific divalent cation[25]. Relative permeabilities can be found in Table S3.1.

Significant differences in cation permeability of different AgOr combinations were determined by ANOVA and post-hoc comparisons were made using a Bonferroni correction.

References

1. Jones, P. L., Pask, G. M., Rinker, D. C. & Zwiebel, L. J. Functional agonism of insect odorant receptor ion channels. *Proceedings of the National Academy of Sciences* **108**, 8821–8825 (2011).

2. Wicher, D. *et al.* Drosophila odorant receptors are both ligand-gated and cyclic-nucleotide-activated cation channels. *Nature* **452**, 1007–1011 (2008).

3. Sato, K. *et al.* Insect olfactory receptors are heteromeric ligand-gated ion channels. *Nature* **452**, 1002–1006 (2008).

4. Nichols, A. S., Chen, S. & Luetje, C. W. Subunit contributions to insect olfactory receptor function: channel block and odorant recognition. *Chem Senses* **36**, 781–790 (2011).

5. Hallem, E. A., Ho, M. G. & Carlson, J. R. The molecular basis of odor coding in the Drosophila antenna. *Cell* **117**, 965–979 (2004).

6. Bönigk, W. *et al.* The native rat olfactory cyclic nucleotide-gated channel is composed of three distinct subunits. *J Neurosci* **19**, 5332–5347 (1999).

7. Cheng, W., Yang, F., Takanishi, C. L. & Zheng, J. *Thermosensitive TRPV channel subunits coassemble into heteromeric channels with intermediate conductance and gating properties*. *J Gen Physiol* **129**, 191–207 (2007).

8. Corringer, P. J., Le Novère, N. & Changeux, J. P. Nicotinic receptors at the amino acid level. *Annu. Rev. Pharmacol. Toxicol.* **40**, 431–458 (2000).

9. Takken, W. & Knols, B. G. Odor-mediated behavior of Afrotropical malaria mosquitoes. *Annu Rev Entomol* **44**, 131–157 (1999).

10. Wang, G., Carey, A. F., Carlson, J. R. & Zwiebel, L. J. Molecular basis of odor coding in the malaria vector mosquito Anopheles gambiae. *Proceedings of the National Academy of Sciences* **107**, 4418–4423 (2010).

11. Carey, A. F., Wang, G., Su, C.-Y., Zwiebel, L. J. & Carlson, J. R. Odorant reception in the malaria mosquito Anopheles gambiae. *Nature* **464**, 66–71 (2010).

12. Pitts, R. J., Rinker, D. C., Jones, P. L., Rokas, A. & Zwiebel, L. J. Transcriptome Profiling of Chemosensory Appendages in the Malaria Vector Anopheles gambiae Reveals Tissue- and Sex-Specific Signatures of Odor Coding. *BMC Genomics* **12**, 271 (2011).

13. Lu, T. *et al.* Odor coding in the maxillary palp of the malaria vector mosquito Anopheles gambiae. *Curr Biol* **17**, 1533–1544 (2007).

14. Xia, Y. *et al.* The molecular and cellular basis of olfactory-driven behavior in Anopheles gambiae larvae. *Proceedings of the National Academy of Sciences* **105**, 6433–6438 (2008).

15. Pelletier, J., Hughes, D. T., Luetje, C. W. & Leal, W. S. An odorant receptor from the southern house mosquito Culex pipiens quinquefasciatus sensitive to oviposition attractants. *PLoS ONE* **5**, e10090 (2010).

16. Bohbot, J. D. *et al.* Conservation of indole responsive odorant receptors in mosquitoes reveals an ancient olfactory trait. *Chem Senses* **36**, 149–160 (2011).

17. Eisenman, G. Cation selective glass electrodes and their mode of operation. *Biophys J* **2**, 259–323 (1962).

18. Eisenman, G. & Dani, J. An introduction to molecular architecture and permeability of ion channels. *Annual review of biophysics and biophysical chemistry* **16**, 205–226 (1987).

19. Lee, C. O. & Fozzard, H. A. Electrochemical properties of hydrated cation-selective glass membrane. A model of K+ and Na+ transport. *Biophys J* **14**, 46–68 (1974).

20. Nakagawa, T., Sakurai, T., Nishioka, T. & Touhara, K. Insect sex-pheromone signals mediated by specific combinations of olfactory receptors. *Science* **307**, 1638–1642 (2005).

21. Cibulsky, S. M. & Sather, W. A. Block by ruthenium red of cloned neuronal voltage-gated calcium channels. *J Pharmacol Exp Ther* **289**, 1447–1453 (1999).

22. Kaissling, K.-E. Single Unit and Electroantennogram Recordings in Insect Olfactory Organs. *in Experimental Cell Biology of Taste and Olfaction* 361–377 (1995).

23. Zufall, F., Stengl, M., Franke, C., Hildebrand, J. G. & Hatt, H. Ionic currents of cultured olfactory receptor neurons from antennae of male Manduca sexta. *J Neurosci* **11**, 956–965 (1991).

24. Su, C.-Y., Martelli, C., Emonet, T. & Carlson, J. R. Temporal coding of odor mixtures in an olfactory receptor neuron. *Proc Natl Acad Sci USA* (2011).doi:10.1073/pnas.1100369108

25. Voets, T. *et al.* Molecular determinants of permeation through the cation channel TRPV4. *Journal of Biological Chemistry* **277**, 33704 (2002).

Supporting Information

Table S3.1 The relative permeabilities of the AgOrs to the mono- and divalent cations in the contexts of both VUAA1 and odorant agonism

AgOr	Agonist	P_{Rb}/P_{Na}	P_{K}/P_{Na}	P_{Cs}/P_{Na}	P_{Li}/P_{Na}	P_{Ca}/P_{Na}	P_{Mg}/P_{Na}
AgOrco	VUAA1	1.82 ± 0.08	1.60 ± 0.05	1.19 ± 0.04	0.73 ± 0.02	0.34 ± 0.03	0.31 ± 0.02
AgOrco + AgOr10	VUAA1	1.56 ± 0.07	1.45 ± 0.03	1.22 ± 0.03	0.81 ± 0.02	0.72 ± 0.03	0.60 ± 0.03
	benzaldehyde	1.84 ± 0.11	1.72 ± 0.13	1.28 ± 0.03	0.90 ± 0.01	0.68 ± 0.07	0.58 ± 0.06
AgOrco + AgOr28	VUAA1	2.40 ± 0.17	2.05 ± 0.10	1.11 ± 0.09	0.71 ± 0.03	0.35 ± 0.02	0.30 ± 0.02
	2,4,5-tri-methylthiazole	2.80 ± 0.32	2.87 ± 0.38	1.19 ± 0.06	0.81 ± 0.02	0.27 ± 0.05	0.24 ± 0.03
AgOrco + AgOr65	VUAA1	1.62 ± 0.16	1.51 ± 0.12	1.14 ± 0.04	0.77 ± 0.02	0.36 ± 0.05	0.30 ± 0.04
	eugenol	1.80 ± 0.15	1.75 ± 0.14	1.13 ± 0.01	0.92 ± 0.01	0.66 ± 0.06	0.58 ± 0.07
AgOrco + AgOr8	VUAA1	1.25 ± 0.06	1.23 ± 0.05	1.10 ± 0.04	0.76 ± 0.02	0.32 ± 0.04	0.27 ± 0.03
	1-octen-3-ol	1.94 ± 0.06	1.70 ± 0.07	0.98 ±0.04	0.84 ± 0.04	0.48 ± 0.04	0.42 ± 0.05

Table S3.2 Activation kinetics for responses to 100 μM VUAA1. The 10-90% activation time was calculated using the statistics tool in pCLAMP 10 (Axon Instruments), and subsequent statistical significance was determined through a one-factor ANOVA and a post-hoc Bonferroni correction.

AgOr	10-90% activation time (sec)
AgOrco	13.6 ± 0.65
AgOrco + AgOr10	5.53 ± 0.89[a]
AgOrco + AgOr28	15.89 ± 0.60
AgOrco + AgOr65	15.73 ± 0.27
AgOrco + AgOr8	12.78 ± 1.40

[a] Significantly different from each other receptor combination ($p < 0.001$)

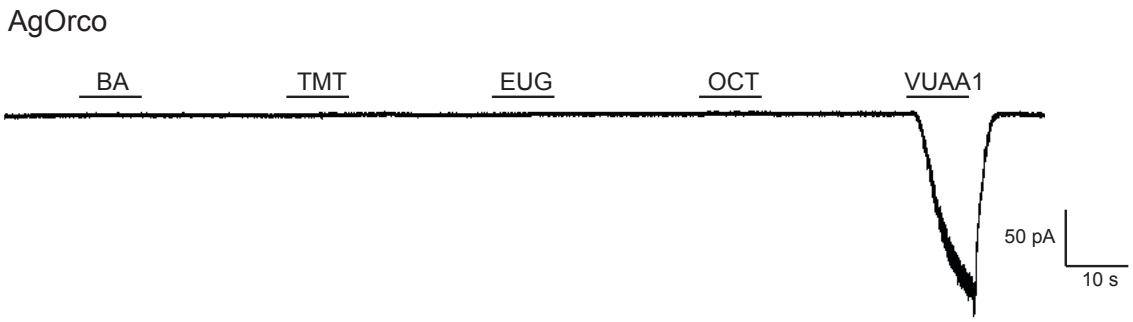

Figure S3.1 Cells expressing only AgOrco do not respond to odorants. The holding potential for each recording is -60 mV (n=5). Concentrations and abbreviations: 100 μM benzaldehyde (BA), 100 μM 2,4,5-trimethylthiazole (TMT), 100 nM eugenol (EUG), 100 μM 1-octen-3-ol (OCT), 100 μM VUAA1.

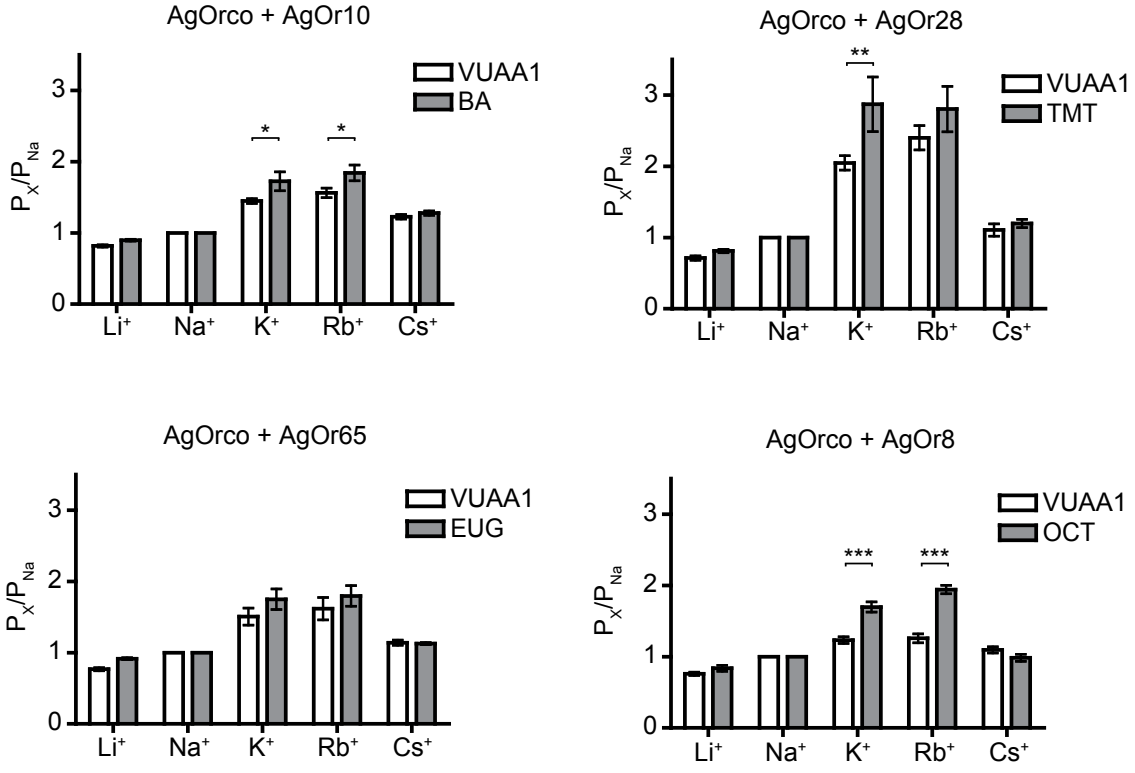

Figure S3.2 Comparison of monovalent cation permeability by agonist from Figures 3.1 and 3.2. Odorant concentrations and abbreviations: 100 μM benzaldehyde (BA), 100 μM 2,4,5-trimethylthiazole (TMT), 100 nM eugenol (EUG), 100 μM 1-octen-3-ol (OCT). Statistical significance was determined by a two-factor ANOVA ($p<0.05$), and a Bonferroni correction was performed for individual comparisons (*** = $p<0.001$, ** = $p<0.01$, * = $p<0.05$).

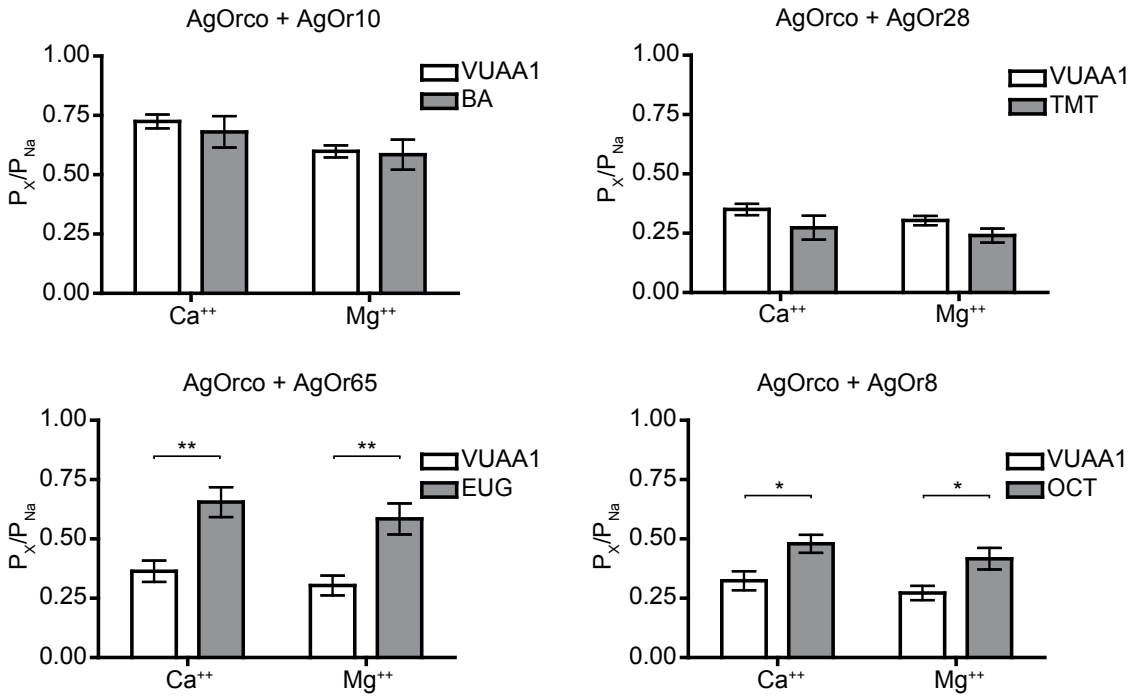

Figure S3. Comparison of divalent cation permeability by agonist from Figures 3.3 and 3.4. Odorant concentrations and abbreviations: 100 μM benzaldehyde (BA), 100 μM 2,4,5-trimethylthiazole (TMT), 100 nM eugenol (EUG), 100 μM 1-octen-3-ol (OCT). Statistical significance was determined by a two-factor ANOVA ($p<0.05$), and a Bonferroni correction was performed for individual comparisons (** = $p<0.01$, * = $p<0.05$).

CHAPTER IV

BLOCKADE OF INSECT ODORANT RECEPTOR CURRENTS BY AMILORIDE DERIVATIVES

Gregory M. Pask, Yuriy V. Bobkov, Elizabeth A. Corey,

Barry W. Ache, and Laurence J. Zwiebel

Preface

This work was published in *Chemical Senses* (2013, *epub ahead of print*) and is a result of collaboration with the Ache lab. Yuriry Bobkov performed the initial amiloride derivative experiments with two Zwiebel lab cell lines (Figures 4.2 and 4.3). I then explored the candidate blockers further by using VUAA1, examining the effect of HMA across Orco orthologs, and examining the mechanism of the current block. I wrote the manuscript with comments from the other coauthors. This work was supported by the National Institute of Allergy and Infectious Disease [AI056402] to L.J.Z and the National Institute on Deafness and Other Communication Disorders (NIDCD) [DC001655] to B.W.A. at the National Institutes of Health, and the Foundation for the National Institutes of Health through the Grand Challenges in Global Health Initiative [VCTR121] to L.J.Z. G.M.P was supported by the NIDCD through an NRSA F31 [DC011989].

Introduction

The recent discovery of an Orco family agonist, VUAA1, has provided insight into insect OR structure and function[1]. When expressed alone, Orco subunits from several insect species can form functional homomeric channels, susceptible to activation by VUAA1 [1]. In addition, differences in the pore-specific properties between several heteromeric OR complexes suggest that the odorant-specific OR contributes to the pore structure[2-4]. Further examination of the structure-activity relationship of VUAA1 has yielded several more potent Orco agonists, as well as antagonists capable of reducing both VUAA1- and odorant-evoked currents through competitive and noncompetitive mechanisms, respectively[5,6]. The identification of new insect OR modulators will provide additional pharmacological tools that can be useful in continuing to advance our understanding of the insect olfactory system.

To block insect OR responses, previous studies have utilized ruthenium red, a non-specific blocker of numerous cation channels[1-3,7,8]. The identification of other channel blockers with greater selectivity than ruthenium red would provide useful probes for the study of insect OR function. One candidate group of agents consists of amiloride and several related analogs, which have been shown to block epithelial sodium channels (ENaCs), acid-sensing ion channels, and Na^+/H^+ exchangers[9,10]. In arthropod olfactory systems, amiloride and its derivatives have been studied extensively in the lobster where they reversibly inhibit odorant-evoked activity, and more recently amiloride has been shown to block *Drosophila melanogaster* chemosensory IRs[11,12].

Therefore, we have explored the ability of a panel of amilorides to block currents of 2 heteromeric OR channels from *An. gambiae*, as well as homomeric Orco channels from 4 insect orders. We demonstrate that insect ORs display varying degrees of susceptibility to channel blockade by amiloride derivatives, and we propose their use in pharmacological studies of insect OR function.

Results

Whole-cell patch clamp assays were performed to test the effect of a panel of amilorides on *An. gambiae* ORs (AgOrs) heterologously expressed in HEK cells. The panel of derivatives consisted of amiloride, as well as amiloride analogs with varying substituents at the 5 position of the pyrazine ring and the terminal nitrogen of the guanidinium group (Figure 4.1). This panel was tested against cells expressing either AgOr48, a lactone receptor, or AgOr65 which is sensitive to eugenol, each co-expressed with AgOrco[13,14]. Increasing concentrations of amiloride derivative were applied once agonist-induced currents reached a steady-state level.

During the application of a strong agonist, δ-decalactone, each of the amiloride derivatives caused substantial concentration-dependent blockade of odorant-evoked currents from AgOr48-expressing cells (Figure 4.2). Of these, amiloride was the least potent, with all structural modifications resulting in more potent blockade. The potency sequence for AgOr48 + AgOrco is HMA ~ MIA > EIPA > DMA ~ DCBA > Phenamil > Amiloride (see Table S4.1 for IC_{50} values). The effects of many of the amiloride analogs were partially irreversible at high

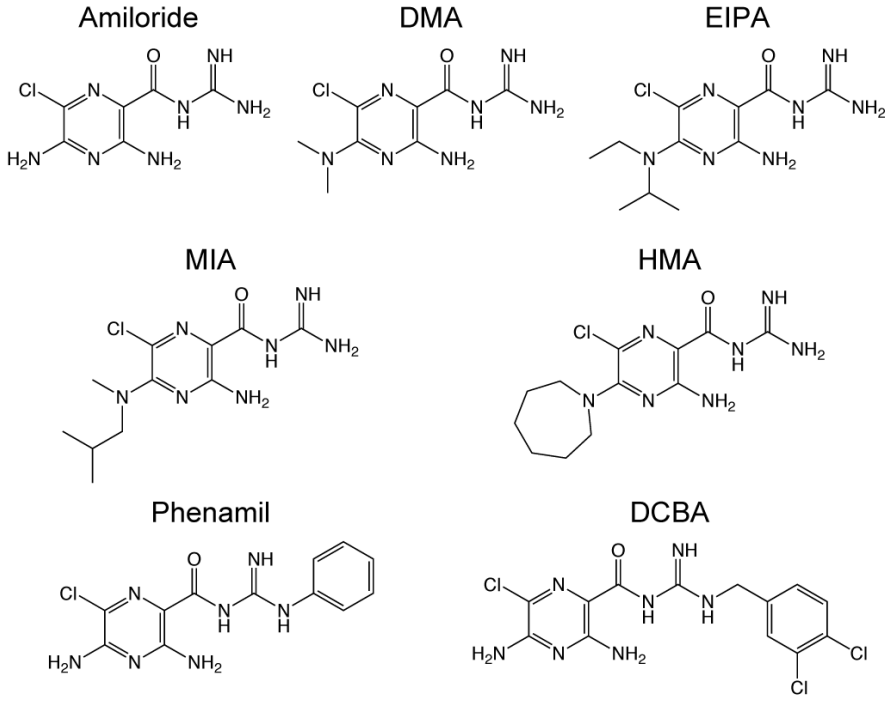

Figure 4.1 Chemical structures and abbreviations of the amiloride derivatives involved in this study.

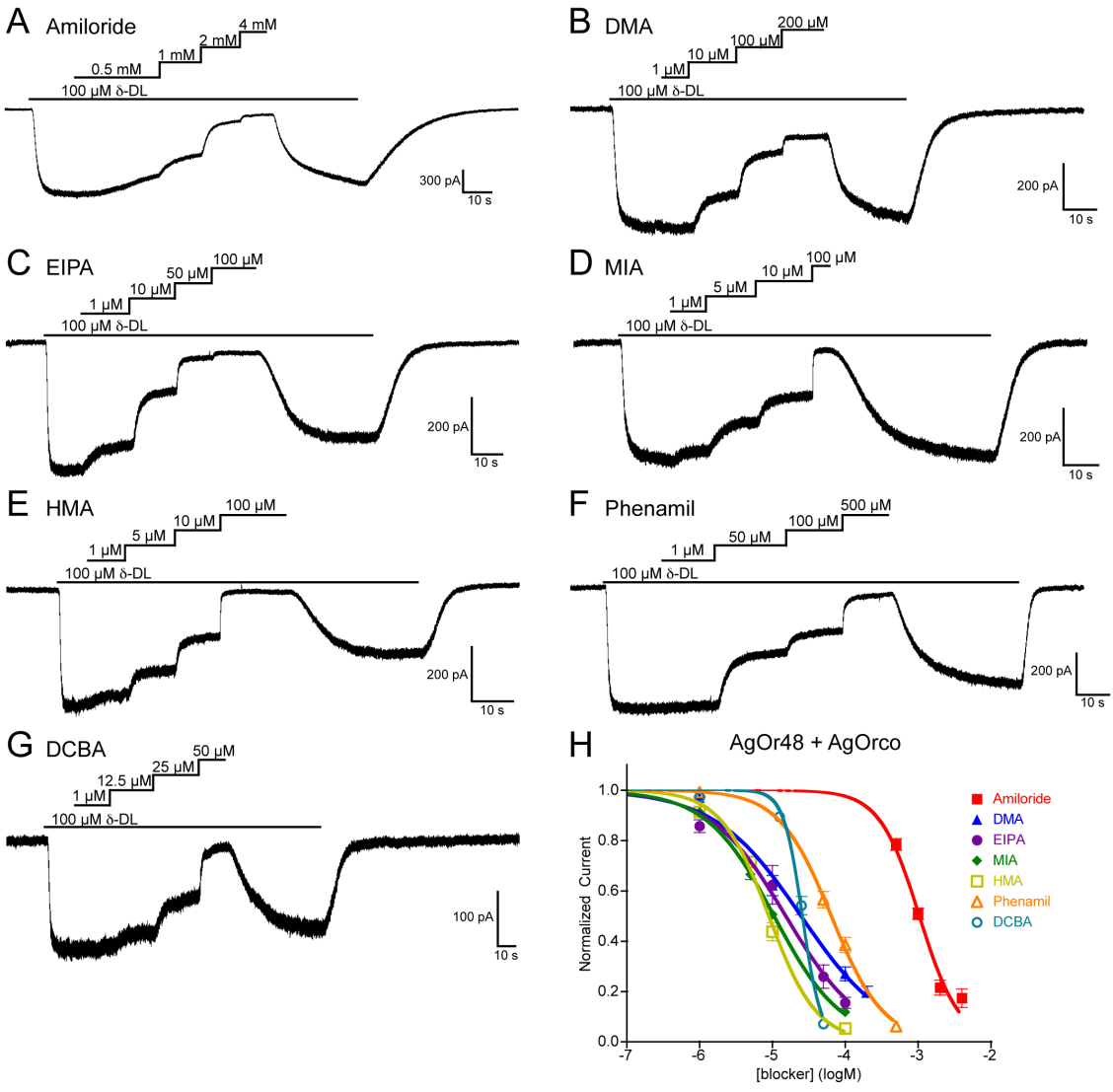

Figure 4.2 Amiloride derivatives block odorant-evoked whole-cell currents in AgOr48 + AgOrco cells. (**A-G**) Representative whole-cell recordings of HEK cells expressing AgOr48 + AgOrco. Cells were first stimulated by 100 µM δ-decalactone, and then simultaneously subjected to increasing concentrations of the indicated amiloride derivative. Holding potentials ranged from -60 to -50 mV and the solutions were Extracellular 1 and Internal 1. (**H**) Inhibition curves for each of the amiloride derivatives, with data points representing the normalized mean ± SEM of the current reduction. IC_{50} values and the number of trials (*n*) can be found in Table S4.1.

concentrations, as indicated by the observation that current amplitudes after wash-out of the blocker did not return to their initial levels. This decrease was not the result of constant agonist application, as δ-decalactone-evoked currents reached a steady state and did not decrease over time (Figure S4.1). Overall, HMA (IC_{50} = -5.05 ± 0.02 logM) and MIA (IC_{50} = -4.98 ± 0.02 logM) were found to be the most potent channel blockers of the AgOr48 + AgOrco complex.

When the same panel of derivatives was applied to AgOr65 + AgOrco cells, they were, once again, all capable of blocking odorant-evoked currents at varying potencies (Figure 4.3). The AgOr65 complex displayed a similar potency sequence of HMA > MIA > DCBA ~ EIPA > Phenamil > DMA > Amiloride (see Table S4.1 for IC_{50} values). Interestingly, 1 amiloride derivative, DMA, was significantly less potent (P<0.001) against the AgOr65 complex (IC_{50} = -3.79 ± 0.03 logM) compared with AgOr48 (IC_{50} = -4.61 ± 0.05 logM), suggesting that the odorant-specific tuning OR contributes to the site of DMA blockade.

We next examined whether amiloride derivatives could block insect OR currents when elicited by the Orco agonist, VUAA1[1]. Here, the most robust blockers from the odorant studies, HMA and MIA, also caused a concentration-dependent reduction in the VUAA1 currents of HEK cells expressing AgOrco together with either AgOr48 or AgOr65 (Figures 4.4 and S4.2). The IC_{50} values for HMA (-5.41 ± 0.04 logM) and MIA (-5.40 ± 0.04 logM) against the AgOr48 complex were very similar to each other, which was also observed when activated by δ-decalactone. Cells expressing AgOr65 + AgOrco displayed significantly higher sensitivity (P<0.001) to HMA (-5.68 ± 0.03 logM) than MIA

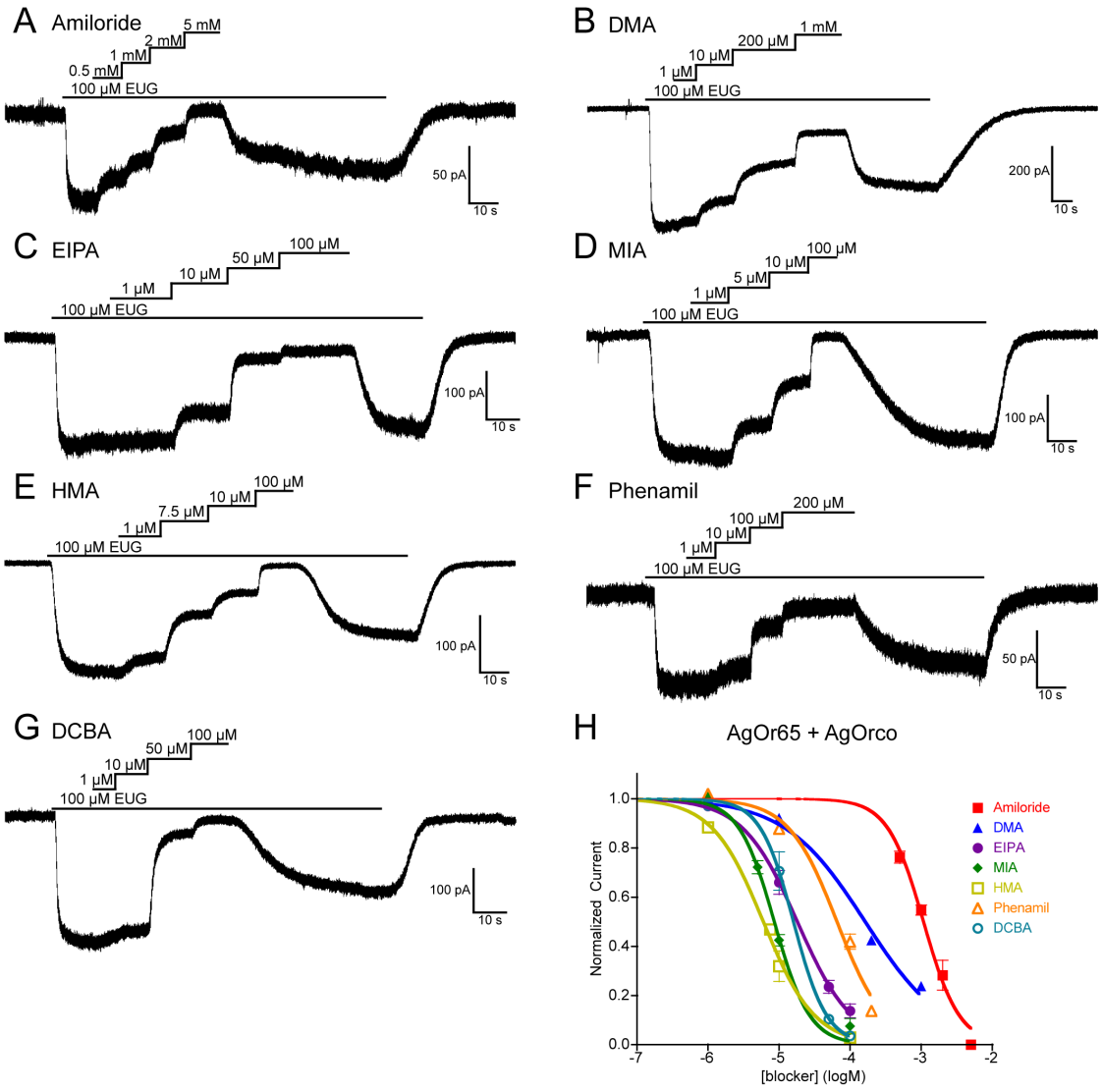

Figure 4.3 Odorant-evoked currents of the AgOr65 complex can be blocked by amiloride derivatives. (**A-G**) Representative whole-cell recordings of HEK cells expressing AgOr65 + AgOrco. After initial steady-state responses to 100 µM eugenol, increasing concentrations of the amiloride derivative were applied to each preparation. Holding potentials ranged from -60 to -50 mV and the solutions were Extracellular 1 and Internal 1. (**H**) Inhibition curves for each of the amiloride derivatives, with data points representing the normalized mean ± SEM of the current reduction. IC_{50} values and the number of trials (*n*) are in Table S4.1.

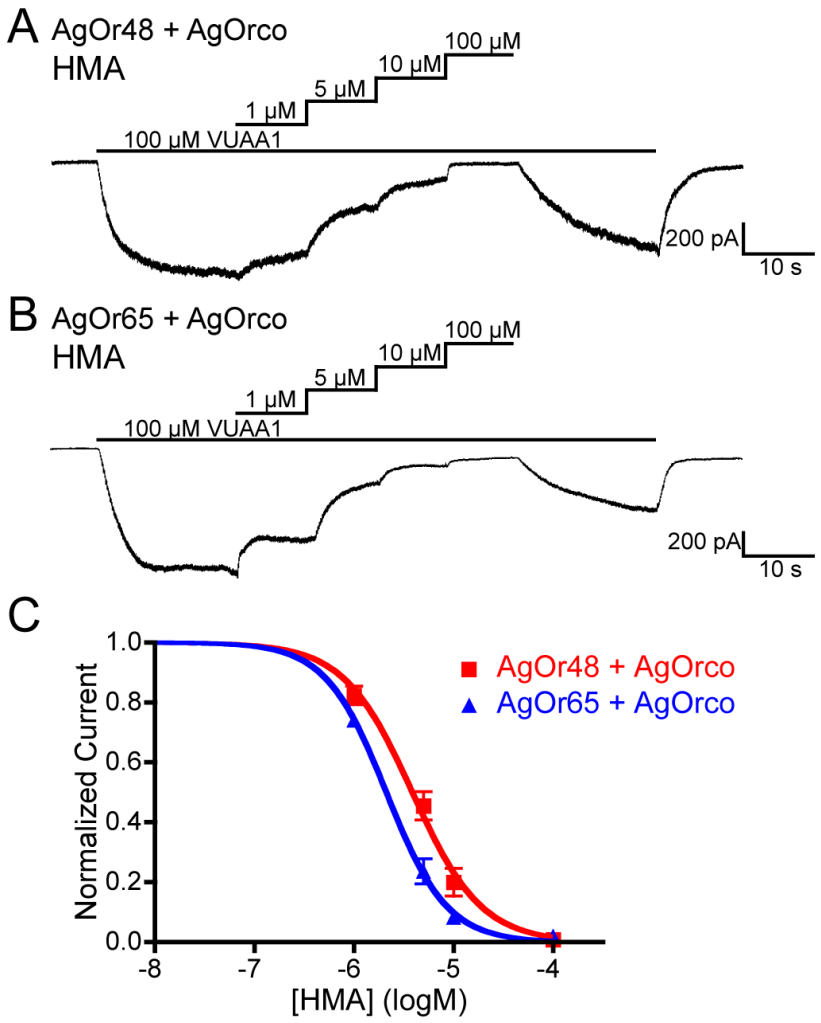

Figure 4.4 VUAA1-evoked currents are blocked by HMA. (**A-B**) Representative current traces from either AgOr48 or AgOr65 cells during stimulation with 100 µM VUAA1. Increasing amounts of HMA resulted in a reduction of VUAA1-evoked current that was partially irreversible after amiloride wash-out. The holding potential for each recording is -60 mV and the solutions were Extracellular 2 and Internal 2. (**C**) Inhibition curves for HMA for each complex, with data points representing the normalized mean ± SEM of the current reduction. IC_{50} values and the number of trials (*n*) can be found in Table S4.1.

(-5.38 ± 0.06 logM), a difference that was also observed in the eugenol studies. Both AgOr complexes were more susceptible to blockade when activated by VUAA1, suggesting that the VUAA1-bound channel is more accessible to HMA and MIA (Table S4.1). Again, the effects of blockade appeared to be slightly irreversible and independent of prolonged VUAA1 stimulation (Figure S4.1). These results demonstrate that amiloride derivatives are capable of blocking heteromeric AgOr complexes gated by VUAA1.

To determine if amiloride derivatives could also block homomeric Orco channels, we applied HMA and MIA to cells expressing AgOrco alone. Here, homomeric AgOrco channels were considerably more sensitive to HMA and MIA than any of the heteromeric AgOr complexes, with IC_{50} values of -5.86 ± 0.02 logM and -5.72 ± 0.04 logM, respectively (Figures 4.5A and S4.2C-D). In addition, we explored the effect of HMA on homomeric Orco channels from 3 other insect orders—*Harpegnathos saltator* (Hymenoptera, HsOrco), *Heliothis virescens* (Lepidoptera, HvOrco), and *Lygus hesperus* (Hemiptera, LhOrco)—to assess whether amiloride blockade was specific to AgOrs[15-17]. In these studies, VUAA1 currents from each Orco ortholog were reduced with increasing concentrations of HMA, (Figures 4.5B-D). Moreover, HsOrco displayed the greatest sensitivity to HMA (-6.07 ± 0.04 logM) whereas LhOrco was the least sensitive to current blockade (-5.62 ± 0.04, Figure 5E). These results indicate that amiloride derivatives possess a broad ability to block Orco-containing complexes and can therefore be utilized to explore OR channel function across several insect taxa.

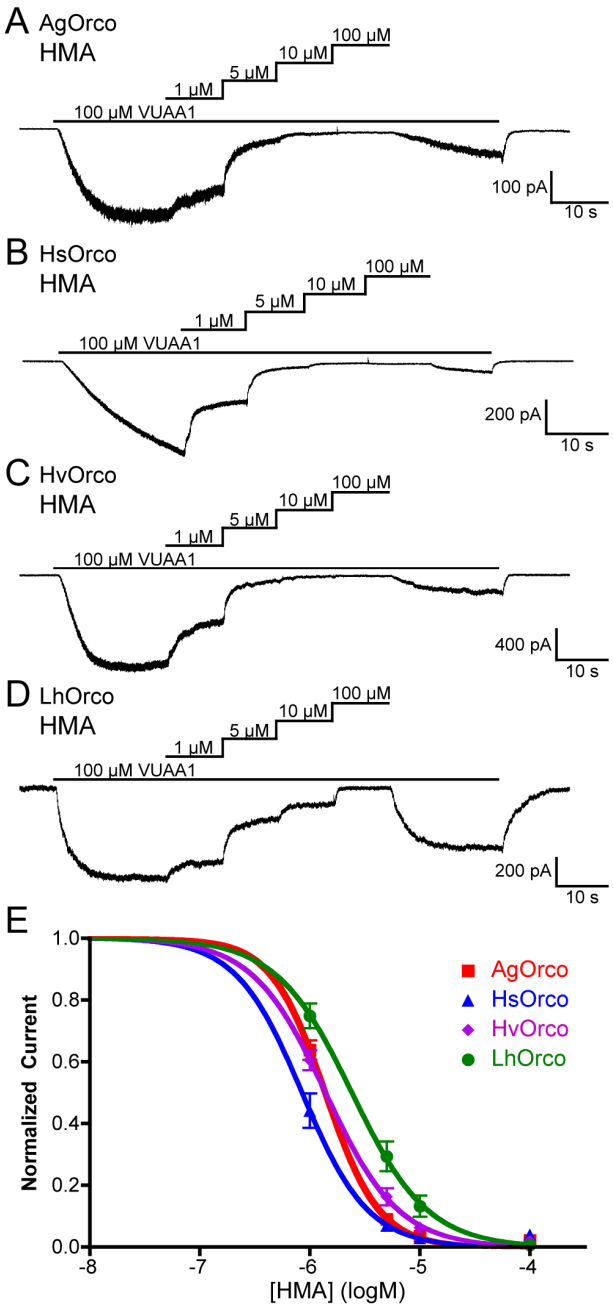

Figure 4.5 HMA also blocks homomeric Orco channels from four insect species. (**A-D**) Whole-cell responses from cells expressing Orco channels from *Anopheles gambiae* (**A, AgOrco**), *Harpegnathos saltator* (**B, HsOrco**), *Heliothis virescens* (**C, HvOrco**), or *Lygus hesperus* (**D, LhOrco**) to an application of 100 μM VUAA1. HMA reduced VUAA1-mediated currents in a concentration-dependent manner. The holding potential for each recording was -60 mV and the solutions were Extracellular 2 and Internal 2. (**E**) Inhibition curves for HMA and MIA against AgOrco or HsOrco, with data points representing the normalized mean ± SEM of the current reduction. IC_{50} values and the number of trials (*n*) can be found in Table S4.1.

We next investigated the kinetics of the current inhibition on AgOr complexes by applying a high concentration of HMA (100 μM) to steady-state currents evoked by either VUAA1 or odorant. When applied, HMA exhibited significantly different inhibition kinetics (as defined as the time required to transition from 90% to 10% steady-state current amplitudes) across several of the AgOr complexes (Figure 4.6A-E). By this measure, VUAA1-induced currents in AgOrco cells displayed the most rapid current inhibition with an inhibition time of 319.4 ± 97.4 ms (Figure 4.6F).

To explore the mechanism of current block, we next examined whether HMA could bind AgOr complexes in the absence of agonist. The assay design consisted of 3 recording sweeps each containing an application of agonist, with 100 μM HMA applied and washed out in Sweep 3 just before the third agonist stimulation (Figure 4.7A). With Sweep 1 serving as a normalization factor, potential differences in activation kinetics and current amplitude between Sweeps 2 and 3 were compared to determine if the pre-application of HMA had an effect. In all instances, pre-exposure to HMA significantly reduced both the activation rate and current amplitude during Sweep 3, demonstrating that HMA can bind the AgOr complex in the absence of agonist (Figure 4.7B-H). Furthermore, during the pre-agonist HMA application to AgOr48+AgOrco-expressing cells, there was a consistent upward deflection in the baseline current that was not observed with either AgOr65+AgOrco or AgOrco cells (Figure S4.3). This observation provides

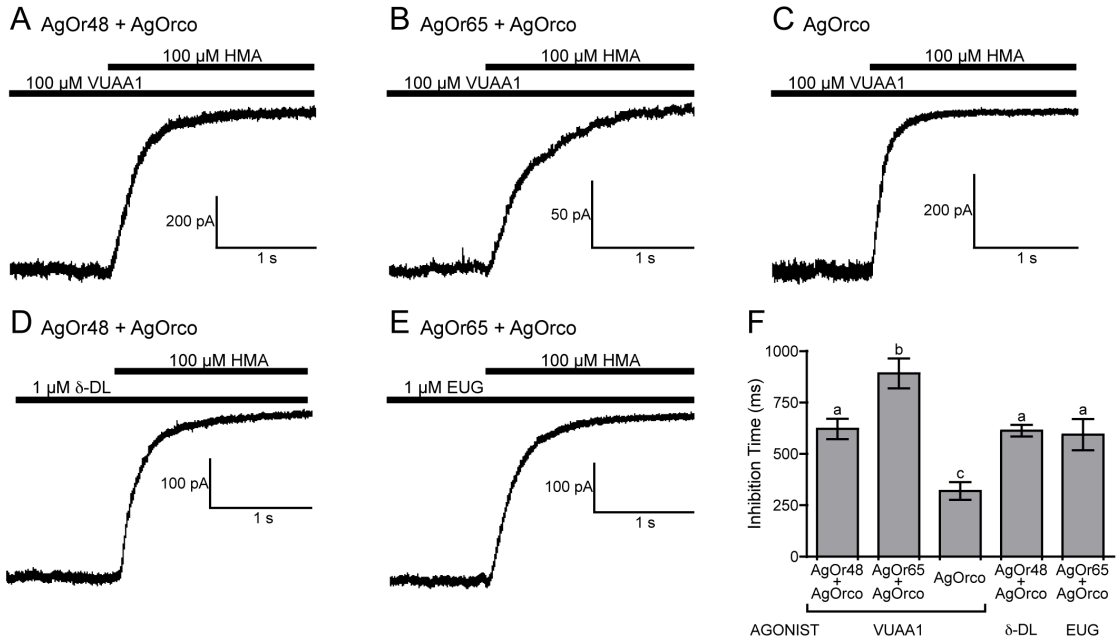

Figure 4.6 The rate of current inhibition by HMA varies among AgOr complexes. (**A-E**) Representative whole-cell currents of steady-state activation by either VUAA1 (100 µM) or odorant (1 µM) that were subsequently blocked by application of 100 µM HMA. (**F**) Histogram of the inactivation time (mean ± SEM, *n* = 5), or the time required to reduce the steady-state current from 90% maximal current to 10%, of the AgOr complexes. The holding potential for each recording was -60 mV and the solutions were Extracellular 2 and Internal 2. Statistically different groups determined by an ANOVA and a Bonferroni post test ($P<0.05$) are denoted by a, b, and c.

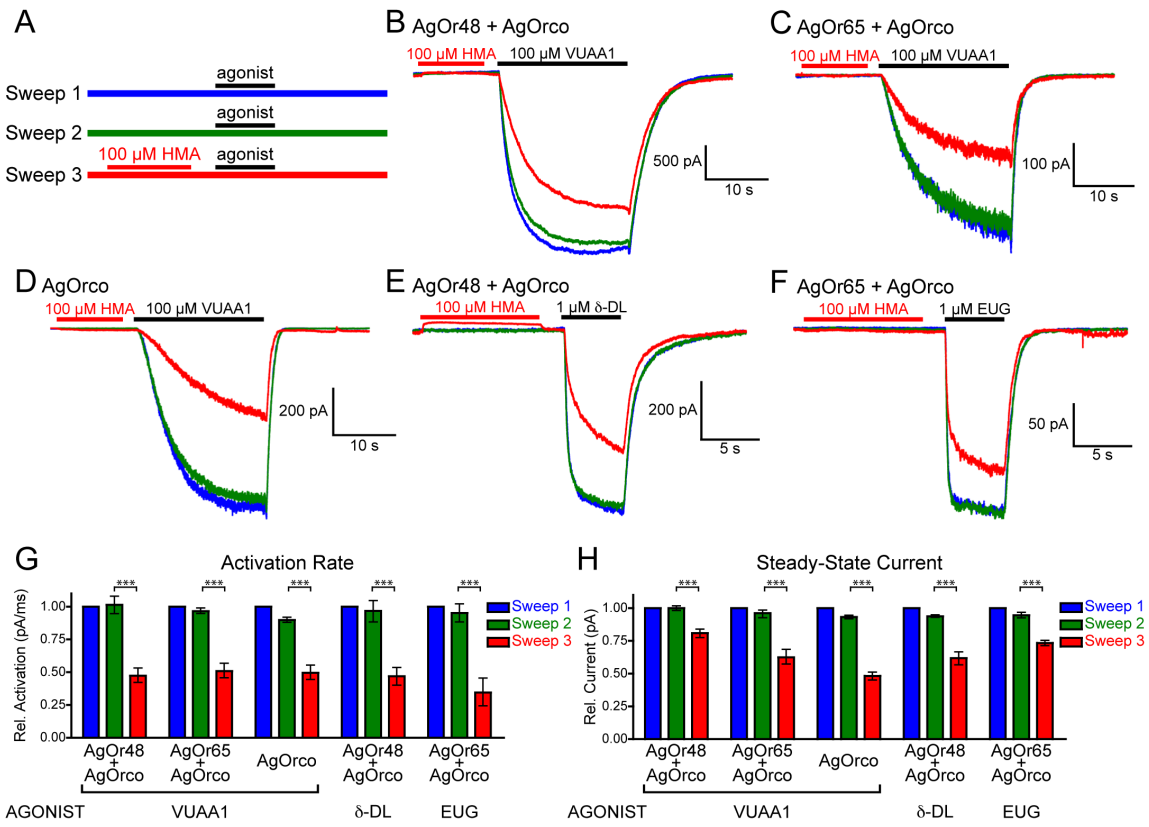

Figure 4.7 HMA can bind AgOr complexes in the absence of agonist. (**A**) Schematic of the assay consisting of 3 recording sweeps each containing a stimulation of agonist. Before the agonist application in Sweep 3, a 10 s pulse of HMA (100 µM) was applied to the cell. (**B-F**) Whole-cell recordings on several AgOr complexes as described in Figure 7A. The holding potential for each recording was -60 mV and the solutions were Extracellular 2 and Internal 2. The effect of HMA on AgOr48 + AgOrco baseline currents is further examined in Figure S3. (**G-H**) Histograms of both the activation rate from 10% to 90% maximal current (**G**) and the steady-state current (**H**) for each sweep (n = 5). The values for Sweeps 2 and 3 are normalized to Sweep 1 and compared with an ANOVA and Bonferroni post test (*** = P<0.001)

evidence that HMA can bind to and block the spontaneous opening currents of the AgOr48 complex and suggests that this complex has a higher rate of spontaneous opening than other AgOr complexes.

Discussion

This study identifies several amiloride derivatives that are capable of blocking insect OR ion channels when activated by an odorant ligand. The most potent blockers were HMA and MIA, and these derivatives were also able to block both heteromeric and homomeric currents during VUAA1 activation. Although the OR amiloride-binding domain remains uncharacterized, these data suggest that this site retains its susceptibility to amiloride derivatives, independent of the type of OR agonist or the tuning OR subunits present in the channel complex.

Though all of the OR complexes tested were susceptible to amiloride blockade, significant differences in sensitivity to the different analogs were observed. Indeed, the potencies of 3 amiloride derivatives were found to vary significantly between AgOr48 and AgOr65, the greatest of which was DMA, with nearly an order of magnitude difference in the IC_{50} values. Assuming that the site of amiloride blockade is within the OR channel pore as it is in ENaC, these data are in agreement with previous findings that the odorant-specific OR makes a significant contribution to the pore domain[2-4,18].

Interestingly, both the AgOr48 and AgOr65 cell lines were more susceptible to HMA and MIA blockade when activated by VUAA1 compared with

gating by an odorant molecule. This effect could be due to the presence of functional homomeric Orco channels in the heteromeric AgOr cell lines or could suggest that the VUAA1-bound open state is more susceptible to amiloride blockade than the odorant-gated state. Homomeric AgOrco currents were more sensitive to HMA blockade than the heteromeric AgOr complexes, suggesting that the lack of an odorant-binding OR subunit results in a unique pore structure that is more sensitive to amilorides. These observations support the current model in which each insect OR complex exhibits a diverse channel pore, with significant contributions from both the Orco coreceptor and the odorant-sensitive OR [2-4]. Moreover, the differences in HMA susceptibility among Orco orthologs suggest that, despite the high conservation of this protein across insect taxa, the non-conserved residues give rise to observable functional differences.

Although the precise mechanism of insect OR channel block by amiloride derivatives is still unknown, it appears that HMA is capable of binding and blocking ORs in the absence of agonist. In light of the well-established spontaneous opening of OR complexes, it cannot be determined whether HMA can bind to any channel state or only to the open channel[1,8]. We believe the reduction of baseline current upon HMA application observed in AgOr48 + AgOrco cells reflects a higher spontaneous opening probability for AgOr48+AgOrco complexes than either AgOr65 + AgOrco and AgOrco channels. It is reasonable to assume these OR-specific channel properties underlie the differences in spontaneous spike frequency previously observed in *Drosophila* ORNs in both endogenous neurons and the empty neuron[19].

These studies demonstrate that amiloride derivatives can serve as potent pharmacological blockers of OR channels across 4 insect orders and can likely facilitate future mechanistic studies of these complexes, whether carried out in heterologous or *in vivo* systems. Furthermore, although both amilorides and ruthenium red have the ability to block many other types of ion channels, the large library of amiloride analogs may ultimately foster the identification of more specific blockers of insect ORs. Along with other molecular and pharmacological tools, the utilization of amiloride derivatives can lead to a greater understanding of the complex mechanisms involved in OR-based signal transduction in insects. This may ultimately lead to the development of novel approaches to modulate critical olfactory behaviors in agricultural pests, disease vectors and other insects of global importance.

Materials and Methods

Chemicals

The odorants, δ-decalactone (CAS 705-86-2) and eugenol (CAS 97-53-0), were purchased from Sigma-Aldrich. VUAA1 (N-(4-ethylphenyl)-2-((4-ethyl-5-(3-pyridinyl)-4H-1,2,4- triazol-3-yl)thio)acetamide) was purchased from ChemBridge corporation (ID# 7116565). The following amiloride derivatives were ordered from Sigma-Aldrich: Amiloride hydrochloride hydrate (**Amiloride**), CAS 2016-88-8; 5-(*N*,*N*-Dimethyl)amiloride hydrochloride (**DMA**), CAS 1214-79-5; 5-(N-Ethyl-N-isopropyl)amiloride (**EIPA**), CAS 1154-25-2; 5-(N-Methyl-N-isobutyl)amiloride (**MIA**), CAS 96861-65-3; 5-(N,N-Hexamethylene)amiloride (**HMA**), CAS

1428-95-1; Phenamil methanesulfonate salt (**Phenamil**), CAS 1161-94-0; and 3',4'-Dichlorobenzamil hydrochloride (**DCBA**), CAS 1166-01-4. All of the above compounds were initially dissolved in DMSO and subsequently diluted in extracellular solution at a final concentration of 0.2% DMSO.

Cell Culture and Patch Clamp Electrophysiology

The generation and use of OR-expressing cell lines have been previously described[20]. Cells were incubated with 0.3 µg/mL tetracycline for 16-24 h before the assay to induce OR expression.

Whole-cell patch clamp recordings were measured using an Axopatch 200B amplifier (Molecular Devices) and a Digidata 1322A (Molecular Devices) with a sampling rate of 10kHz and low-pass filtered at 5kHz. Holding potentials were between -60 and -50 mV, and all compound solutions were applied under continuous focal perfusion with either a Perfusion Pencil (Automate Scientific) or an RSC-160 rapid solution changer (Bio-Logic Science Instruments). Extracellular solutions contained (in mM) 140 NaCl; 1 $CaCl_2$; 0-1 $MgCl_2$; 5 KCl; 10 HEPES (Extracellular 1) or 130 NaCl, 34 glucose, 10 HEPES, 1.5 $CaCl_2$, 1.3 KH_2PO_4, 0.5 $MgSO_4$ (Extracellular 2) and the internal solutions contained either 140 NaCl; 1-2 EGTA; 10 HEPES (Internal 1) or 120 KCl, 30 glucose, 10 HEPES, 2 $MgCl_2$, 1.1 EGTA, 0.1 $CaCl_2$ (Internal 2). All solutions had a pH 7.35-7.4 and were adjusted with either Trizma-base (Sigma) or NaOH.

Data Analysis

Current recordings were analyzed in pCLAMP 10 (Molecular Devices) and inhibition curves were generated with Prism 4 (Graphpad). Curves were fit with a sigmoidal dose-response (variable slope) Hill equation with 1.0 set as the top curve constraint. An ANOVA with a Bonferroni post test were used for all IC_{50} and histogram comparisons and were performed in Prism 4 (Graphpad).

References

1. Jones, P. L., Pask, G. M., Rinker, D. C. & Zwiebel, L. J. Functional agonism of insect odorant receptor ion channels. *Proceedings of the National Academy of Sciences* **108**, 8821–8825 (2011).

2. Nichols, A. S., Chen, S. & Luetje, C. W. Subunit contributions to insect olfactory receptor function: channel block and odorant recognition. *Chem Senses* **36**, 781–790 (2011).

3. Pask, G. M., Jones, P. L., Rützler, M., Rinker, D. C. & Zwiebel, L. J. Heteromeric Anopheline odorant receptors exhibit distinct channel properties. *PLoS ONE* **6**, e28774 (2011).

4. Nakagawa, T., Pellegrino, M., Sato, K., Vosshall, L. B. & Touhara, K. Amino Acid residues contributing to function of the heteromeric insect olfactory receptor complex. *PLoS ONE* **7**, e32372 (2012).

5. Chen, S. & Luetje, C. W. Identification of New Agonists and Antagonists of the Insect Odorant Receptor Co-Receptor Subunit. *PLoS ONE* **7**, e36784 (2012).

6. Jones, P. L. *et al.* Allosteric antagonism of insect odorant receptor ion channels. *PLoS ONE* **7**, e30304 (2012).

7. Nakagawa, T., Sakurai, T., Nishioka, T. & Touhara, K. Insect sex-pheromone signals mediated by specific combinations of olfactory receptors. *Science* **307**, 1638–1642 (2005).

8. Sato, K. *et al.* Insect olfactory receptors are heteromeric ligand-gated ion channels. *Nature* **452**, 1002–1006 (2008).

9. Kleyman, T. R. & Cragoe, E. J. Amiloride and its analogs as tools in the study of ion transport. *J Membr Biol* **105**, 1–21 (1988).

10. Ugawa, S. *et al.* Amiloride-blockable acid-sensing ion channels are leading acid sensors expressed in human nociceptors. *J. Clin. Invest.* **110**, 1185–1190 (2002).

11. Bobkov, Y. V. & Ache, B. W. Block by amiloride derivatives of odor-evoked discharge in lobster olfactory receptor neurons through action on a presumptive TRP channel. *Chem Senses* **32**, 149–159 (2007).

12. Abuin, L. *et al.* Functional architecture of olfactory ionotropic glutamate receptors. *Neuron* **69**, 44–60 (2011).

13. Wang, G., Carey, A. F., Carlson, J. R. & Zwiebel, L. J. Molecular basis of odor coding in the malaria vector mosquito Anopheles gambiae. *Proceedings of the National Academy of Sciences* **107**, 4418–4423 (2010).

14. Pask, G. M., Romaine, I. M. & Zwiebel, L. J. The Molecular Receptive Range of a Lactone Receptor in Anopheles gambiae. *Chem Senses* **38**, 19-25 (2013)

15. Zhou, X. *et al.* Phylogenetic and transcriptomic analysis of chemosensory receptors in a pair of divergent ant species reveals sex-specific signatures of odor coding. *PLoS Genet* **8**, e1002930 (2012).

16. Wang, G., Vásquez, G. M., Schal, C., Zwiebel, L. J. & Gould, F. Functional characterization of pheromone receptors in the tobacco budworm Heliothis virescens. *Insect Mol Biol* **20**, 125–133 (2011).

17. Hull, J. J., Hoffmann, E. J., Perera, O. P. & Snodgrass, G. L. Identification of the western tarnished plant bug (Lygus hesperus) olfactory co-receptor Orco: Expression profile and confirmation of atypical membrane topology. *Arch Insect Biochem Physiol* **81**, 179–198 (2012).

18. Kelly, O. *et al.* Characterization of an amiloride binding region in the alpha-subunit of ENaC. *Am. J. Physiol. Renal Physiol.* **285**, F1279–90 (2003).

19. Hallem, E. A., Ho, M. G. & Carlson, J. R. The molecular basis of odor coding in the Drosophila antenna. *Cell* **117**, 965–979 (2004).

20. Bohbot, J. D. *et al.* Conservation of indole responsive odorant receptors in mosquitoes reveals an ancient olfactory trait. *Chem Senses* **36**, 149–160 (2011).

Supporting Information

Table S4.1 IC_{50} values for the amiloride derivatives on each receptor complex

Receptor Complex	Agonist	Amiloride Derivative	# of trials (n)	IC_{50} value (logM ± SEM)
AgOr48 + AgOrco	δ-decalactone	Amiloride	5	-2.97 ± 0.03
		DMA	9	-4.61 ± 0.05
		EIPA	9	-4.82 ± 0.07
		MIA	9	-4.98 ± 0.02
		HMA	7	-5.05 ± 0.02
		Phenamil	10	-4.19 ± 0.02
		DCBA	9	-4.59 ± 0.01
	VUAA1	MIA	5	-5.40 ± 0.04
		HMA	5	-5.41 ± 0.04
AgOr65 + AgOrco	eugenol	Amiloride	4	-2.97 ± 0.03
		DMA	8	-3.79 ± 0.03
		EIPA	7	-4.74 ± 0.04
		MIA	7	-5.07 ± 0.02
		HMA	9	-5.22 ± 0.04
		Phenamil	7	-4.19 ± 0.04
		DCBA	8	-4.80 ± 0.04
	VUAA1	MIA	5	-5.38 ± 0.06
		HMA	5	-5.68 ± 0.03
AgOrco	VUAA1	MIA	5	-5.72 ± 0.04
		HMA	5	-5.86 ± 0.02
HsOrco	VUAA1	HMA	5	-6.07 ± 0.04
HvOrco	VUAA1	HMA	5	-5.86 ± 0.03
LhOrco	VUAA1	HMA	5	-5.62 ± 0.04

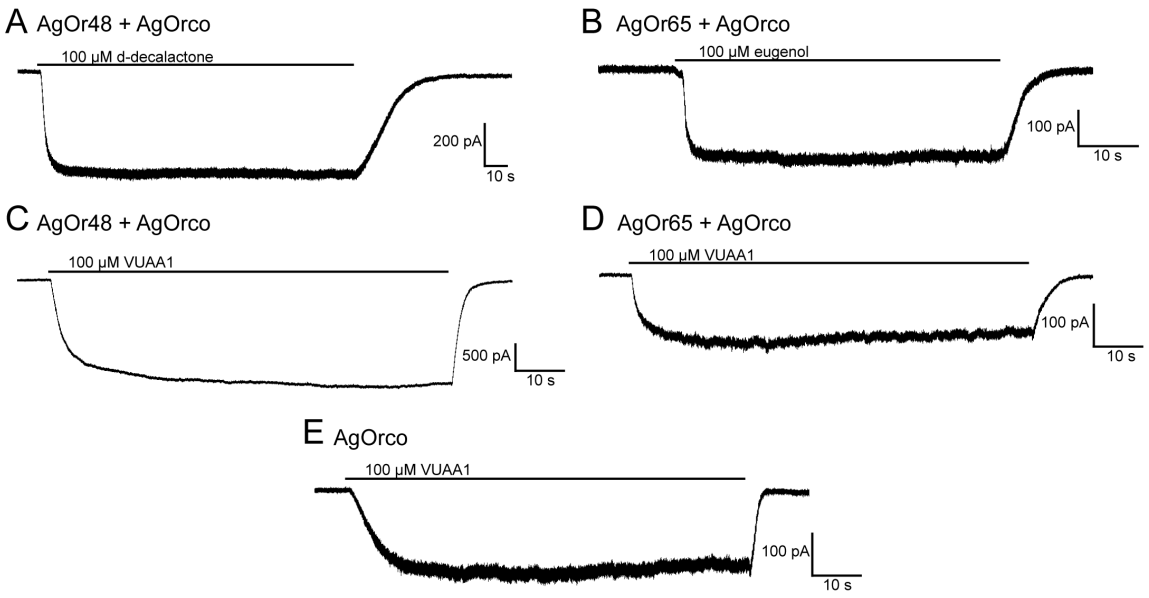

Figure S4.1 Prolonged agonist application produces steady-state currents that do not decrease over time. Holding potentials for each recording were -60mV.

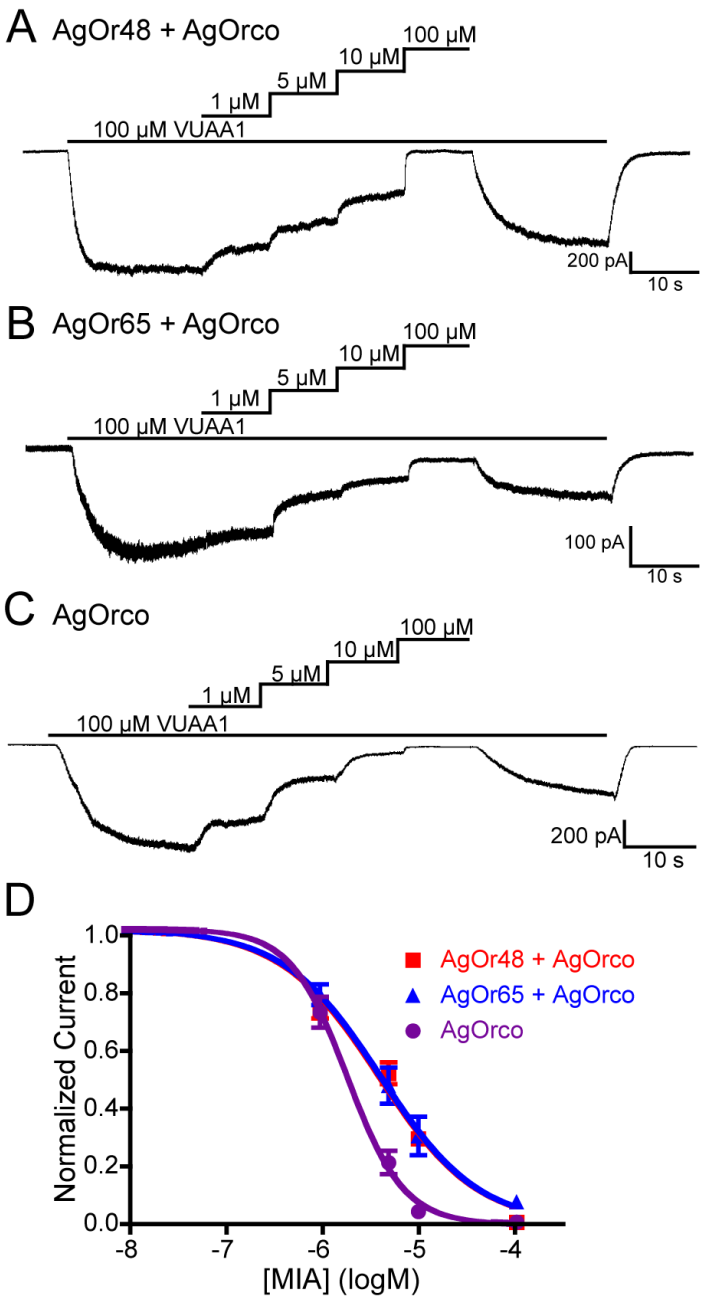

Figure S4.2 VUAA1-evoked currents are blocked by MIA. (**A-C**) Representative current traces from either AgOr48 + AgOrco (**A**), AgOr65 +AgOrco (**B**), or AgOrco (**C**) cells during stimulation with 100µM VUAA1. Increasing amounts of MIA resulted in a reduction of VUAA1-evoked current that was partially irreversible after amiloride wash-out. The holding potential for each recording is -60 mV and the solutions were Extracellular 2 and Internal 2. (**D**) Inhibition curves for MIA for each complex, with data points representing the normalized mean ± SEM of the current reduction. IC_{50} values and the number of trials (*n*) can be found in Table S4.1.

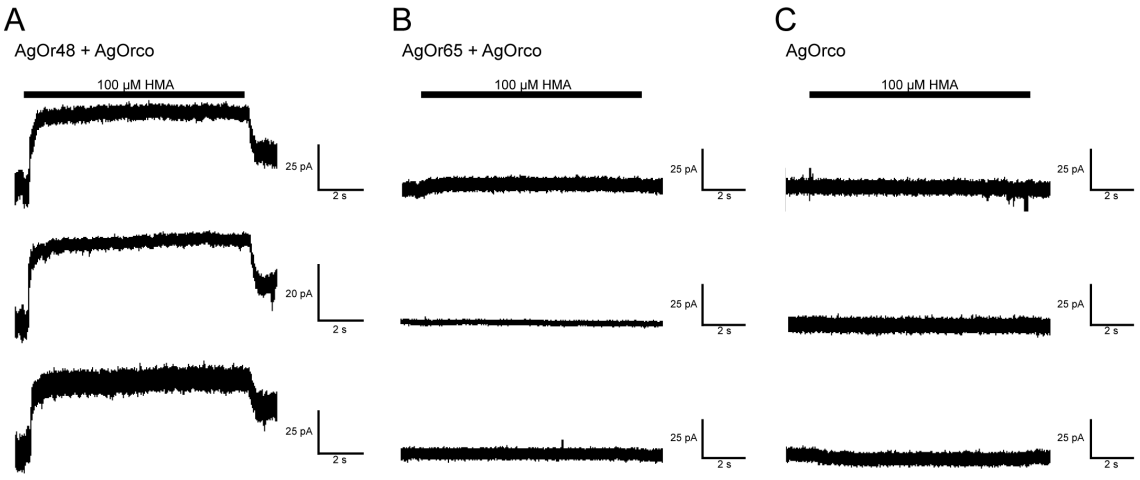

Figure S4.3. HMA reduces the current baseline of AgOr48 + AgOrco cells. (**A-C**) Three representative whole-cell currents during application of 100 µM HMA to each AgOr complex. Note that the baseline in in AgOr48 + AgOrco cells does not return to the original current level after HMA washout, suggesting the presence of bound HMA to the complex

CHAPTER V

THE MOLECULAR RECEPTIVE RANGE OF A LACTONE RECEPTOR IN *ANOPHELES GAMBIAE*

Gregory M. Pask, Ian M. Romaine, Laurence J. Zwiebel

Preface

The work from this chapter was published in *Chemical Senses* (2013, 38(1) pp. 19-25) and examines the structural features of odorant agonist that are necessary in activating a specific AgOr complex. Here, I designed and performed all experiments, while Ian Romaine synthesized two ε-lactones that were not commercially available. I wrote the manuscript with comments from the other coauthors. This work was supported by the National Institutes of Health [AI056402] and the Foundation for the National Institutes of Health through the Grand Challenges in Global Health Initiative [VCTR121] to L.J.Z. I am supported in part by the National Institute on Deafness and Other Communication Disorders at the National Institutes of Health through an NRSA F31 [DC011989].

Introduction

Although several studies have identified odorant ligands for numerous tuning ORs of various insects, the molecular mechanisms underlying ligand-OR activation, binding, and gating remain uncertain. Defining the molecular receptive range of an OR can provide insight into its interaction with an odorant ligand. Through functional screens with a wide range of odorants, the chemical characteristics (function groups, ring size, chain length, etc.) that are critical for

receptor activation can be determined[1]. Further examination of the chemical properties can be used to support a pharmacophore model, a generalized ligand structure that provides insight into the presumed OR binding pocket.

In an effort to better understand the olfactory system of *Anopheles gambiae*, the principal afro-tropical malaria vector, heterologous screens using broad panels of odorant stimuli have deorphanized several of the *An. gambiae* ORs (AgOrs)[2-4]. However lactones, or cyclic esters, which have been identified as important semiochemicals in mosquitoes and other insects were under-represented in the odorant panels utilized in these studies. For example, erythro-6-acetoxy-5-hexadecanolide has been identified as the major component of oviposition pheromone in egg rafts of *Culex pipiens fatigans*[5]. In hermit beetles, *Osmoderma eremita*, males produce R-(+)-γ-decalactone as a sex pheromone, and are known for their fruity, peach-like odor profile[6]. In addition to these animal sources of lactones, numerous flower and fruit volatiles contain mixtures of lactones[7]. One study utilized several lactones identified in ripe peaches to elicit olfactory responses in the antennae of the fruit-piercing moth, *Oraesia excavata*[8]. Also, volatile fractions from some monofloral honeys have been found to contain different lactone species, and honey is attractive to both male and female *An. gambiae* seeking a sugar meal[9,10]. Taken together, animal- and plant-derived lactones may have a role in the chemical ecology of *An. gambiae*, specifically in the selection of sugar sources and oviposition sites.

In initial odorant panel screenings of tuning ORs from *An. gambiae*, γ-decalactone elicited the strongest responses from *Xenopus* oocytes expressing

AgOr48 and AgOrco, with much weaker responses from 2-nonanone and 1-octanol[3]. AgOr30 and AgOr57 also responded to γ-decalactone, albeit with lower sensitivity; each of these AgOr's also responded more strongly to several other agonists[3]. AgOr48 is expressed in antennal structures during the larval and adult stages and was found to respond to another lactone, δ-undecalactone[2,11,12]. In this study, we further explored the molecular receptive range of AgOr48 by determining the effects of chain length, ring size, and chirality on agonist potency and have determined a preliminary pharmacophore.

Results

In order to assay odorants of potential ecological relevance to *An.* gambiae, the panel used in this study represents lactones commonly found in nature. These consist of various lactone ring sizes, including five- (γ), six- (δ), and seven- (ε) membered rings; α- and β- lactones are less common due to the decreased stability of the three- and four- membered rings, respectively. Additionally, lactones with variation in the carbon side chain length were selected to determine the optimal chain length for agonist activity. Altogether, the selected panel of lactones examines the effects of ring size and side chain length on the efficiency of AgOr48 agonists.

A panel of γ-lactones with side chains ranging from two to eight carbons was applied to AgOr48 + AgOrco-expressing HEK cells at a concentration of 1μM (Figure 5.1A). In whole cell patch clamp studies, larger current amplitudes were elicited by γ-lactones with five- to seven-carbon side chains, with

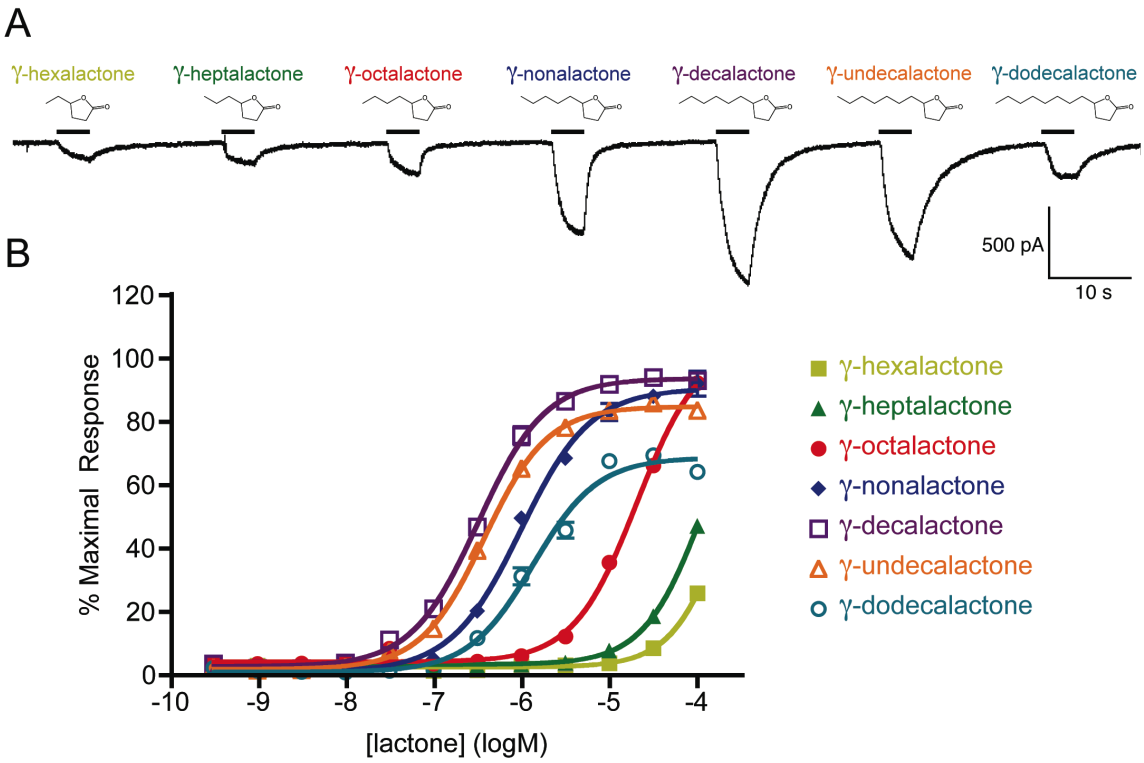

Figure 5.1 AgOr48-expressing HEK cells respond to γ-lactones. (**A**) Whole-cell recording of an AgOr48 + AgOrco cell responding to 1μM concentrations of lactone. Holding potential is −60mV. (**B**) Concentration-response curves generated from Ca^{++}-imaging assays on AgOr48 + AgOrco cells (n=4). Data points represent the mean ± SEM and percent maximal response is normalized to the plate standard, δ-decalactone. EC_{50} values from the curve fit can be found in Table S5.1.

γ-decalactone producing the largest. In these studies, repeated stimulation with the lactone panel resulted in decreased current amplitudes for some strong agonists (Figure S5.1). Calcium mobilization assays were subsequently performed in order to generate concentration-response curves and remove the desensitization effects of repeated agonist application (Figure 5.1B). The general trend observed in the whole-cell recording of Figure 5.1A correlated with the concentration-response curve data, as γ-decalactone was the most potent agonist with an EC_{50} value of −6.49 ± 0.02 logM. These observations suggest that with a γ-lactone ring structure, the six-carbon chain yields the optimal agonist activity.

We next examined the responses to a series of δ-lactones with side chains of three to nine carbons, where several δ-lactones elicited robust currents in the AgOr48 + AgOrco cells (Figure 5.2A). The concentration-response curves from Ca^{++}-imaging assays reveal three lactone agonists, δ-decalactone (−6.84 ± 0.03 logM), δ-undecalactone (−6.81 ± 0.03 logM), and δ-dodecalactone (−7.01 ± 0.03 logM) that are clearly more potent than the other compounds (Figure 5.2B). As was the case with the γ-lactones, the five- to seven- carbon chain δ-lactones elicited the most potent AgOr48 responses.

In order to test a series of ε-lactones, we synthesized both ε-undecalactone and ε-tridecalactone to supplement ε-decalactone and ε-dodecalactone, which are commercially available (see Materials and methods). Initial whole-cell recordings showed current responses to all ε-lactones at 1μM, with the largest amplitudes resulting from ε-undecalactone and ε-dodecalactone

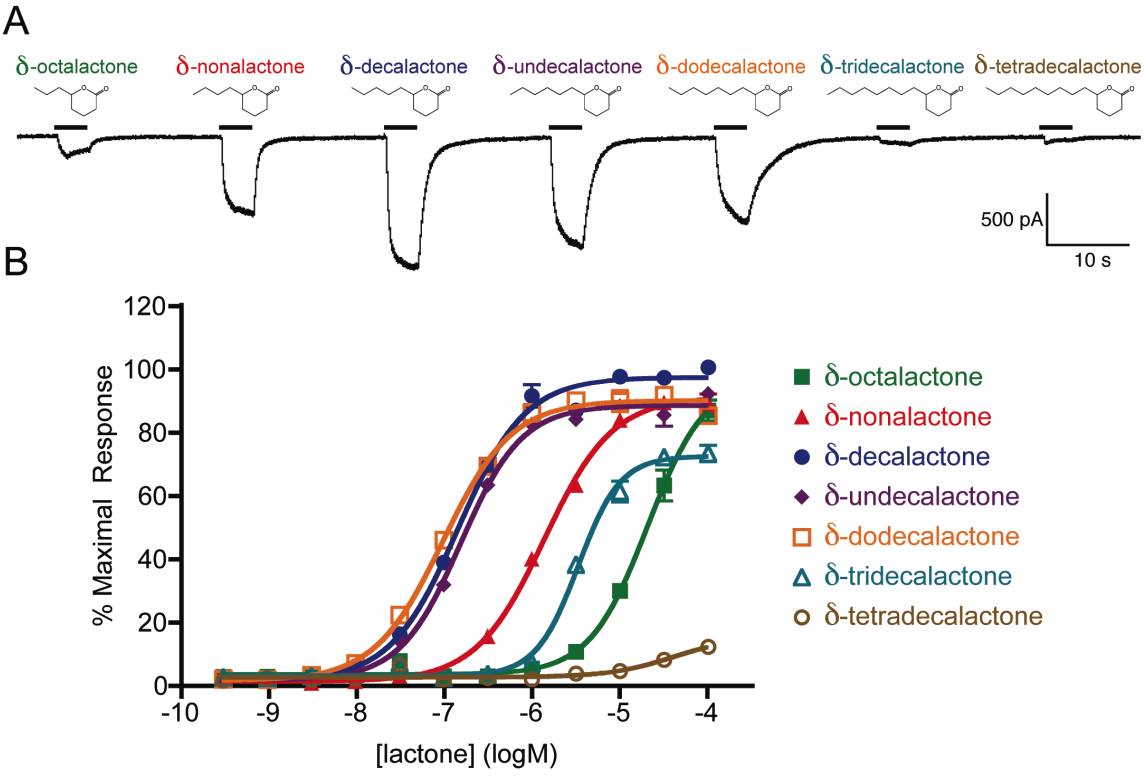

Figure 5.2 Several δ-lactones gate the AgOr48 complex. (**A**) Current responses of an AgOr48 + AgOrco-expressing cell during application of various δ-lactones (1μM). Holding potential is −60mV. (**B**) Concentration-response curves generated from Ca^{++}-imaging assays on AgOr48 + AgOrco cells (n=4). Data points represent the mean ± SEM and percent maximal response is normalized to the plate standard, δ-decalactone. EC_{50} values from the curve fit can be found in Table S5.1.

(Figure 5.3A). The most potent ε-lactone was ε-dodecalactone, with an EC_{50} value of −6.69 ± 0.04 logM (Figure 5.3B). Also, agonist potency decreased greatly with the addition of a single carbon to the side chain (ε-tridecalactone, −5.83 ± 0.03 logM).

These studies of the molecular receptive range of AgOr48 to lactone agonists facilitate the construction of an initial pharmacophore model. From the EC_{50} values of each agonist, it appears that lactones with a six-carbon chain are the most potent in gating the AgOr48 complex (Figure 5.4). Additionally, the δ-lactone ring offers the most flexibility in chain length in terms of potency, with the five- or seven-carbon chain δ-lactones displaying near-equal potencies. It is also interesting to note that AgOr48 displays relatively high sensitivity (≤1μM) to several of the lactones in the panel.

Because the carbon that links the side chain to the lactone ring is chiral, we next determined if AgOr48 is enantioselective, and thus able to differentiate between the R-(+) and S-(−) forms of a lactone agonist. AaOr8, an enantioselective mosquito OR from *Aedes aegypti*, is ~100-fold more sensitive to R-(−)-1-octen-3-ol than the S-(+) form[13]. Both enantiomers of the strong AgOr48 agonist, δ-decalactone, were commercially available and elicited differential currents at equimolar concentrations (Figure 5.5A). Indeed, these differences were observed in the concentration-response curves where R-(+)-δ-decalactone (EC_{50} −7.01 ± 0.02 logM) was a significantly more potent AgOr48 agonist than the S-(−) enantiomer (EC_{50} −6.41 ± 0.02 logM) (Figure 5.5B). These results

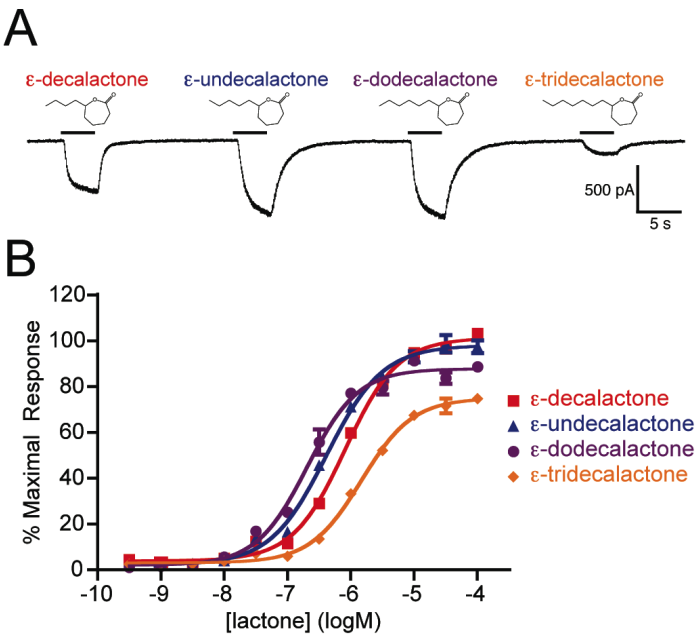

Figure 5.3 The AgOr48 complex responds to ε-lactones. (**A**) Representative whole-cell currents of an AgOr48 + AgOrco cell during application of various ε-lactones (1μM). Holding potential is −60mV. (**B**) Concentration-response curves generated from Ca^{++}-imaging assays on AgOr48 + AgOrco cells (n=4). Data points represent the mean ± SEM and percent maximal response is normalized to the plate standard, δ-decalactone. EC_{50} values from the curve fit can be found in Table S5.1.

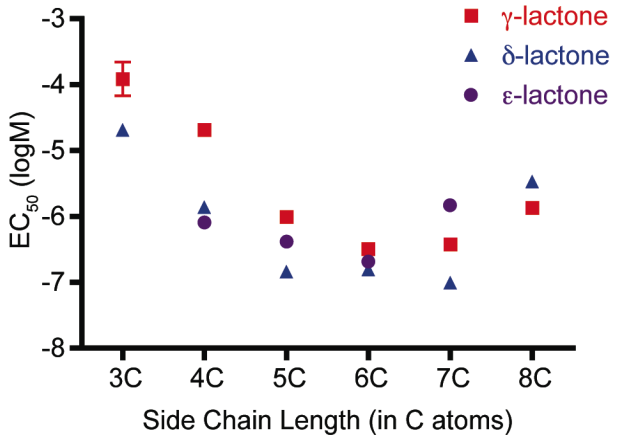

Figure 5.4 Lactone potency depends on side chain length and ring size. Plot of EC_{50} values by number of carbons in the side chain and the lactone ring structure. Data points represent mean ± SEM, and exact values can be found in Table S5.1.

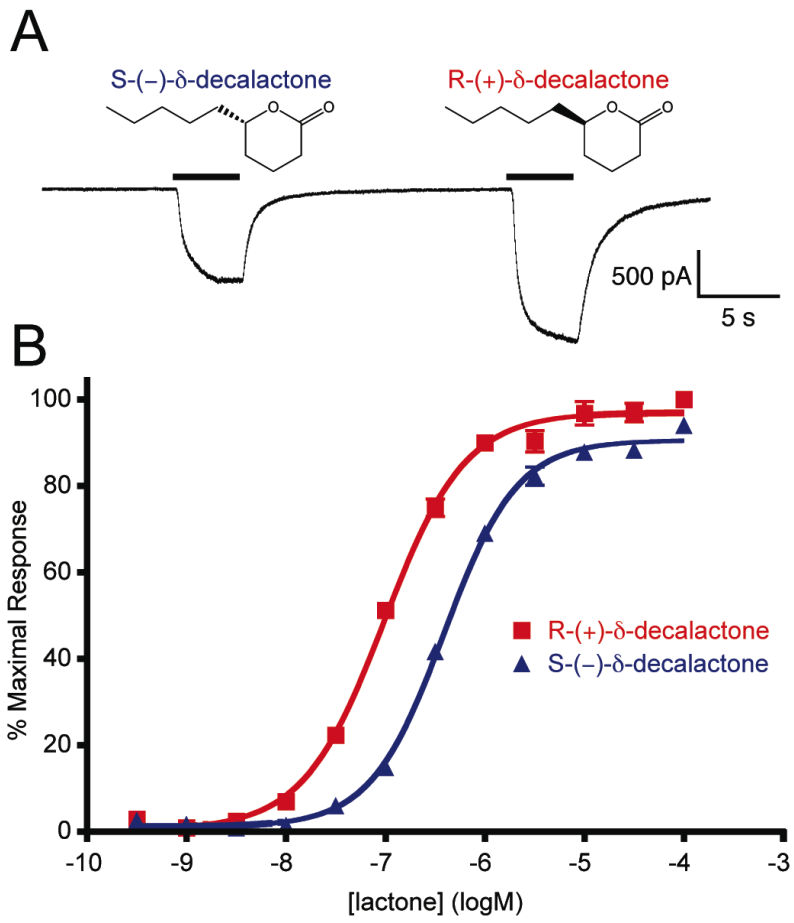

Figure 5.5 Enantiomers of δ-decalactone display different agonist potencies on AgOr48 cells. (**A**) A current recording from an AgOr48 + AgOrco cell during a 1μM application of S-(–)-δ-decalactone and R-(+)-δ-decalactone. Holding potential is –60mV. (**B**) Concentration-response curves generated from Ca^{++}-imaging assays on AgOr48 + AgOrco cells (n=4). Data points represent the mean ± SEM and percent maximal response is normalized to the plate standard, δ-decalactone. The EC_{50} values from the curve fit differ significantly between the R- and S-enantiomers (P<0.0001, F test) and can be found can be found in Table S5.1.

demonstrate that the AgOr48 complex is able to effectively discriminate between these chiral lactone agonists.

Discussion

We have used an odorant panel of straight-chain lactones to explore the molecular receptive range of AgOr48 and have identified several additional potent agonists. From these data, we can conclude that AgOr48 is most sensitive to lactones with a five- to seven-carbon side chain, and that the six-membered δ-lactone ring structure typically results in more potent agonists. It should be noted that several ketones and alcohols are capable of eliciting less potent responses from AgOr48, and it remains unclear whether this occurs at the same site as lactone recognition[3,4]. Furthermore, AgOr48 appears to be enantioselective, with a preference towards the R-(+) configuration of δ-decalactone. These differences are not as sizeable when compared with the previously observed enantioselective mosquito OR, but suggest that the lactone-binding site of AgOr48 is capable of discriminating the two side chain positions on the lactone ring[14]. In addition, the R-(+) configuration of the larger straight chain lactones (five carbons and above) appears to be more abundant in several fruit species[15]. The resulting preliminary pharmacophore for AgOr48 lactone agonists consists of a six-membered lactone ring (± one carbon) with a side chain of five to seven carbons in an R-(+) conformation at the chiral center.

Our initial hypothesis was that the specificity of AgOr48 to lactones might play a role in the chemical ecology of *An. gambiae*. We were specifically

interested in nectar-feeding and oviposition, as several of the strong lactone agonists identified here are naturally abundant in a range of plant flowers and fruits[7]. This would be consistent with our hypothesis that lactones function as semiochemicals, signaling a potential sugar source for *An. gambiae*. Indeed, several fruits that have recently been associated with field-caught *An. gambiae* contain many of these lactones in their volatile profiles. One study observed an abundance of *An. gambiae* males associated with *Mangifera indica*, the common mango tree, and observed attraction to *M. indica* odor using a Y-shaped olfactometer[16]. The aroma of *M. indica* is largely dependent on a mixture of several straight chain γ- and δ-lactones, many of which display agonist activity against AgOr48[7,17]. Another field study in Mali found that the most attractive fruits to both male and female *An. gambiae* were guava (*Psidium guajava*) and honey melon (*Cucumis melo*)[18]. In studies analyzing the volatile constituents of these fruits, γ-decalactone has been implicated as a major component of guava odor, and the skin and pulp of the honey melon contain several γ- and δ-lactones[7,19]. Taken together, although we recognize that AgOr48 may be part of a larger suite of dedicated ORs that cooperatively discriminate among structurally-divergent lactones, it is likely that the lactone specificity of AgOr48 plays a role in the attraction of adult *An. gambiae* to sugar sources.

AgOr48 displayed high sensitivity (≤1μM) to nine of the tested lactones, and this may play a significant role in detecting mixtures of lactones from fruit volatiles. In nature, lactone-containing fruit volatiles typically consist of complex odor blends that are comprised of several compound species in distinct ratios,

rather than a single lactone[15]. Olfactory-driven behaviors in insects are often driven by blends rather than single odorants, as observed in field experiments with *O. excavata*[8]. Although the moth responded robustly to several individual lactones in electroantennograms, which can be used to assess peripheral signaling, only the mixture of lactones was effective in capturing *O. excavate* in field traps[8]. Similarly, complex blends of lactones, as well as other odorants, are likely required for *An. gambiae* in locating a sugar source.

This study extends our characterization of AgOr48 as a lactone receptor, capable of activation by several straight-chain lactones at relatively low concentrations. Although its exact role in *An. gambiae* chemical ecology is still unknown, we suggest that AgOr48 plays a role in locating lactone containing sugar sources. Finally, we have investigated the molecular receptive range and proposed a preliminary lactone pharmacophore of AgOr48, which provides further insight into the mechanisms of odorant-OR interaction.

Materials and Methods

Chemicals

Supplier information and CAS numbers for purchased lactones are provided in Table S5.1. All assay compounds were first diluted in DMSO and subsequently diluted in assay buffer with a final DMSO concentration of 0.1%.

Synthesis of ε-undecalactone and ε-tridecalactone

General: All non-aqueous reactions were performed in flame-dried or oven dried round-bottomed flasks under an atmosphere of argon. Stainless steel syringes or cannulae were used to transfer air- and moisture-sensitive liquids. Reaction temperatures were controlled using a thermocouple thermometer and analog hotplate stirrer. Reactions were conducted at room temperature (RT, ~23°C) unless otherwise noted. Analytical thin-layer chromatography (TLC) was performed on E. Merck silica gel 60 F254 plates and visualized using UV, ceric ammonium molybdate, potassium permanganate, and anisaldehyde stains. Yields were reported as isolated, spectroscopically pure compounds.

Materials: Solvents were obtained from either an MBraun MB-SPS solvent system. Commercial reagents were used as received.

Procedure: To a solution of either 2-pentylcyclohexanone or 2-heptylcyclohexanone (100 mg, 0.59 mmol) in 11.5 mL of CH_2Cl_2 at 0^oC was added a solution of *m*-CPBA (205.4 mg, 1.19 mmol) in 2 mL of CH_2Cl_2. After 48 h at RT, saturated $NaHCO_3$ (50 mL) was added and the resulting solution stirred for 10 min. The aqueous layer was extracted with CH_2Cl_2 (3 x 50 mL). The combined organic layers were dried ($MgSO_4$), and concentrated to a residue. Each residue was purified by column chromatography with EtOAc/Hexane (1:4) to afford 35 mg (32%) of ε-undecalactone or 49 mg (45%) of ε-tridecalactone: ^1H NMR data matched published data for each product[20].

Cell culture, electrophysiology, and calcium imaging

The AgOr48 + AgOrco stable HEK cell line was previously generated[12]. Whole-cell patch clamp recording from AgOr48 + AgOrco cells were performed using previously described methods[21]. The calcium mobilization assays were performed using Fluo-4 AM dye and an FDSS600 plate reader (Hamamatsu) as described previously[21]. In a 384-well plate, each well contains an identical number of cells and is given a single agonist treatment to prevent desensitization due to repeated stimulations. Each of the 12 concentrations was done in quadruplicate. The generation of concentration response curves and the statistical analysis of the fitted curves values were completed in Prism 4 (GraphPad).

References

1. Bestmann, H. J., Wu, C. H., Dohla, B., Li, K. & Kaissling, K. E. Functional group recognition of pheromone molecules by sensory cells of Antheraea polyphemus and Antheraea pernyi (Lepidoptera: Saturniidae). *Z. Naturforsch* **42C**, 435–441 (1987).

2. Xia, Y. *et al.* The molecular and cellular basis of olfactory-driven behavior in Anopheles gambiae larvae. *Proceedings of the National Academy of Sciences* **105**, 6433–6438 (2008).

3. Wang, G., Carey, A. F., Carlson, J. R. & Zwiebel, L. J. Molecular basis of odor coding in the malaria vector mosquito Anopheles gambiae. *Proceedings of the National Academy of Sciences* **107**, 4418–4423 (2010).

4. Carey, A. F., Wang, G., Su, C.-Y., Zwiebel, L. J. & Carlson, J. R. Odorant reception in the malaria mosquito Anopheles gambiae. *Nature* **464**, 66–71 (2010).

5. Laurence, B. R. & Pickett, J. A. Erythro-6-acetoxy-5-hexadecanolide, the major component of a mosquito oviposition attractant pheromone. *J. Chem. Soc., Chem. Commun.* 59–60 (1982).

6. Svensson, G. P. & Larsson, M. C. Enantiomeric specificity in a pheromone-kairomone system of two threatened saproxylic beetles, Osmoderma eremita and Elater ferrugineus. *J Chem Ecol* **34**, 189–197 (2008).

7. Grab, W. Blended flavourings In: Ziegler, E. & Ziegler, H., editors *Flavourings: Production, Composition, Applications, Regulations*. Wiley-VCH, (1998).

8. Tian, R. *et al.* Electroantennographic responses and field attraction to peach fruit odors in the fruit-piercing moth, Oraesia excavata (Butler)(Lepidoptera: Noctuidae). *Applied entomology and zoology* **43**, 265–269 (2008).

9. Moreira, R. F. A., Trugo, L. C., Pietroluongo, M. & De Maria, C. A. B. Flavor composition of cashew (Anacardium occidentale) and marmeleiro (Croton species) honeys. *J. Agric. Food Chem.* **50**, 7616–7621 (2002).

10. Foster, W. A. & Takken, W. Nectar-related vs. human-related volatiles: behavioural response and choice by female and male Anopheles gambiae (Diptera: Culicidae) between emergence and first feeding. *Bull Entomol Res* **94**, 145–157 (2004).

11. Pitts, R. J., Rinker, D. C., Jones, P. L., Rokas, A. & Zwiebel, L. J. Transcriptome Profiling of Chemosensory Appendages in the Malaria Vector Anopheles gambiae Reveals Tissue- and Sex-Specific Signatures of Odor Coding. *BMC Genomics* **12**, 271 (2011).

12. Jones, P. L. *et al.* Allosteric antagonism of insect odorant receptor ion channels. *PLoS ONE* **7**, e30304 (2012).

13. Bohbot, J. & Dickens, J. Chiral Selectivity of an Insect Odorant Receptor. 1–14 (2009).

14. Bohbot, J. D. & Dickens, J. C. Characterization of an enantioselective odorant receptor in the yellow fever mosquito Aedes aegypti. *PLoS ONE* **4**, e7032 (2009).

15. Bernreuther, A., Christoph, N. & Schreier, P. Determination of the enantiomeric composition of γ-lactones in complex natural matrices using multidimensional capillary gas chromatography. *Journal of chromatography* **481**, 363–367 (1989).

16. Gouagna, L. C. *et al.* Patterns of sugar feeding and host plant preferences in adult males of An. gambiae (Diptera: Culicidae). *J Vector Ecol* **35**, 267–276 (2010).

17. Wilson, C., III, Shaw, P. & Knight, R., Jr Importance of some lactones and 2, 5-dimethyl-4-hydroxy-3 (2H)-furanone to mango (Mangifera indica L.) aroma. *J. Agric. Food Chem.* **38**, 1556–1559 (1990).

18. Müller, G. C. *et al.* Field experiments of Anopheles gambiae attraction to local fruits/seedpods and flowering plants in Mali to optimize strategies for malaria vector control in Africa using attractive toxic sugar bait methods. *Malar J* **9**, 262 (2010).

19. Aubert, C. & Pitrat, M. Volatile compounds in the skin and pulp of Queen Anne's pocket melon. *J. Agric. Food Chem.* **54**, 8177–8182 (2006).

20. Fellous, R., Lizzani-Cuvelier, L., Loiseau, M. & Sassy, E. Resolution of racemic-lactones. *Tetrahedron: Asymmetry* **5**, 343–346 (1994).

21. Jones, P. L., Pask, G. M., Rinker, D. C. & Zwiebel, L. J. Functional agonism of insect odorant receptor ion channels. *Proceedings of the National Academy of Sciences* **108**, 8821–8825 (2011).

Supporting Information

Table S5.1 Potency and efficacy of each lactone on the AgOr48 complex.

Name	CAS	Supplier	EC_{50} (logM)	% Maximal Response[b]
γ-hexalactone	695-06-7	Sigma	-3.61±1.32[a]	25.65±1.10
γ-heptalactone	105-21-5	Sigma	-3.91±0.26[a]	46.73±0.59
γ-octalactone	104-50-7	Sigma	-4.67±0.03	91.79±1.59
γ-nonalactone	104-61-0	Sigma	-6.01±0.03	91.55±3.95
γ-decalactone	706-14-9	Sigma	-6.49±0.02	92.50±1.41
γ-undecalactone	104-67-6	Sigma	-6.42±0.02	83.10±1.47
γ-dodecalactone	2305-05-7	Sigma	-5.87±0.04	63.86±2.15
δ-octalactone	698-76-0	Wako	-4.69±0.05	86.44±3.27
δ-nonalactone	3301-94-8	Wako	-5.86±0.02	88.91±2.71
δ-decalactone	705-86-2	Sigma	-6.84±0.03	100.00±1.55
δ-undecalactone	710-04-3	Sigma	-6.81±0.03	91.64±1.84
δ-dodecalactone	713-95-1	Sigma	-7.01±0.03	84.80±2.05
δ-tridecalactone	7370-92-5	Wako	-5.47±0.02	72.93±2.54
δ-tetradecalactone	2721-22-4	Wako	-4.39±0.35[a]	12.16±0.36
ε-decalactone	5579-78-2	Wako	-6.09±0.03	103.34±1.37
ε-undecalactone	N/A	synthesized	-6.39±0.03	97.62±2.76
ε-dodecalactone	16429-21-3	Wako	-6.69±0.04	88.81±1.06
ε-tridecalactone	N/A	synthesized	-5.83±0.03	74.92±1.24
R-(+)-δ-decalactone	2825-91-4	Wako	-7.01±0.02	100.00±0.82
S-(-)-δ-decalactone	59285-67-5	Wako	-6.41±0.02	94.02±0.87

[a] Low-potency CRCs do not reach a maximum efficacy, resulting in crude EC_{50} values.
[b] Relative to d-decalactone maximal response

CHAPTER VI

SUMMARY AND FUTURE DIRECTIONS

Summary

The findings presented in the previous chapters have furthered our understanding of the mechanisms of insect OR function. The identification of the Orco agonist, VUAA1, provides a powerful pharmacological tool that is already being used throughout the field to address questions in insect olfaction. We have used VUAA1 to examine the channel pore of different heteromeric OR complexes to determine the role of the tuning OR in conductive properties. In addition, several amiloride derivatives have been described as channel blockers and have elucidated functional differences in insect OR complexes. Finally, the molecular receptive range of a lactone receptor, which may have a role in sugar feeding, has been investigated and provides insight into the selectivity of odorant binding.

While much has been made about the potential activity of VUAA1 in the mass media, I feel it is still a long shot for this molecule to have an impact on insect control due to its lack of volatility and low potency. Additionally, the more potent VUAA1-analogs that have been identified all have increases in molecular weight. That said, I feel the concept of broad range activation of Orco-mediated neural circuits has the potential to significantly alter insect behavior. Collaboration with the lab of Jurgen Liebig has provided strong support of this theory. The antennae of an ant can be treated with VUAA1, and the individual displays a range of aggression behaviors toward its nestmates, presumably

because the ant can no longer recognize the odor profile of its own colony (personal communication).

Our work has identified that VUAA1 can activate Orco-containing channel complexes, but perhaps there are other binding sites on Orco that also allow for gating by small molecules. I propose that another small molecule screen on cells expressing only Orco (with VUAA1 as a positive control) could yield another set of exciting lead compounds. It would be ideal if the compound library used in the screen contained volatile molecules, as these could have a greater impact in modifying insect behavior as potential repellents. In addition to this screen, below are several other projects that I have proposed, some of which are currently in progress. Enjoy!

Using VUAA1 Analogs to Examine Orco Structure/Function

In relation to the work with the Orco agonist, VUAA1, our lab has generated several structural analogs to explore the structure/activity relationship (SAR). Some of these analogs have been shown to be more potent agonists, and others were identified as Orco antagonists[1,2]. Several of the other analogs have had no activity at all and it has lead to the idea that SAR around VUAA1 and its presumed binding pocket is rather tight[1].

Although we have do not have any insight into the location of a VUAA1-binding pocket on Orco, the use of this extensive library of VUAA1 analogs could be used to identify candidate binding pockets. Our lab has cloned or sub-cloned nine different Orcos, spanning four different insect orders, all of which respond to

VUAA1 (Figure 6.1). In addition, we have generated stable HEK lines expressing each of these orthologs. Through a parallel screen on each Orco cell line, the activities of each VUAA1-analog can be compared across the nine Orco orthologs. The proposed screen could reveal that some analogs are more potent on certain orthologs. A result like this could lead to further development from a chemical synthesis angle, where VUAA1-like agonists could be engineered to target a specific insect order.

This screen could also be informative from a structure/function standpoint. We could use potential differences in activation between Orco orthologs to highlight regions of the primary amino acid sequence. Although the Orco family is highly conserved, areas of divergence do exist and could give rise to altered activation by a VUAA1 analog. This result could prompt some elegant mutagenesis or chimeric studies, in which divergent residues or areas between Orco proteins could be swapped and then assayed for functional changes. Finally, these studies could point to residues in Orco that may be critical for VUAA1 binding.

I would like to put forth a few thoughts on the presumed binding pocket for VUAA1 and its analogs. Because of its complexity and lack of volatility, it seems very unlikely that an insect would encounter a molecule like VUAA1 in its lifetime. In this light, it is unusual that a VUAA1 binding site would be maintained through evolutionary history across different insect orders, as shown in Figure 6.1. Therefore, I believe that VUAA1 must interact with a site that is critical for Orco function, perhaps residues involved in channel gating, subunit oligomerization,

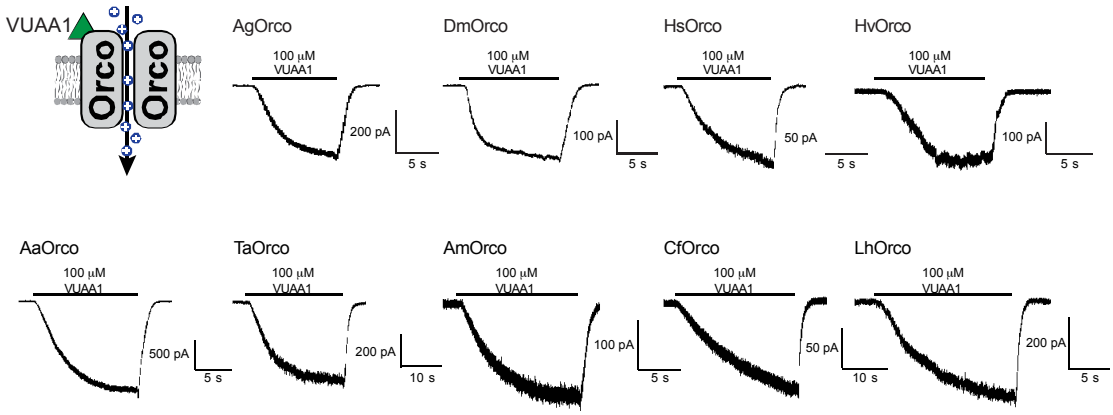

Figure 6.1 VUAA1 can gate homomeric Orco channel orthologs from four insect orders. Whole-cell recordings from HEK cells expressing an Orco ortholog. The species organized by insect order are the following: Diptera (*Anopheles gambiae*, AgOrco; *Aedes aegypti*, AaOrco; *Toxorhynchites amboinensis*, TaOrco; *Drosophila melanogastor*, DmOrco), Hymenoptera (*Apis mellifera*, AmOrco; *Harpegnathos saltator*, HsOrco; *Camponotus floridanus*, CfOrco), Lepidoptera (*Heliothis virescens*, HvOrco), and Hemiptera (*Lygus hesperus*, LhOrco).

etc. We may not know any of this information until a structure is determined, but perhaps a VUAA1-like molecule might be used in obtaining an open-state structure in the future.

High-throughput Deorphanization of Insect ORs

Our lab has mostly utilized cell-based high-throughput assays to search for small molecule modulators, like VUAA1, I believe this system has great potential in OR deorphanization with odorant ligands. Understandably so, the compound library at Vanderbilt Institute of Chemical Biology High-Throughput Screening Core does not contain many, if any, volatile compounds that would be classified as odorants. The following method would be an efficient way to identify ligands for orphan ORs as well as find new and/or stronger ligands for ORs.

After an OR has been cloned, it can next be sub-cloned into a set of mammalian expression vectors. The first vector can then be used for transient expression and also incorporates an N-terminal GFP tag, which has been shown to retain function. Once the OR of interest is in in the GFP vector, it can be co-transfected with Orco into HEK cells. If the GFP fluorescence appears to be associated with the membrane, which can be determined by confocal microscopy, then it is likely that a functional OR complex has formed.

Next, the OR of interest can be sub-cloned into a dual expression vector (already with Orco) containing FLP recombinase sites and can be used to generate stable cell lines. OR expression in isolated colonies can be validated by application of VUAA1 or by PCR from genomic DNA. While generating the

stable lines, the next step is to set up the odorant panel for screening. Though this task requires a couple of long and smelly days in and out of the odorant refrigerator, a single plating can be frozen and used for several screens.

I would also like to point out that many of the OR deorphanization publications in the past have used a generic panel of odorants. However, the insect of interest would never encounter several odorants in such panels, with some odorants not even existing in a natural environment. With our increasing knowledge of chemical ecology, I believe that OR deorphanization screens would have greater success and relevance by utilizing biologically-relevant odorant panels.

Once the Orco+ORX cell line has been generated and the odorant panel has been plated into 384 well plates, one can then perform the Ca^{++}-imaging screen[3]. Using the well-established Fluo4-based Ca^{++}-mobilization assays, the orphan OR complex can be exposed to 384 odorants at a time. After the initial run, positive odorant hits can be revalidated in a concentration-dependent manner, thus producing a CRC in the process. The largest odorant panels used for OR-deorphanization studies have consisted of 110 odorants and have been limited by the low to medium throughput of the *Drosophila* empty neuron and *Xenopus* oocyte systems. This high-throughput HEK-based assay can then produce tuning curves with great chemical diversity. If several ORs are deorphanized in this manner, the data can then be used to define the odor space of the insect.

Sugar-Feeding Assays with Lactones

As a next step from the lactone-AgOr48 publication, I had performed some preliminary sugar-feeding assays involving several of the strong lactone agonists[4]. The assay involved treating the 10% sucrose with either a lactone compound or vehicle alone (DMSO). The solutions were then turned either blue or red with food coloring and placed in a glass bottle with a cotton wick. 3-day old mosquitoes (sugar starved for 24 hours) were then added to a Bug Dorm that contained both a blue and red solution of either treatment or vehicle. Mosquitoes were then checked for either blue or red color in the abdomen. My preliminary findings showed a preference for 100 μM *∂*-decalactone in the treatment and no preference in the cages with two sugar sources of vehicle alone. I did not see a strong effect in later assays, and that may be due to residual odorant in the Bug Dorms, as I did not clean them after each use.

I believe that the next step to characterize odorants as sugar-source attractants would involve some changes in the assay. First, I believe that using pupae instead of 3-day old adults would give a stronger and more reliable effect. Previous research has shown that recently eclosed *An. gambiae* females prefer a sugar meal to a blood meal[5]. In addition, without any prior sugar meals, it should be relatively easy to observe the colored abdomen.

It would also be wise to test mixtures of different lactones at various concentrations. I have also been curious to see whether a weak agonist at high concentrations could trigger the same behavioral response as a strong agonist at low concentrations, an effect that has been recently shown in the olfactory

periphery of *Drosophila*[6]. It would also be worthwhile to test some fruit extracts from mangos or guava, which have been shown to be attractive to *An. gambiae*[7,8].

Determination of Subunit Stoichiometry of Insect ORs

One of the more elusive questions in the field relates to the subunit stoichiometry of an insect OR complex. How many Orco and tuning OR subunits does it take to form a functional heteromeric complex? In the past, subunit stoichiometry of ion channels has been determined through co-expression of WT and mutant subunits, affinity purification, and FRET-based techniques[9-11]. With the lack of knowledge about insect OR structure, other techniques may prove useful in determining the stoichiometry.

In 2007, a new method to count subunits in membrane-bound receptors using single molecule imaging was described[12]. Using Total Internal Reflection Fluorescence (TIRF) microscopy, the group demonstrated that one could observe puncta of fluorophore-tagged receptors on the membrane surface. The photobleach steps can then be counted for each punctum while a high intensity laser excites the fluorophores. As the fluorophore:subunit ratio is 1:1, the photobleach steps correlate directly to the tagged-subunits in the complex.

I proposed to do the following experimental setups:

1) N-EmGFP-AgOrco + AgOrX, to determine number of AgOrco subunits in the heteromeric complex

2) AgOrco + N-EmGFP-AgOrX, to determine number of AgOrX subunits in the heteromeric complex
3) N-EmGFP-AgOrco + N-EmGFP-AgOrX, to determine the total number of subunits in the heteromeric complex
4) N-EmGFP-AgOrco, to determine the number of AgOrco subunits in the homomeric complex

For the AgOrXs, both AgOr10 and AgOr65 will be used to determine if the stoichiometry changes according to the tuning OR. I have generated the required EmGFP-AgOr fusion constructs and these constructs are fully functional when expressed in HEK cells (Figure 6.2). Initial attempts at single molecule imaging of transfected cells showed membrane-associated puncta at 3 hours post transfection. However, the majority of the tagged protein remained on the intracellular compartments and lead to increased background, prompting the need for a controllable expression system for the EmGFP-tagged constructs.

Through subcloning all of the EmGFP constructs into the pTRE plasmid, which contains a tetracycline response element (TRE) upstream from a CMV promoter that can control expression of the gene of interest. These plasmids can then be transiently transfected into Tet-Off HEK cells, which stably express a modified Tet-repressor protein, tTA, that functions as a tetracycline-controlled transactivator of the TRE site. In the absence of tetracycline, tTA binds to the TRE and induces expression. Consequently, when tetracycline is present, it binds to tTA and stops expression of the gene of interest. By adding tetracycline at different time points post transfection, one can allow a small subset of OR

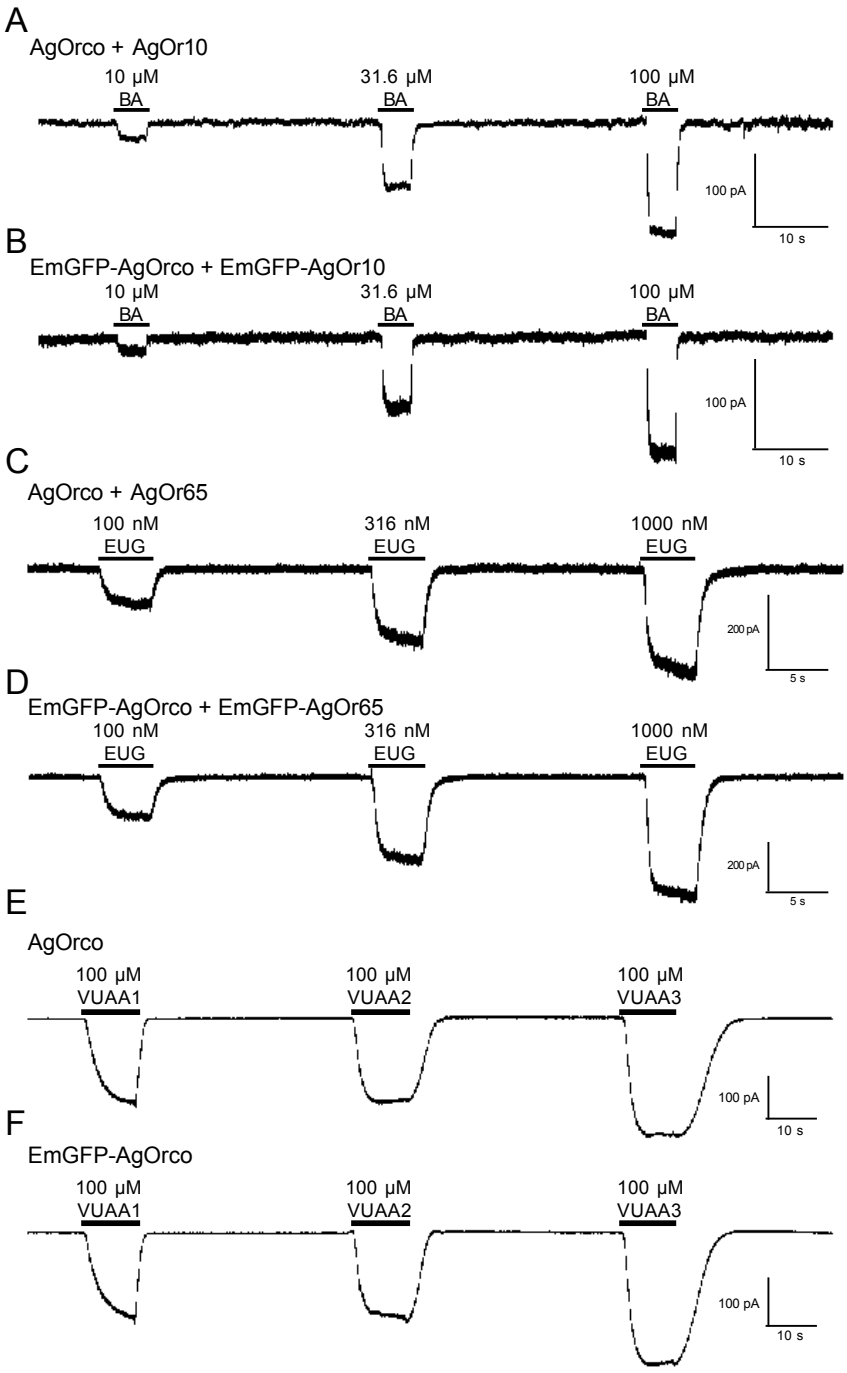

Figure 6.2 EmGFP tagged AgOr constructs function as wild type. Whole-cell responses of WT and EmGFP-tagged AgOr complexes to different concentrations of agonist. The AgOrco + AgOr10 (**A-B**), AgOrco + AgOr65 (**C-D**), and AgOrco (**E-F**) complexes showed similar responses independent of the N-terminal EmGFP tag.

complexes to localize to the plasma membrane with relatively little present in intracellular compartments.

These studies are currently underway and hopefully will yield conclusive data and a high impact publication. Both Dave Piston and Matt Tyska have been extremely helpful in assisting me in TIRF microscopy and single molecule imaging.

References

1. Taylor, R. W. *et al.* Structure-Activity Relationship of a Broad-Spectrum Insect Odorant Receptor Agonist. *ACS Chem. Biol.* (2012).doi:10.1021/cb300331z

2. Jones, P. L. *et al.* Allosteric antagonism of insect odorant receptor ion channels. *PLoS ONE* **7**, e30304 (2012).

3. Rinker, D. C. *et al.* Novel high-throughput screens of Anopheles gambiae odorant receptors reveal candidate behaviour-modifying chemicals for mosquitoes. *Physiol Entomol* **37**, 33–41 (2012).

4. Pask, G. M., Romaine, I. M. & Zwiebel, L. J. The Molecular Receptive Range of a Lactone Receptor in Anopheles gambiae. *Chem Senses* **38**, 19–25 (2013).

5. Foster, W. A. & Takken, W. Nectar-related vs. human-related volatiles: behavioural response and choice by female and male Anopheles gambiae (Diptera: Culicidae) between emergence and first feeding. *Bull Entomol Res* **94**, 145–157 (2004).

6. Münch, D., Schmeichel, B., Silbering, A. F. & Galizia, C. G. Weaker Ligands Can Dominate an Odor Blend due to Syntopic Interactions. *Chem Senses* (2013).doi:10.1093/chemse/bjs138

7. Gouagna, L. C. *et al.* Patterns of sugar feeding and host plant preferences in adult males of An. gambiae (Diptera: Culicidae). *J Vector Ecol* **35**, 267–276 (2010).

8. Müller, G. C. *et al.* Field experiments of Anopheles gambiae attraction to local fruits/seedpods and flowering plants in Mali to optimize strategies for malaria vector control in Africa using attractive toxic sugar bait methods. *Malar J* **9**, 262 (2010).

9. Mano, I. & Teichberg, V. A tetrameric subunit stoichiometry for a glutamate receptor-channel complex. *Neuroreport* **9**, 327 (1998).

10. Grudzinska, J., Schemm, R., Haeger, S. & Nicke, A. The [beta] Subunit Determines the Ligand Binding Properties of Synaptic Glycine Receptors. *Neuron* (2005).

11. Zheng, J., Trudeau, M. & Zagotta, W. Rod cyclic nucleotide-gated channels have a stoichiometry of three CNGA1 subunits and one CNGB1 subunit. *Neuron* **36**, 891–896 (2002).

12. Ulbrich, M. H. & Isacoff, E. Y. Subunit counting in membrane-bound proteins. *Nature Publishing Group* **4**, 319–321 (2007).